Carrying Capacity Study of Teesta Basin in Sikkim

Volume-V

AIR ENVIRONMENT

Commissioned by :

Ministry of Environment & Forests, Government of India

Sponsored by :

National Hydroelectric Power Corporation Ltd., Faridabad

CENTRE FOR INTER-DISCIPLINARY STUDIES OF
MOUNTAIN & HILL ENVIRONMENT
CISMHE UNIVERSITY OF DELHI, DELHI

Carrying Capacity Study of Teesta Basin in Sikkim

Volume-V

AIR ENVIRONMENT

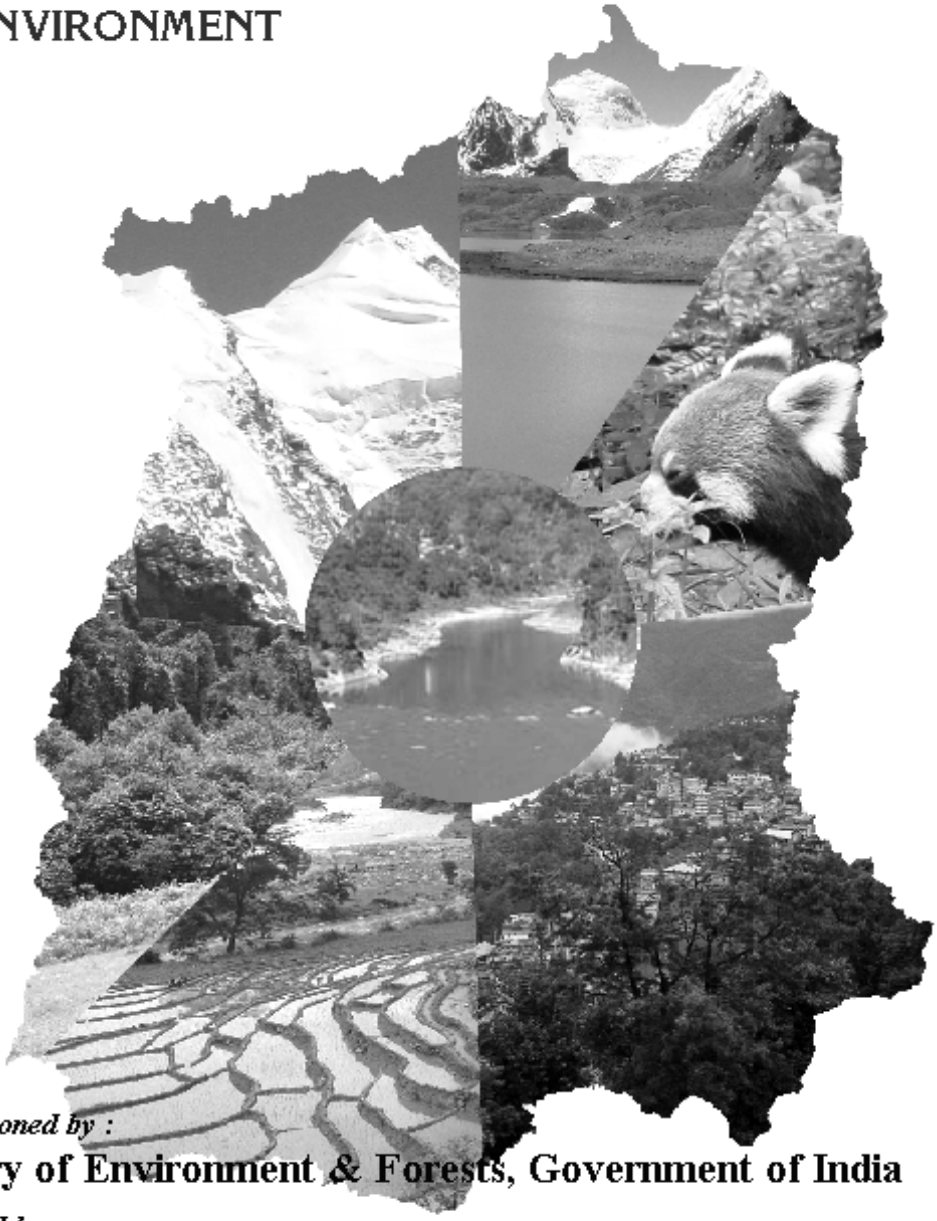

Commissioned by :

Ministry of Environment & Forests, Government of India

Sponsored by :

National Hydroelectric Power Corporation Ltd., Faridabad

CISMHE **CENTRE FOR INTER-DISCIPLINARY STUDIES OF MOUNTAIN & HILL ENVIRONMENT**
UNIVERSITY OF DELHI, DELHI

&

Centre for Atmospheric Sciences, Indian Institute of Technology, Delhi

CARRYING CAPACITY STUDY OF TEESTA BASIN IN SIKKIM

Principal Investigator

Prof. (Mrs.) Pramila Goyal

CENTRE FOR ATMOSPHERIC SCIENCES
INDIAN INSTITUTE OF TECHNOLOGY, DELHI
HAUZ KHAS, NEW DELHI-110016

PARTICIPATING INSTITUTIONS

- **Centre for Inter-disciplinary Studies of Mountain & Hill Environment, University of Delhi, Delhi**

- **Centre for Atmospheric Sciences, Indian Institute of Technology, Delhi**

- **Centre for Himalayan Studies, University of North Bengal, Distt. Darjeeling**

- **Department of Geography and Applied Geography, University of North Bengal, Distt. Darjeeling**

- **Salim Ali Centre for Ornithology and Natural History, Anaikatti, Coimbatore**

- **Water and Power Consultancy Services (India) Ltd., Gurgaon, Haryana**

- **Food Microbiology Laboratory, Department of Botany, Sikkim Government College, Gangtok**

VOLUMES INDEX*

*For Volume-wise Detailed Index – Refer to the end of the report

PREFACE

Rapid urbanization and industrialization has changed the whole scenario of urban cities. Hence it became necessary that alternative to further growth of these cities should be identified, which is consistent with the objectives of economic growth and social development. A city cannot have infinite carrying capacity and sustainable development can be achieved only if the development is within the carrying capacity of the region. This carrying capacity study, accordingly, covers the analysis of supportive as well as assimilative capacities to ensure sustainable development of the region.

At the instance of the Ministry of Environment and Forests (MoEF), a study on “Carrying Capacity of Teesta Basin in Sikkim” has been initiated with financial assistance from National Hydroelectric Power Corporation (NHPC) in view of a series of hydro-power development schemes envisaged in the Teesta Basin and is being undertaken by the Centre for Inter-disciplinary Studies of Mountain and Hill Environment (CISMHE), University of Delhi. The scope of the study, inter-alia, includes.

- Assessment of supportive and assimilative capacities.
- Optimization of resource allocation strategy.
- Evaluation of state development plan as well as business as usual scenario.
- Preparation of short and long term action plans to be implemented by concerned agencies through technological and policy planning interventions.

- Development of alternate scenarios including prioritization of preferred scenarios.

The Indian Institute of Technology Delhi was entrusted with the task of preparing a sustainable development model of Sikkim through assimilative capacity of air environment which will be useful for carrying capacity planned development in the state. The main activities of IIT Delhi are the estimation of assimilative capacity of air resources for most critical environmental areas in Teesta basin and to develop and validate air quality models for Sikkim. The present study includes the monitored air quality at different locations and the emission inventory of air resources based on secondary data acquired from different sources which are used to estimate assimilative capacity of air environment.

Assimilative capacity of air environment is the maximum amount of pollution load that can be discharged without violating the best designated use of the air resource in the planning region. The phenomena governing the assimilative capacity of air environment include dilution, dispersion and deposition. The air pollution assimilative potential of an airshed can be estimated as the ventilation coefficient for the area. The ventilation coefficient is an indicator of horizontal as well as vertical mixing potential. Estimation of assimilative capacity for an environment involves: Delineation of an airshed based on topography of the area and identification of micro-climatic zones depending topography and wind fields data, preparation of inventory and quantification of pollution loads.

The assimilative capacity of Sikkim has been estimated by pollution potential, which has been estimated by using dispersion models in terms of concentration of pollutants, and is inversely proportional to the assimilative capacity of the atmosphere. Dispersion models for point, area and line sources have been used to predict the spatial and temporal distribution of three pollutants namely sulphur dioxide (SO_2), suspended particulate matter (SPM) and oxides of nitrogen (NO_X). These models have been validated against the observed data.

Predictions of temporal and spatial variations in air pollutants concentrations for existing sources using multiple source-receptor model to establish source-receptor relationship. Upper limits of pollution load have been established in critical pockets, after comparing with standards.

The trust reposed by the Ministry of Environment and Forests (MoEF) in the Centre for Atmospheric Sciences (CAS), IIT Delhi for awarding of this challenging project is gratefully acknowledged. The cooperation and advice provided by Prof. M.K. Pandit and Dr. Arun Bhaskar (CISHME) deserve special thanks.

Coordinator also wishes to thank Mr. Sankalp Anand and Mr. Bharat Pradhan, CAS, IIT Delhi for their contribution to the study.

(Prof. Pramila Goyal)
(Coordinator)

CONTENTS

LIST OF TABLES

LIST OF FIGURES

CHAPTER - 1

CARRYING CAPACITY BASED DEVELOPMENT PLANNING PROCESS

1.1 INTRODUCTION

Urban areas are characterized by high population density and economic development. The resulting pollutant emissions place an increasing pressure in the air quality of these areas. Whereas in the past the major reasons for poor air quality were industrial activity and domestic heating but, nowadays as a result of the rapid increase in mobility the major current urban air pollutants come from road traffic (Sturm *et al*., 1997). This is particularly significant for developing countries, where the rapid rates of both urbanization and growth in vehicle fleet (Faiz, 1993) are expected to be the highest in the world (World Health Organization/United Nations Environment Program, 1992). The simple reason being means of transportation is an important infrastructural facility. These play a very important role in the overall development of a country. As the numbers of vehicles are increasing rapidly, it has slowly but surely started hindering our atmospheric purity with the vehicular and noise pollution. The pollutants emitted from these are transported, dispersed or deposited by meteorological and topographical conditions. Thus, the resulting ground level concentration patterns have to be estimated to save the environment and indirectly the human race. It’s for this reason that the assessment of assimilative

capacity is urgently required especially for a place like Sikkim which is environmentally fragile and eco-sensitive.

1.1.1 Concept of Carrying Capacity

The concept of carrying capacity is very important for developmental planning and hence needs to be defined properly. Carrying capacity, in broad terms, is an indicator of potential for future growth keeping in view the resources such as air, water, land etc. Air environment is more important as most of the developmental activities tend to have an impact on the surrounding air quality.

1.1.2 Framework for Carrying Capacity Based Development Planning

The development of framework for carrying capacity based planning involves, mainly, identification of the resources of the region and scope of their utilization *vis*-à-*vis* environmental impacts. The carrying capacity of air environment gives a rough estimate of the emission load (from various sources; man-made and natural) it can sustain under a set of specific conditions (release, topographic and atmospheric).

We should put our efforts to explore strategies for planned and sustainable development of Sikkim region. For example, proper scheduling of operations of industries (in view of the assimilative capacity of the atmosphere) should be done in order to release the pressure on the environment due to the industries.

1.1.3 Assimilative Capacity Dimensions of Air Environment

The term “assimilative capacity” of the atmosphere is believed to be used interchangeably with the “carrying capacity”. The assimilative capacity of the atmosphere gives roughly an idea of the extent to which the atmosphere is capable of sustaining the pollution load from various emission sources. Thus, a thorough study of the assimilative capacity is essential for judging proper sitting of new industrial units and for regulating the operating of the industries according to the atmospheric conditions. The assimilative capacity depends on various physical parameters such as the atmospheric stability, the topography of the region etc. The atmospheric stability is a crucial parameter which is based on solar insulation, mean wind speed and temperature profile.

The assimilative capacity of the atmosphere is directly proportional to the ventilation coefficient and inversely proportional to the pollution potential. Further, the ventilation coefficient is expressed as a product of the mixing height and the transport wind speed within the mixing layer. The use of atmospheric stability for the estimation of assimilative capacity is manifested in the mixing height and the transport wind. A region with large pollution potential would have less carrying capacity.

1.1.4 Resource Allocation Strategies

Optimum and proper utilization of the resources is an important aspect of the carrying capacity based development. For an integrated approach towards sustainable development there is a need to evolve

proper strategies for balanced allocation of the resources in the region. The knowledge of assimilative capacity would be desirable for determining the resource allocation strategies for various parts of the region. This is very essential for decision making related to overall regional development in Sikkim.

1.2 THE STUDY AREA – SIKKIM

Sikkim (Fig. 1.1) is a small Himalayan state in north-east India situated between 27^0 00' 46" to 28^0 07' 48" N latitude and 88^0 00' 58" to 880 55' 25" E longitude with geographical area of 7,096 sq km constituting only 0.22% of total geographical area of India. It has a human population of 5,40,493 as per Census, 2001, which constitutes only 0.05% of India's total population. The state is somewhat rectangular in shape with maximum length from north to south of about 112 km and maximum width of 90 km from east to west. The state is bounded in the north by the Tibetan plateau, by China (Tibet) on the northeast, by Pangola range of Bhutan on the southeast, by Darjeeling district of West Bengal on the south and Singalila range and Khangchendzonga on the west and northwest. Entire state of Sikkim constitutes upper basin of Teesta river except for a small area of 75.62 sq km in extreme southeast that of Jaldhaka River, which originates in east Sikkim and flows through West Bengal parallel to Teesta River to meet Brahmaputra River. In southernmost part of Sikkim, Teesta River flows in southwest direction and defines the inter-state boundary between Sikkim and West Bengal up to Melli Bazar where it is joined by Rangit River which drains West

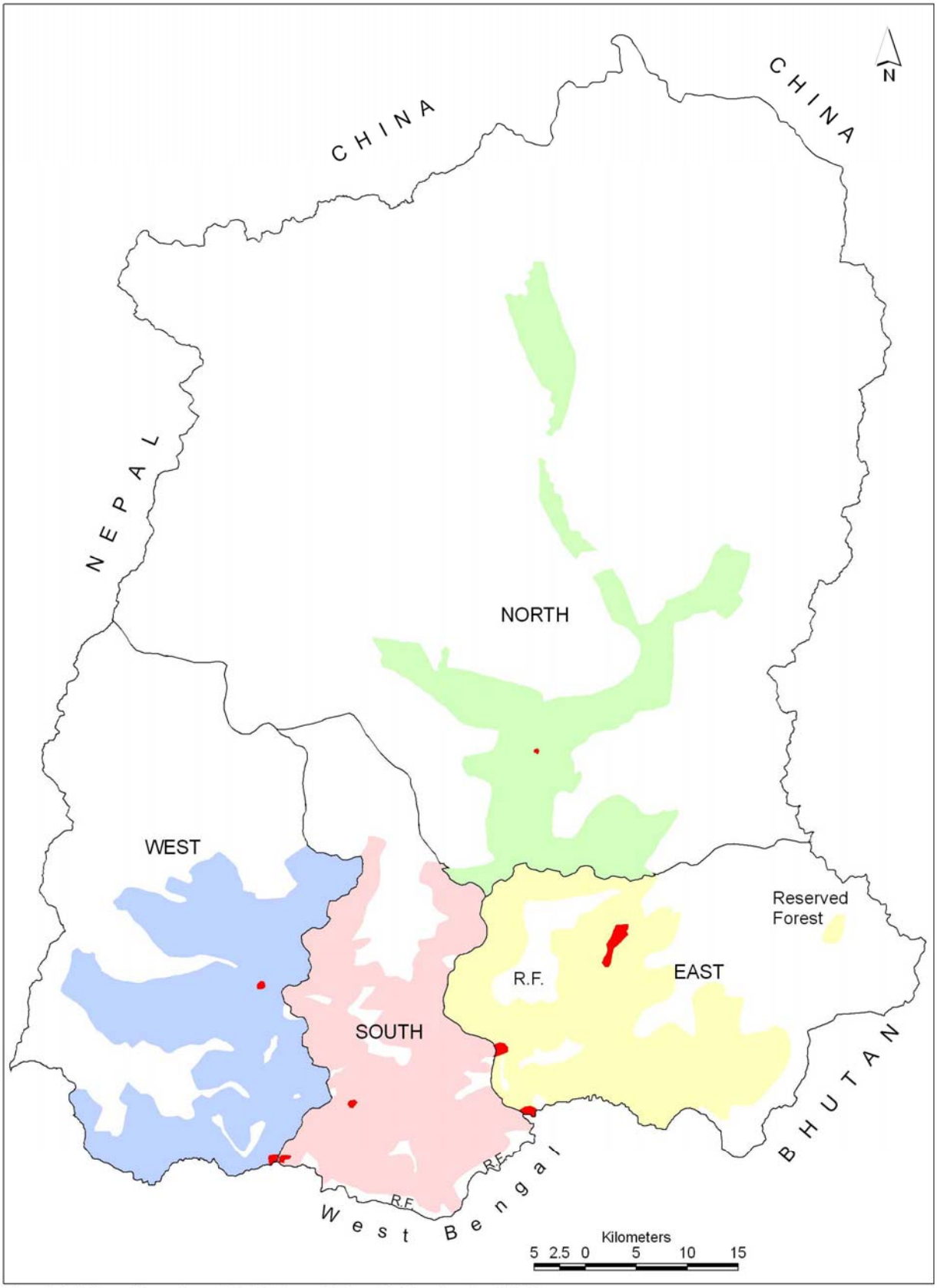

Fig.1.1 Map showing districts of Teesta basin in Sikkim

Sikkim district. Rangit River, the largest tributary of Teesta River Sikkim, from Nayabazar point flows in southeast direction and marks the interstate boundary between Sikkim and West Bengal in the southwest.

The state of Sikkim has been administratively divided into four districts *viz*. North Sikkim, South Sikkim, East Sikkim and West Sikkim using water divides of major and minor tributaries of Teesta River as criteria. North Sikkim is the largest district with an area of 4,226 sq km constituting about 60% of the entire state. The West, East and South districts constitute about 16%, 13% and 11% of the geographical area of the state, respectively. The state capital is located at Gangtok in East Sikkim. Each district has been further divided into two sub-divisions each, except East Sikkim, which has been divided into three sub-divisions. All the districts together have 407 revenue blocks and 42 forest blocks. East Sikkim is the most populated district having 45.29% of state's total population and North Sikkim is the least populated with 7.59% share of the total human population.

Human population of Sikkim is comprised mainly of Nepali, Bhutias and Lepchas. Main languages of the state are Nepali, Bhutia and Lepcha. Majority of the population speaks Nepali, which is the main medium of instruction in educational institutions along with English. The inhabitants of the state are predominantly Buddhists. Majority of residents depends upon agriculture and related activities for their

livelihood. Maize, large Cardamom, rice and wheat are principal crops grown in the state.

1.2.1 Brief History of Sikkim

In pre-historic times, Sikkim was inhabited by 3 tribes *viz*., Naong, Chang and the Mon. Later, the Lepchas entered and occupied it completely. They resorted to the practice of electing a leader whose advice and counsel was sought on crucial matters.

The Tibetan migration in early 17th century led the Lepchas to shift their habitats so as to avoid conflict. Meanwhile they struggled among the followers of the “Yellow Hats” and the “Red Hats” which forced the latter to seek refuge in Sikkim, where they attained the status of aristocracy and gradually dominated the state. In order to avoid any possible opposition from the Lepchas these immigrants chose one venerable person Phuntsog Namgyal as the temporal and spiritual head of Sikkim. He relocated his capital to Yuksam and established a centralized government.

Tensung Namgyal who succeeded his father in 1670 moved his capital to Rabdentse. During the reign of Tashi Namgyal who was throned in 1914, Sikkim underwent a number of reforms. Forced labour was abolished. Gambling was made illegal. Landlords’ courts were abolished. Developmental plans were drawn up for which aid from India was sought. Executive and judicial powers were decentralized. Tashi

Namgyal died on 2nd December 1962 and was succeeded by his son Palden Thondup. He was married to a Tibetan lady Sangey Deki. Growing agitation in 1973 against the monarchy led to the administration's collapsed and Indian troops stepped in which was followed by political arm wrestling for power. In 1975 Sikkim was merged to become India's 22nd State.

1.2.2 Physical Features

The topography of Sikkim is characterized by great variation in elevation, ranging from 243 to 8,595 m. Most of Sikkim is in the Lesser and Greater Himalayan Zone. The state is girdled by high ridges on the north, east and west. To the north the convex arc of Greater Himalayas separates the state from Tibetan highlands. A number of peaks built up of crystalline rocks accentuate the demarcation between Tibet (China) and Sikkim. The longitudinal Chola range separates the state from Tibet on the eastern side while the Singalila range, another longitudinal offshoot of the Himalayan arc, marks the boundary between Sikkim and Nepal in the west.

The girdling ridges on the three sides of the state contain some imposing peaks and high altitude passes. The exalted peak of Khangchendzonga (8,595 m), Siniolchu (6,895 m), Pandim (6,706 m), and high altitude passes like Nathu La (4,728 m), Jelep La (4,040 m), etc, are all located within this Himalayan state.

Sikkim is in the upper part of the Teesta basin, which virtually marks the state boundary. The present landscape of the state owes

much to the drainage network of the river Teesta. The structural slope of the land is from north to south; hence all the major rivers of the state have a southerly flow. The northwestern part of the state is highly elevated and therefore, remains under snow cover almost throughout the year. The resultant topography is that of a typical moraine deposits. Besides, there are numerous glacial lakes, which freeze during winter.

1.2.3 Climate

Sikkim has its own climatic peculiarities caused by its geographical location, relief and altitudinal variation. As such, temperature conditions vary from sub-tropical in the southern lower parts to that of cold deserts. It is the most humid place in the whole of the Himalayan range because of its proximity to the Bay of Bengal and exposure to the effects of the moisture laden southwest monsoon.

Sikkim is a land of great climatic contrasts within very short distances. The region is located within the subtropical climatic regime. But due to the presence of high mountains, one can experience varying climate such as temperate, alpine and sometimes even arctic type. The differences in the climatic types are due not only to the differences in altitude but also to the configuration of the neighboring mountain ranges, which largely affects air movement, rainfall and temperature. Pradhan (2004) has broadly classified the climate of Sikkim into the following types.

1. ***Subtropical Humid Type***- Such type of climatic condition prevails in the areas lying below 1500m. At Namchi in South Sikkim, the summer maximum is 35^0 C while the winter minimum is 6^0 C. The

average annual rainfall is high, but it varies from place to place (1500-3500 mm). While Tadong (1,500 m) in East Sikkim receives more than 3000mm of annual rainfall, Namchi (1,500 m) in South Sikkim receives barely 1550 m of annual rainfall. Again Mangan (1,310 m) in North Sikkim receives 3200 mm of annual rainfall while Dentam (1,372 m) in the west Sikkim records 2300 mm. In the sub-tropical climatic zone, the humid period is very long, extending for almost six months from April to September. Nighttime showers are common in the summer months, thus rendering cool nights even in hottest summer days. Winters are usually cool and dry.

2. ***Semi temperate Type-*** This type of climatic condition is experienced in areas lying between 1,500-2,000 m. Mean annual temperature ranges from 8^0 C in winter to 26^0 C in summer. Rainfall is usually heavy, with annual mean of 2400 mm. It is exceptionally heavy in June, July and August when the south-west monsoon breaks. At Gangtok (1,800 m), the mean minimum temperature is 2^0 C while the mean maximum temperature is 26^0 C. The average annual rainfall is very high, about 3500mm and snowfall is very rare.

3. ***Temperate Type-***The hill slopes lying between 2000-3000 m come under this type of climate. Here the annual temperature ranges from freezing point in winter to 15^0 C in summer. Precipitation is medium to heavy, which occurs both in the form of rain and snow. At Lachen (2,697 m) and Lachung (2,633 m) valleys of north Sikkim, the average annual rainfall is 1700 mm. Within this zone, the summer months are never hot and the winter

months are always very cold. Winter snow is common. Frost is also common at nights almost round the year.

4. ***Alpine Snow-Forest Type***-This climate is experienced between 3000-4000 m. Temperature remains very low for more than five months of the year, i.e., from November to March especially, December, January and February which are extremely cold. Rainfall begins from the end of May and continues till the end of September. In winter months, precipitation occurs in the form of snow. Tsangu (3,840 m) in the east Sikkim records 2900 mm of annual rainfall. The precipitation decreases at regular pace towards the north, for example Yumthang (3,673 m) records annual precipitation of about 1400 mm while Thangu (3,812 m) records only 800 mm. The major part of this area is uninhabited due to harsh climate.

5. ***Alpine Meadow***-This climate is prevalent only around the peripheries of the snow-capped areas in the extreme northern, eastern and western sections of Sikkim. The average elevation is more than 4000m. Here air temperature is always very low, night temperatures often dropping below the freezing point. Atmospheric pressure is also low and uncomfortable for living. Precipitation is mainly through snowfall, except in the summer months. Summer is brief, barely of three months duration, when alpine shrubs and grasses appear in the region. The ground remains snow covered and the soil remains frozen about four months of the year. No permanent settlement is found in this region.

6. ***Arctic Type-***This type of climate is prevalent only in the extreme northwestern part of the state where a number of snow peaks soar above 6,000 m. The snow peaks of the Khangchendzonga, Kabru, Siniolchu and all snow clad peaks are located within this climatic zone. The entire zone is bare of vegetation and animal life.

1.2.4 Temperature

Gangtok, the capital of Sikkim, enjoys a mild, temperate climate all year round owing to its sheltered environs and elevation. Temperatures range from a peak high of 25°C in summer to a peak low of about 3°C in winter. Although snow does not fall within city limits during winter, it does fall within a kilometer of the city, on slightly elevated areas. During particularly cold winters, the lows sometimes plummet below freezing. During this season the weather is often unsettled, and can often suddenly change from bright sunshine with clear skies to heavy rain in a couple of hours.

1.2.5 Rainfall

Sikkim is a region of heavy rainfall. It is usually heavier in the central region, but it increases rapidly towards the Khangchendzonga side. The maximum rainfall occurs at a place where there is no barrier for the penetration of monsoon clouds, such as Chungthang and even at Lachen. The rainfall decreases substantially towards the northern side. Gangtok and Rangli in the east get 300 cm of rainfall. Thangu in the

north gets only 85cm of rainfall. The downpour on a single day is heavy at certain places. There are, however, dry places also, where the monsoon cannot reach easily as for example in Lhonak valley. The monsoon is exhausted as they reach the northern region and, therefore, there is comparatively less rainfall.

1.2.6 Winds

The wind intensity is not high except when accompanied by pre-monsoon thunderstorms. However, in the afternoon they are comparatively more severe. Their direction is generally southeasterly in the mornings and sometimes changes to northwesterly in the evenings.

1.2.7 Population

As per the 2001 census, the population of Sikkim is 5,40,493 as against 4,06,000 in 1991. The male population is 2,88,217 and the female is 2,52,276. Its density of population per sq. km is 76. Sikkim has around 0.22% of the total area of India and its population constitutes 0.05% of the national total. This clearly indicates that the state is still sparsely populated.

According to Rishley (1894), Nepalis with 56% constituted a majority of the population followed by the Lepchas (19%) and Bhutias (16%). At present, the Lepcha population has gone down to 14% whereas that of the Nepalis climbed to almost 70% with the Bhutias constituting more or less the same proportion (Lama, 2001). All these

three ethnic groups have their own language, culture and social practices, and have a strong socio-cultural bond among themselves (Rishley, 1894).

District-wise comparison of the population profile shows that the east district, where the state capital lies, is the most populated which accounts almost 50% of the state population. The north district has the lowest population According to Census of 2001, 48.72% people in Sikkim are workers and the remaining 51.28% are non-workers. Of the 48.72% workers, 49.9% are cultivators, 6.4% agricultural laborers, 1.2% engaged in household industries and the remaining 42.4% belonging to other kinds of vocations.

1.3 OBJECTIVES

The main aim of this study is to prepare a sustainable development model of Sikkim through assimilative capacity of air environment which will be useful for carrying capacity planned development in the state.

The following are the proposed objectives-

- Estimation of assimilative capacity of air environment through meteorological parameters (Mixing Height and Wind Speed).
- Installation of Sodar for measuring Mixing/Inversion height in the study region of Sikkim.
- Analysis of Ventilation Coefficient for different months to estimate the status of assimilative capacity.

- Development of detailed source inventory of air resources from secondary data acquired from different sources in study area.
- Assimilative capacity through air quality dispersion model based on emission inventory and meteorological parameters.
- Validation of air quality models based on air quality data monitored in Sikkim.
- Correlation between two different approaches of assimilative capacity to highlight the status of air environment in the study area.
- Discussion of air pollutant levels in the study area by comparing with National Ambient Air Quality Standards (NAAQS) of respective pollutants and their observed values.

1.4 ASSIMILATIVE CAPACITY ASSESSMENT METHODOLOGY

The assimilative capacity of Gangtok's atmosphere has been estimated by two different approaches. First approach is based on ventilation coefficient, which is directly proportional to the assimilative capacity of the atmosphere and has been computed through micro-meteorological parameters. Second approach is through pollution potential, which has been estimated through dispersion models in terms of concentration of pollutants, and is inversely proportional to the assimilative capacity of the atmosphere. Dispersion models for line sources have been used to predict the spatial and temporal distribution of three pollutants namely sulphur dioxide (SO_2), suspended particulate matter (SPM) and oxides of nitrogen (NO_X). These models have been validated using the observed data.

CHAPTER - 2
APPROACH I - ESTIMATION OF ASSIMILATIVE CAPACITY THROUGH VENTILATION COEFFICIENT

2.1 INTRODUCTION

Rapid growth has led to population explosion in many urban cities. Increased population flux and unplanned development of these cities has created serious environmental problem leading to lowering of air quality and basic human needs. In the present situation when new industries are coming up and the existing ones increasing their capacities, it is necessary to study the environmental conditions in terms of Carrying Capacity. This would enable us to draw a plan for sitting new industries and regulating the operational timings of the existing ones. In broad sense, the Carrying Capacity is an indicator of potential for further growth keeping in view the basic resources such as air, water, land etc. Clean air is essential for healthy living and thus, more important in comparison to the other basic requirements. Any developmental activity has direct impact on the surrounding air quality. For this reason, a detailed analysis of Carrying Capacity of air environment is needed. The Carrying Capacity of air environment gives a rough estimate of emission load which it can sustain.

The terms “Carrying Capacity” and “Assimilative Capacity” of the atmosphere are interchangeably used. Assimilative Capacity of the atmosphere gives roughly an idea of the extent to which atmosphere is capable of sustaining the pollution load from various emission sources. The assimilative capacity depends upon the various physical parameters such as atmospheric stability and the topography of the region. The

atmospheric stability is a crucial parameter which depends upon solar insulation, mean wind speed and temperature profile.

The assimilative capacity of the atmosphere is directly proportional to the ventilation coefficient and inversely proportional to the pollution potential. The ventilation coefficient is expressed as a product of mixing height and the transport wind speed within mixing layer. The use of atmospheric stability for the estimation of assimilative capacity is manifested in the mixing height and transport wind.

The pollution potential of the atmosphere indicates its capacity to dilute the pollutants and the resulting effect on the quality of air. A region with high pollution potential has less Carrying Capacity and vice-versa. According to the US National Meteorological Centre and Atmospheric Environment Services, Canada, has classified that high pollution potential occurs when the afternoon ventilation coefficient is less than 6000 $m^2 s^{-1}$ and mean wind speed does not exceed 4 ms^{-1} and during morning hours, the mixing height is less than 500 m and mean wind speed does not exceed 4ms^{-1} (Stack Pole, 1967; Gross, 1970). The same criterion as in the morning has been assumed during night too. Based on this criterion, the study of pollution potential for Sikkim has been made.

2.2 METHODOLOGY AND DATA REQUIREMENT

To estimate the behaviour of assimilative capacity of atmosphere over Sikkim, hourly meteorological data of the year 2001 and 2004 have

been used. Hourly values of the Ventilation Coefficient (VC) have been computed in order to estimate the Assimilative Capacity which is directly proportional to the VC. As mentioned earlier also, VC is expressed as the product of mixing height and average wind speed.

2.2.1 Mixing/ Inversion Height data

A monostatic Sodar capable of probing the dynamics of atmospheric thermal structures in Atmospheric Boundary Layer (ABL), in real time, has been installed at the G.B. Pant Institute of Himalayan Environment & Development, Pangthang near Gangtok, for studies of mixing/inversion height. The Sodar observations made during the period of October 2003 to September 2004 have been examined and analyzed to work out the monthly mean diurnal variation of mixing and inversion heights.

2.2.2 Sodar Measurement

The system is installed at G.B. Pant Institute of Himalayan Environment & Development, Gangtok. The Sodar antenna was set up on the terrace of water tank outside main building while the electronic and recording system was housed in the meteorological laboratory side by a little down below. The system operated at the fixed audio frequency of 2250 Hz. High power audible tone bursts of 100 ms duration are transmitted every 4 seconds which offer a probing range of about 700 m of the lower atmosphere. A parabolic dish of aperture 1.2 m is used as the acoustic antenna. At the focus of the dish a transducer with an

exponential horn assembly is placed. The antenna dish is surrounded by the 2m high conical acoustic shield. The operational frequency, duration of the tone burst and pulse repetition rate (determining the probing range) are selectable through user friendly software of the system. The whole system has been indigenously fabricated at the National Physical Laboratory. The system was installed at Gangtok during October 2003 and since that time it has been operating continuously. Data collected during the year long period (October, 2003-September, 2004) has been analyzed and presented in this report. The detailed Report of the execution of monitored values of Mixing/Inversion height has been enclosed herewith as Annexure – 1.

2.2.3 Site Characteristics

Sikkim is subject to the Indian monsoon that sweeps up from the Bay of Bengal, bringing heavy rainfall from early June until the end of September. The post-monsoon months of October and November provide settled conditions, with clear views of the mountains, although nighttime temperatures above 3,500 m frequently fall below freezing. The Sodar location is more or less on the sloping edge of deep valley on one side and hills on the other side. Since mixing height characteristics are manifestations of the upward transfer of heat flux in the ABL, the micrometeorological factors associated with topographical features of mountain characteristics, winds, frequent clouds, etc. are likely to induce modifications in the normal characteristics of mixing height on a diurnal scale. Sodar echograms (or the facsimile records) provide pictorial view of the occurrence of such modifications in real time.

2.2.4 Sodar Characteristics

The examination of Sodar echogram has revealed that ABL phenomenon such as free/ forced convection, inversions, fumigation, elevated shear layers/waves etc. are occurring in accordance with prevailing meteorological conditions at the observational site in Gangtok.

Typical Sodar records of ABL representing different meteorological phenomenon are shown in Fig 2.1 based on examination of facsimile records, following typical features of ABL thermal structures, at Gangtok, have been observed. It is seen that the clear thermal plumes (Fig 2.1) representing free thermal convection during the day under solar heating of the ground, have been seen during September and October while the diffused thermal plumes (Fig 2.1) under conditions of poor incoming solar radiations, cloud cover and superimposed induced mechanical mixing due to combined action of ambient and mountain winds are seen during other months.

Ground based inversions with more or less flat top (Fig 2.1), representing stable atmospheric conditions and /or spiky inversions layers (Fig 2.1), representing wind induced mechanical mixing within the stable ABL, are seen during night time on all the days of observations.

Eroding inversion (Fig 2.1) representing inversion breakup under the transition phase of the stable to unstable ABL after sunrise, is seen distinctly seen under calm atmospheric conditions during the winter and the clear months of September and October. However, it is seen to be

prolonged till afternoon during the winter months November to January. The observation is similar to what is normally observed over the plain land areas.

Elevated wavy/descending layers (Fig 2.1) associated with the occurrence of wind shear or subsidence etc. is seen on several days of observations. Such layers have also been seen (Singal *et al.* 1984) to be associated with the outburst of dust storm/thunderstorm at NPL, New Delhi.

2.3 RESULTS

The monthly hourly averaged values of mixing height are given in Table 2.1 and plot of diurnal variations of mixing height is shown in Fig 2.2. The study shows that the mixing height of unstable atmospheric boundary layer under sunshine hours during the day is fairly good. The maximum mixing height of about 2 km is seen during the post monsoon month of October while a maximum height of about 800m is seen during the winter month of December. It is seen to vary between these limits during course of the day and seasonal conditions in accordance with incoming solar radiation, prevailing meteorological conditions and time of the day. Singal and Kumar (1998) have reported similar results of observing a mixing height of about 1.7 km for the unstable ABL at Guwahati in the hilly area of Assam.

The average height of stable atmospheric boundary layer (inversion) associated with the maximum cooling (0100-0300 hrs) is

seen to vary between the minimum of 145 m to the maximum of 305 m. The minimum height is seen during the summer month of June while maximum is observed in the winter month of January. Normally the stable ABL or the ground based inversion height is height up to which the effect of radiational cooling of the ground is transmitted. However, in a hilly area with valley topography, there is an additional superimposed contribution of mountain winds or the katabatic winds. These winds carry cold air mass from higher heights down to the slopes and pile the same on to the top of ground based radiation inversion. The effect is more pronounced in winter due to strong inversions. This is considered as the probable cause of the presently observed, increased inversion height during extreme winter period. However, the extent of increase in height will depend upon the altitude and slope of the hill.

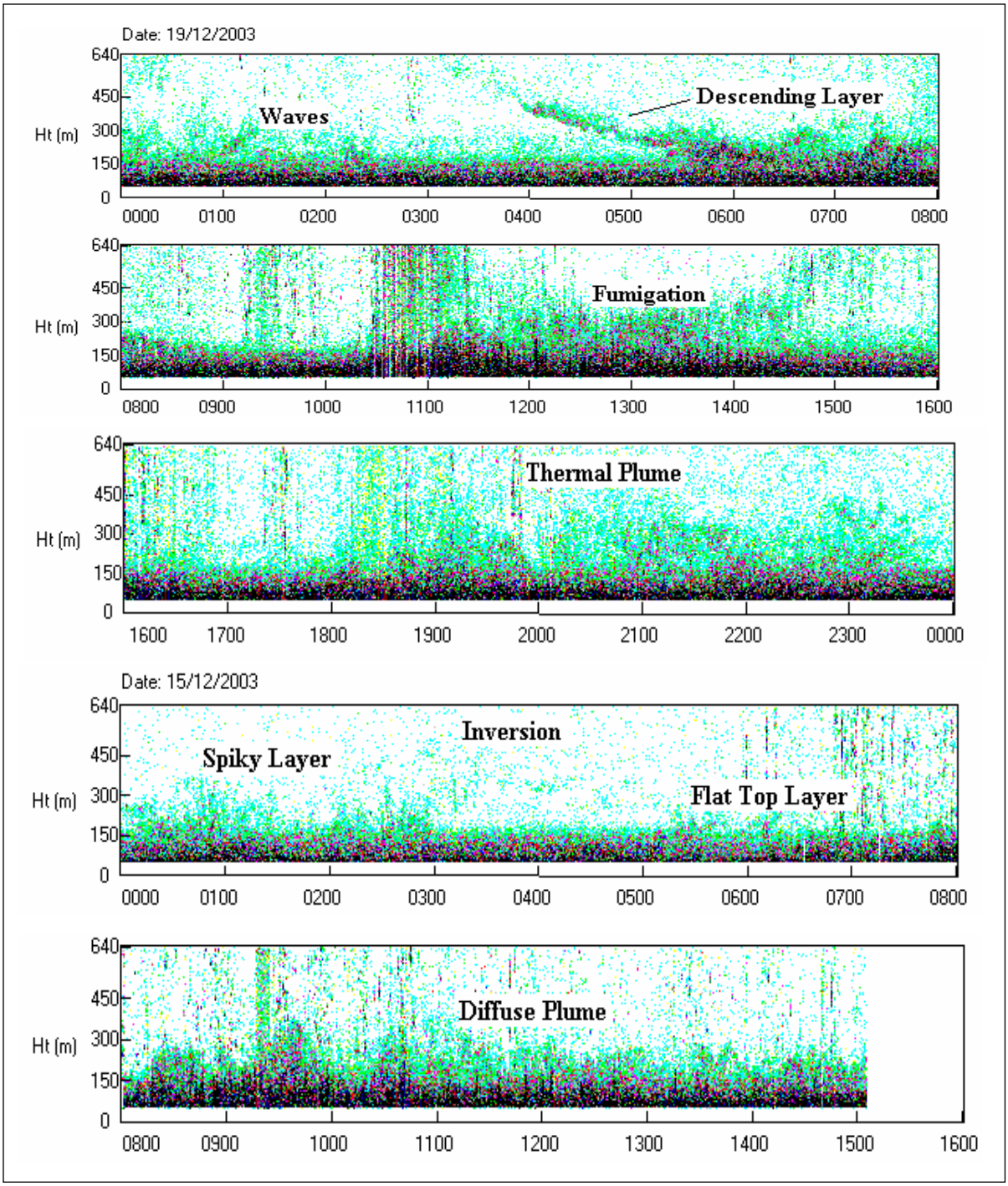

Fig 2.1 Various Sodar structure observed at G.B. Pant Institute, Pangthang, Sikkim

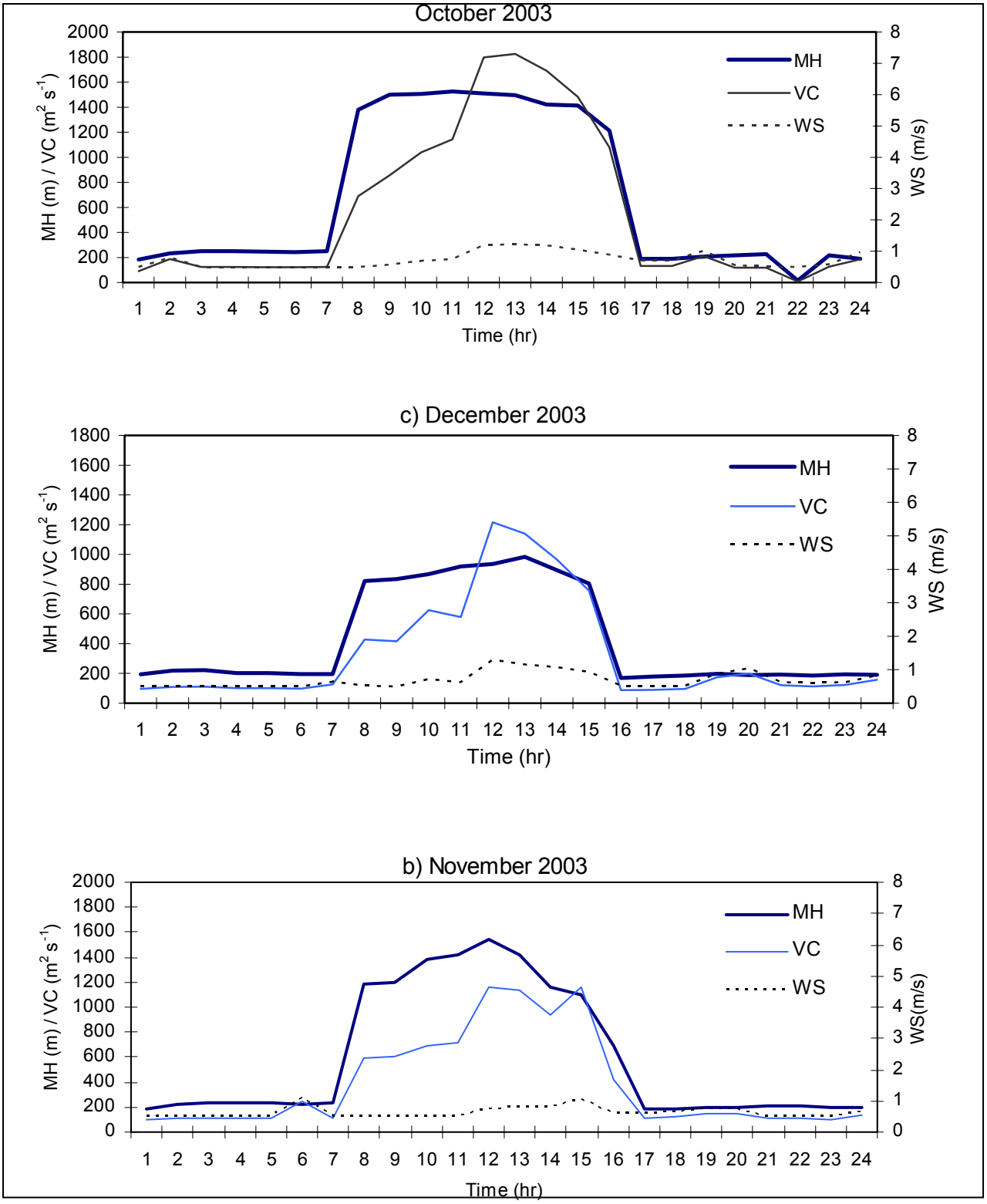
October 2003
MH (m) / VC (m2 s-1)
WS (m/s)
MH
VC
WS
Time (hr)
c) December 2003
MH (m) / VC (m2 s-1)
WS (m/s)
MH
VC
WS
Time (hr)
b) November 2003
MH (m) / VC (m2 s-1)
WS(m/s)
MH
VC
WS
Time (hr)

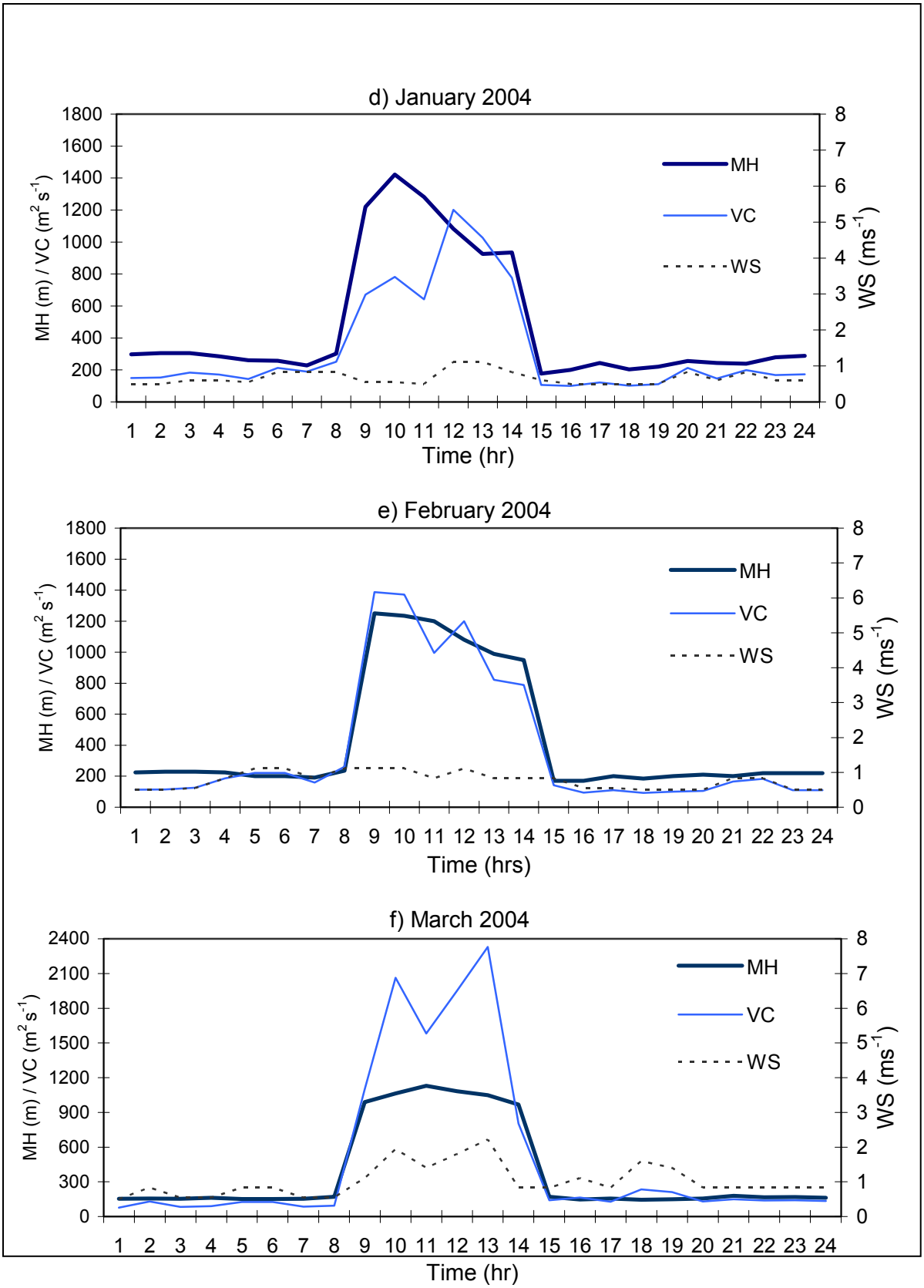
d) January 2004
MH (m) / VC (m^2 s^{-1})
WS (ms^{-1})
MH
VC
WS
Time (hr)
e) February 2004
MH (m) / VC (m^2 s^{-1})
WS (ms^{-1})
MH
VC
WS
Time (hrs)
f) March 2004
MH (m) / VC (m^2 s^{-1})
WS (ms^{-1})
MH
VC
WS
Time (hr)

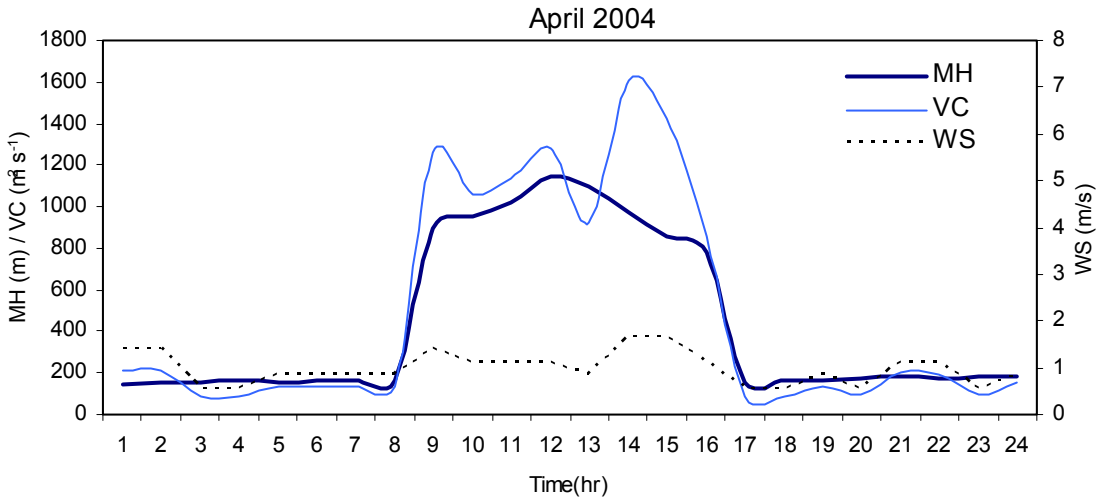
April 2004
MH
VC
WS
MH (m) / VC (m² s⁻¹)
WS (m/s)
Time(hr)

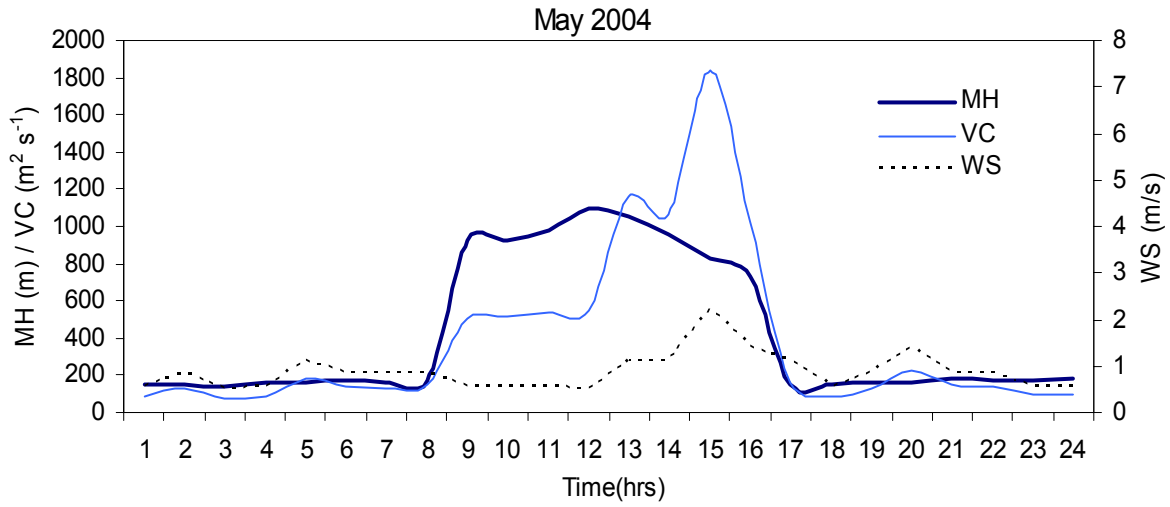
May 2004
MH
VC
WS
MH (m) / VC (m² s⁻¹)
WS (m/s)
Time(hrs)

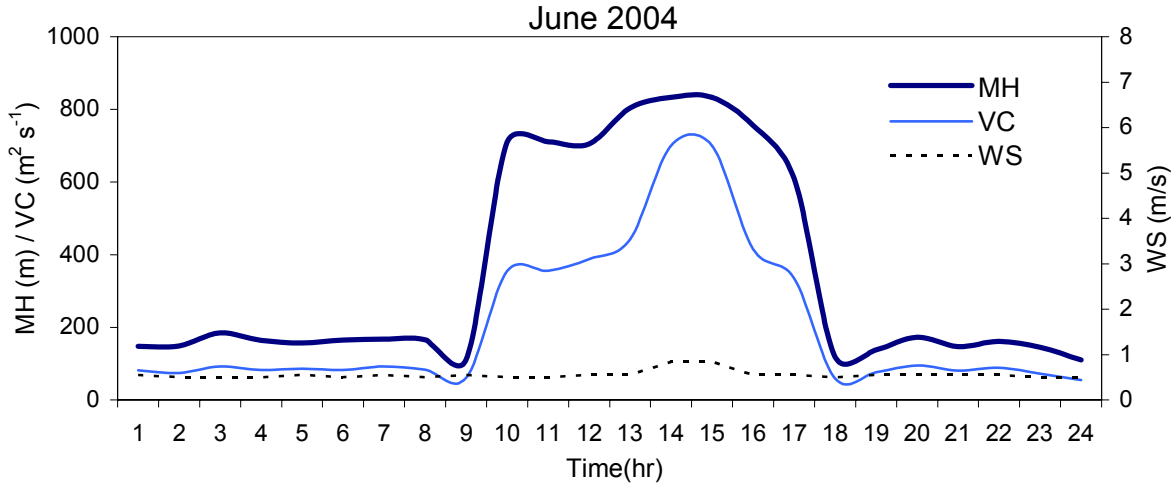
June 2004
MH
VC
WS
MH (m) / VC (m² s⁻¹)
WS (m/s)
Time(hr)

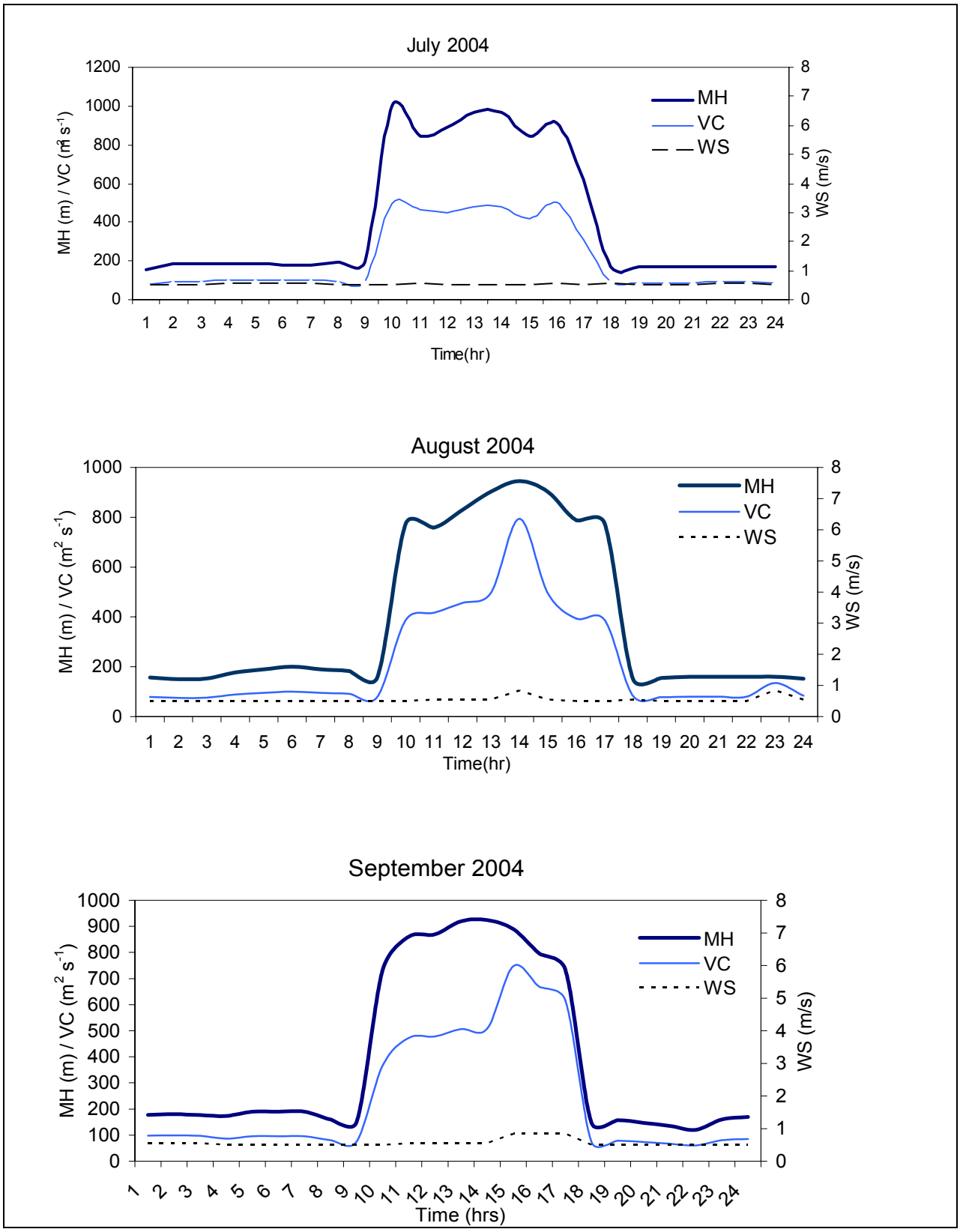

Fig 2.2 Diurnal variation of ventilation coefficient, mixing height & wind speed at Gangtok

CHAPTER - 3
APPROACH II - ASSESSMENT OF POLLUTION POTENTIAL USING AIR

3.1 AIR QUALITY STUDIES USING MODELS

Complicated processes occurring in nature can be described using mathematical models. When a pollution source emits a chemical into the atmosphere at an initial concentration (mass per unit volume of air), the chemical does not remain at that initial concentration. Hence, air pollution modeling can be viewed as the attempt to predict or simulate, by physical or numerical means the ambient concentration of criteria pollutants found within the atmosphere of a domain. Atmospheric processes act to disperse the emissions downwind into less concentrated form. Pollution sources can use dispersion models to show that emission impacts will remain below applicable regulatory standards. Clearly, dispersion model development and application has been largely driven by air quality regulations.

In many instances, a model can provide an acceptable indication of the distribution of a pollutant much more quickly and cheaply than can a monitoring network. Thus air quality models are important tools and can play a crucial role as part of the methodology developed to protect air quality.

To conduct a dispersion modeling analysis, a user enters data in the following four major categories:

Meteorological conditions, such as wind speed, wind direction, stability class, temperature and mixing height; *Emissions parameters*, such as

source location, source height, stack diameter, gas exit velocity, gas exit temperature and emission rate; *Terrain elevations*; and *Building parameters*, such as location, height and width.

3.2 BASELINE ENVIRONMENTAL QUALITY OF AIR

Pure and clean air environment is crucial to healthy living. Various sources of pollution, natural as well as man-made, are responsible for impairing the ambient air quality. While man-made pollution is chiefly the result of modernization, pollution from natural sources is almost inevitable. The sources of air pollution are nearly as numerous as the grains of sand. The preparation of emission inventory is the first step in any air quality study for which we have divided the air pollution sources into the following four major categories:

(1) Vehicular emission sources
(2) Industrial sources
(3) Domestic sources
(4) Power plants

3.2.1 Identification of Air Quality Impacts of a Proposed Project

The major pollutants of our concern are Total Suspended Particulates (TSP), Sulphur Dioxide (SO_2) and Nitrogen Oxides (NOx). The total emissions from different kinds of sources depend upon source configuration, type and amount of fuel used, emission factors,

combustion / burning process rate, and the control devices. The emission factors are obtained from the secondary sources classified by the end-use, type of fuel used and the types of furnace / boiler used in the industries and power plants.

Emission inventory is very important for any air quality study and its preparation for various kinds of sources has to be done category-wise.

Emission factor (Ef) is the average rate at which a pollutant is released into the atmosphere as a result of some activity such as production, divided by the level of that activity. It relates the types and quantities of pollutants emitted to indicators such as production capacity, quantity of fuel burned or vehicle – miles traveled by an automobile.

For conventional air pollutants (such as particulates, CO, HC's and NOx) emission factor information should be readily available.

3.2.2 Compilation of Air Quality Data

The source of information on air quantity monitoring data include the relevant state air pollution agencies and private industries in the area that might be maintaining air quality monitoring programs for their particular interests. Appropriate interpretation of air quality data should include consideration of historical trends as well as information about the monitoring station. Graphical presentation of air quality may be useful.

A common problem in addressing baseline air quality in an area of a proposed project or activity is the absence of data for specific site. One solution is to explore the availability of data from nearby area having similar pollution sources and similar characteristics in term of land usage. The main use of existing air quality data is in determining whether the air quantity exceeds attains or does not comply with relevant standards.

3.2.3 Emission Inventory

An emission inventory provides a summary of the pollutant emission under current condition in the vicinity of the proposed project activity. It should be noted that emission inventories have limitations, since they do not give consideration to atmospheric reactions nor they account for unequal effects of air pollutants on a mass basis. The steps compiling a comprehensive emission inventory are as follows:

i) Classification of all pollutants and sources of emissions in the geographical area being addressed.
ii) Identification and aggregation of information on emission factors for each of the identified pollutants and sources.
iii) Determine the daily quantity of materials handled, processed or burned or unit production information, depending upon the individual identified sources.
iv) Computation of the rate at which each pollutant is emitted to the atmosphere (on Annual Basis).

v) Summation of the specific pollutant emission from each of the identified source category.

Source Inventory should be updated.

3.2.4 Methods of Emission Estimation from Vehicular Traffic

Method 1- This method (Goyal *et al*., 1998) is one of the most common to determine emission rates for line source model. The emission rate of air pollutants on a reasonably straight highway from a continuous line source per unit length, i.e. 'q' (g m^{-1} s^{-1}) can be determined as the product of the emission factor and traffic density

$$TV_{ij}=N_jV_i$$

Where V_i is the speed of the i type vehicle (Km h^{-1}), TV_{ij} is the traffic density of i type vehicle on j type road (vehicles h^{-1}) and N_j is the number of vehicles traveling per unit length of j type of road (vehicles Km^{-1}).

$$Q_{ij}= TV_{ij}e_i$$

Where $q_{i,j}$ is the source strength per unit length (g $m^{-1}s^{-1}$) and e_i is the emission factor of vehicle type i (g km^{-1} $vehicle^{-1}$).

Method II- This method has been used by Singh *et al*. (1990). Three types of roads namely arterial, feeder and residential, based on traffic load have been considered in this method.

Let R^i_a, R^i_f and R^i_r be the lengths of the arterial, feeder and residential roads types in the *i*th city grid and V^i_a, V^i_f and V^i_r be the

volume of traffic on these roads per day. The total Vehicle Kilometer Travel (VKT) in the $_i$th city grid is given by:

$$V^i_T = R^i_a V^i_a + R^i_f V^i_f + R^i_r V^i_r$$

The VKT is the averaged value of different types of vehicles (LTV, MTV and HTV) traveled per km. If the total emission of NO_2 is E_t (g day^{-1}), the NO_2 source strength day^{-1} in grid i is given by

$$E_i = \frac{E_t V_T^i}{\sum_i V_T^i}$$

where $\sum_i V_T^i$ is the total traffic volume of city. The road length within each grid has been obtained from and relative volume of traffic flow per day has been adopted according to Hammerle (1976), and Srinivasan *et al*. (1973).

If e(t) is the city wide emission at time t, the city wide pollutant emission for the whole day is given by-

$$E_t = \int_{day} e(t)\,dt$$

But e(t) is proportional to traffic volume V(t) at time t. Thus knowing the diurnal traffic pattern, the diurnal pattern of emission can be obtained giving the source strength Q_i in the *i*th grid as a function of time in units of g m^{-2}.

3.3 MODEL DESCRIPTION

CALINE-3 is a third generation line source air quality model developed by the California Department of Transportation (Benson,

1979). It is based on the Gaussian diffusion equation and employs a mixing zone concept to characterize pollutant dispersion over the roadway.

The purpose of the model is to assess air quality impacts near transportation facilities in what is known as the microscale region. Given source strength, meteorology, site geometry, and site characteristics, the model can reliably predict pollutant concentrations for receptors located within 150 meters of the roadway.

Gaussian Element Formulation of CALINE-3 divides individual highway links into a series of elements from which incremental concentrations are computed and then summed to form a total concentration estimate for a particular receptor.

The receptor distance is measured along a perpendicular from the receptor to the highway centerline. The lengths of subsequent elements are described by the following formula:

$$EL = W*BASE\ (NE-1)$$

Where, EL = Element Length

W = Highway Width

NE = Element Number

BASE = Element Growth Factor

PHI<20°, BASE=1.1

20°≤PHI<50°, BASE=1.5

50°≤PHI<70°, BASE=2.0

70°≤PHI, BASE=4.0

Where, PHI = the angle between the wind direction and the direction of the roadway. (Note: Capitalized variables shown in text are identical to those used in the computer coding.)

Each element is modeled as an "equivalent" finite line source (EFLS) positioned normal to the wind direction and centered at the element midpoint. A local x-y coordinate system aligned with the wind direction and originating at the element midpoint is defined for each element. The emissions occurring within an element are assumed to be released along the EFLS representing the element. The emissions are then assumed to disperse in a Gaussian manner downwind from the element. The length and orientation of the EFLS are functions of the element size and the angle (PHI, φ) between the average wind direction and highway alignment. Values of PHI=0 or PHI=90 degrees are altered within the program an insignificant amount to avoid division by zero during the EFLS trigonometric computations.

IITLS model is a simple Gaussian type line source model (Wark and Warner, 1981). The model formulation is given by:

$$C(x,0)=\frac{2q}{(2\pi)^{\frac{1}{2}}\,\sigma_z\,u}\exp\left[-\frac{1}{2}\left(\frac{H^2}{\sigma_z}\right)\right] \qquad (1)$$

where

q is the pollutant emission rate per unit length of the road (g m^{-1} s^{-1}),

u is the mean wind (m s^{-1}),

h is the height of the source (m),

σ_z is the vertical dispersion parameter (m) and

C is the concentration of air pollutants at downwind distance x when wind is normal to the line source.

The IITLS model developed by Goyal *et al*. (1995) has further modified for dispersion parameter (σ_z) and source strength (q) as follows.

Dispersion Parameter (σz): A combination of two dispersion parameters is found to be more suitable for dispersion of pollutants from vehicular traffic.

The dispersion parameter may be written as

$$\sigma_z = \sigma_{z0}^2 + \sigma_{zb}^2 \qquad (2)$$

where σ_{zo} is the initial dispersion parameter due to vehicular movement, which has been chosen up to a downwind distance of 500 m and σ_{zb} is the dispersion parameter, applicable beyond 500 m downwind from the source. The value of σ_{zo} has been assumed as 20% of height of mixing in the initial dispersion of pollutants. This assumption has been made by following the other studies of (Okamoto and Shiozawa, 1978 and Kono and Ito, 1990). The value of σ_{zb} has been determined from Brigg's (1973) urban formulae.

3.4 NORTH SIKKIM

3.4.1 Study Area: Chungthang and its Surrounding Areas

Situated in the North district (Fig. 3.1) of Sikkim about 109 km from the Capital town of Gangtok, surrounded by huge hills and lying along the side of the Teesta river is the small idyllic settlement of Chungthang

valley. It has an area of approximately (15 x 18) km^2. Light petrol driven vehicles can go up to Mangan, the headquarters of the northern district, about 79 km from Gangtok. There is a gradual increase in the steepness of the hills as we move northwards from Gangtok and the terrain gets complex with a number of waterfalls along the way. Due to the steep, narrow and highly uphill nature of the roads, only heavy diesel driven vehicles can ply after Mangan. With the exception of Mangan there are only few villages namely Kodyorg, Myang and Thang and the population is very scanty. After about 1km from Chungthang, the Teesta branches off into two tributaries. Being on the border between India and China, there is a huge army camp in Chungthang.

The total population of Chungthang is about 3000 and the civilians are only about half in number. The residents are mostly Bhutias and Nepalese and a few business community people from other parts of the country. The people are very warm, hospitable and live in harmony. They preserve their culture and do not encourage people from outside to settle because of the fear that they their culture might be invaded.

The prominent problems are- there is no proper medical facility. The government only provides rice and their main source of income is from Cardamom cultivation.

From the 2nd week of May to the 3rd week of September, due to heavy rainfall and landslides, the roads get blocked and Chungthang gets virtually cut off from the rest of the state. During this period the problem of electricity and water worsens. Communications also get

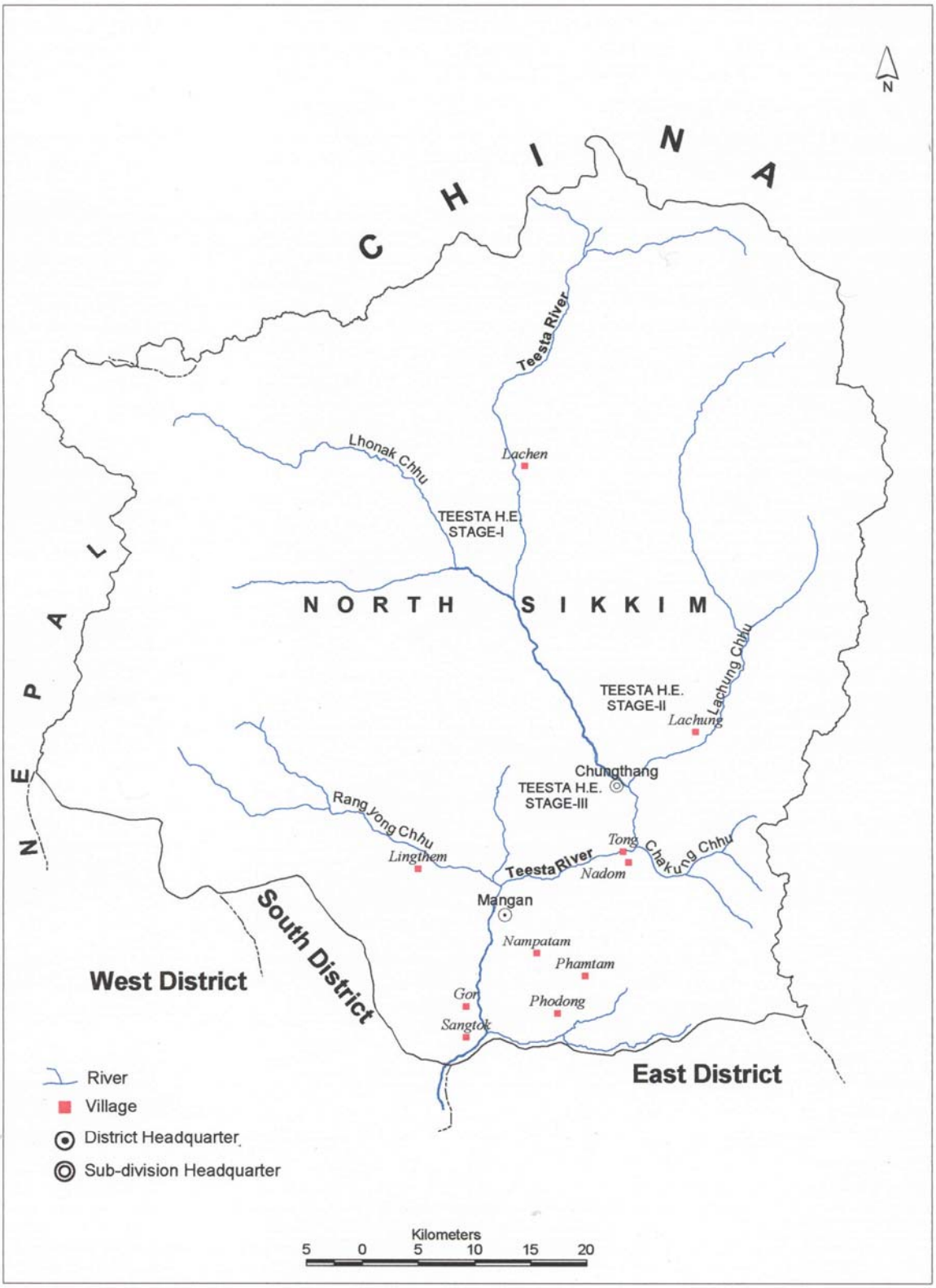

Fig.3.1 Map showing North Sikkim district

disturbed during this period. The food and vegetables also become very expensive. Another major problem is the household fuel. There are only 60 L.P.G connections and a maximum of 120-130 LPG cylinders in the entire area. Only the financially better placed people can afford to use them. LPG cylinders have to be brought and refilled from Gangtok. Due to this the transportation charges are very high and a normal cylinder costs them nearly Rs.350. The transportation of cylinder from Gangtok to Chungthang also becomes very difficult. As a result the people rely entirely on firewood.

The Army however, has proved to be a very big boon to the people in Chungthang. They help the locals for all purposes e.g., free medicines, food and other daily essentials are provided by the army.

3.4.2 Sources of Air Pollution in the Region

The hilly and mountainous nature of the terrain and Sikkim's positioning in relation to the Bay of Bengal, the Teesta valley around this region receives intense rainfall. Landslides are very common here which accounts for the low population in these areas. A lot of clearing work also goes in these regions. Hence major air pollutants are the suspended particulate matter (SPM) which include, dust, both fine and coarse. The heavy diesel driven army vehicles and also other vehicles (around 20-30 in the normal season and 40-50 in the tourist season) emit Nitrogen Oxide, Carbon Monoxide (CO), particulate matter and volatile organic compounds. The high combustion in the diesel engines

provides a temperature which encourages the combustion of atmospheric Nitrogen and Oxygen into Oxides of Nitrogen which are very harmful. SOx and NOx can result in acid formation when they react with rain water. Both wet and dry deposition of SO_2 damages vegetation degrades soils, building materials and water course.

There is also a considerable amount of indoor air pollution in Chungthang which is mostly because of the heavy use of firewood which emit SPM, CO and Sulfur compounds. These pollutants can cause health hazards ranging from simple eye, nose, and throat irritation to severe diseases like cancer and heart problems as CO reduces the oxygen carrying capacity of the blood. This problem becomes even more severe in the winters because at this time, to beat the severe cold, the army people and also the civilians use a lot of charcoal which emits a lot of CO and sulfur compounds. Owing to the geographical nature of the place, the high mountains and hills prevent the escape of pollutants as a result of which they tend to accumulate near the ground level. This causes a lot of air pollution and high concentration of air pollutants at the ground level.

3.4.3 Emission Inventory of Chungthang

A study of Chungthang region revealed that pollution is caused mostly by the vehicles whose number increases in the tourist season. A significant contribution in the winter season is made by the domestic burning of firewood and coal. In the present study, emission of SPM,

NOx and SOx have been calculated by using the daily traffic volume in Chungthang and its surrounding regions. The problem has been modeled as a- continuous emitting finite Line Source while, the contribution of domestic fuel burning to pollution has been estimated by using an area source model.

3.4.4 Emission of Line Source

A gridded source inventory has been developed over an area of (15 x 18) km^2 as shown in Fig. 3.2 below. The area has been divided into grids of size (3.8 x 3) km^2. Five sources have been considered at places Kodyorg, Long Nadom, Theng, Chhateng and Chungthang. Three receptors have been considered at Myang, Ningla and a region around 2 km radius of Chunghtang.

The emission rate of air pollutants in this study has been determined using method I (Table 3.1).

Table 3.1 Emission rate of air pollutants

Type of vehicle	Emission factors (g veh^{-1} km)		
	SO_2	SPM	NO_x
Petrol driven cars (MTV)	0.08	0.33	3.20
Diesel-driven cars (MTV)	0.39	2.00	0.99
Heavy duty vehicles (HTV)	1.50	3.00	21.00

In this study only two types of vehicles have been considered: the heavy duty diesel driven vehicles (army vehicles) and the medium type diesel driven cars which are commonly known as “Pejos” in the region. Over the study area of (15 x 18) km^2, the vehicles have been assumed to travel an average distance of 25 km daily. On the average a total of 25 vehicles travel during the normal season and around 40 vehicles travel during the tourist season. The average speed of the heavy duty vehicles is assumed to be 20 km/hr and that of the medium type vehicles as 25 km/ hr. The source strength of the pollutants due to vehicular emissions in Chungthang is estimated as given in Table 3.2.

Table 3.2 Source Strength of Pollutants

Pollutant	Source Strength ($\mu g\ m^{-1}\ s^{-1}$)
SPM	23.328
NO_X	54.1992
SO_X	6.584

3.4.5 Emission of Area source

The amount of charcoal and firewood used in Chungthang has been estimated from the total amount extracted and sold in Sikkim in the year 2000-2001 (total charcoal is about 8575 kg and firewood is 84000 kg), based on the population of Chungthang (about 3000). Since the firewood used in Chungthang is obtained from unauthorized sources (directly from the forests) a record of its percentage is not available.

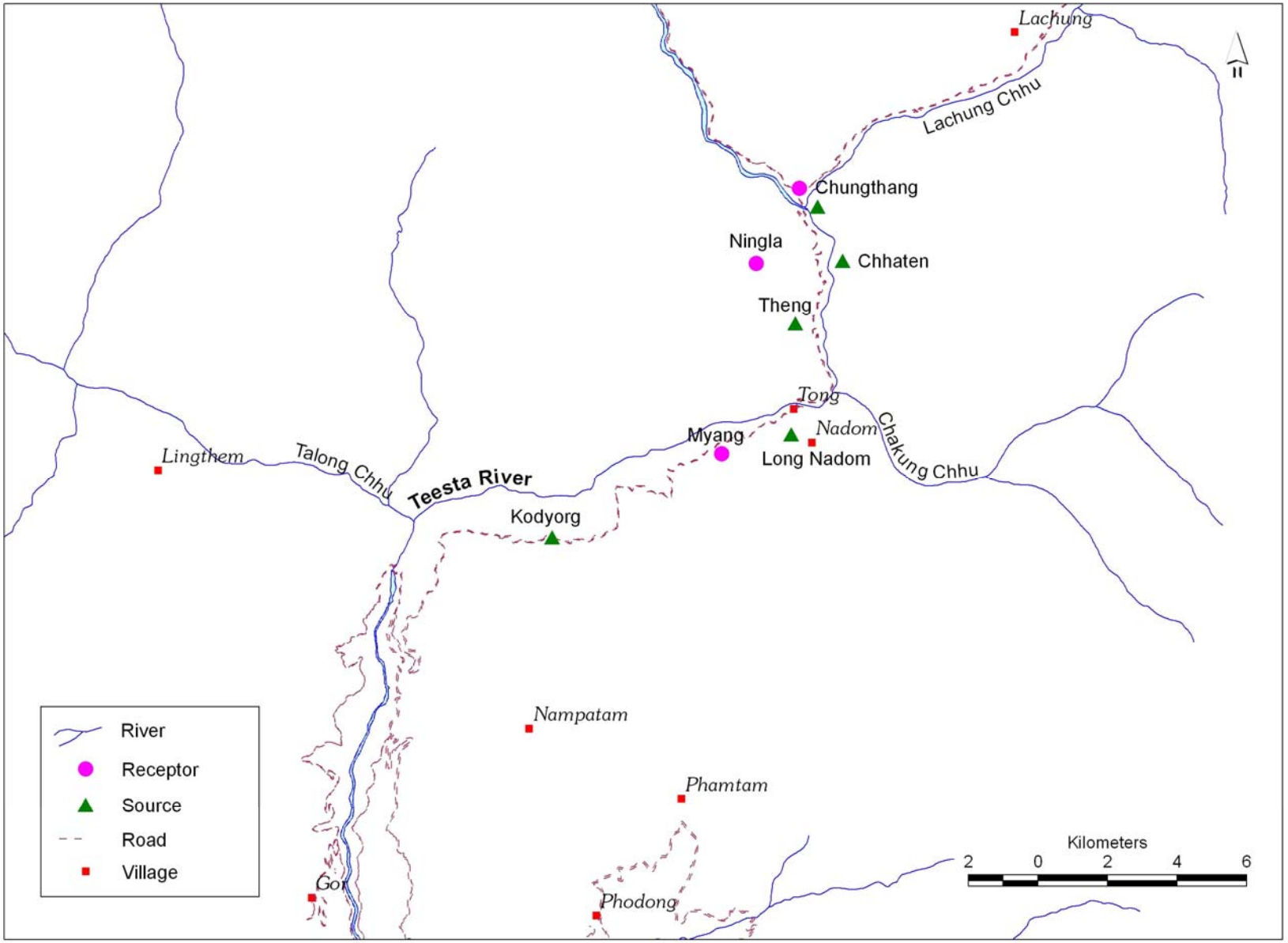

Fig.3.2 Gridded source inventory of North Sikkim region

Hence the actual amount of firewood used in the region may be much more than the estimated value in our study.

3.4.6 Results

The IIT Line and Area source models were used to calculate the concentration of three major pollutants namely suspended particulate matter (SPM), Oxides of Nitrogen (NO_X) and Oxides of Sulfur (SO_X) for the month of April 2002, since this is the month most frequented by the tourists. The values have been averaged over a period of 5 days. The concentration of SPM, SO_X and NO_X in $\mu g\ m^{-3}$ estimated by the IIT Line source model at three receptor points, Myang, Ningla and the region near Chungthang is shown below in Fig. 3.3.

From the above figure, it is evident that concentration of NOx is maximum at all the receptor points. This is justified as the diesel run vehicles provide a temperature high enough for the atmospheric Nitrogen and Oxygen to combine and form NO_X. The result also points to the dominance of vehicular pollution in the region. The low concentration of SO_X at all the receptor points is because of the absence of any industries (in particular, the power plants). The SPM values are also quite comparable with the NO_X due to the use of diesel vehicles.

The emission from domestic burning of charcoal and firewood was found to be of negligible i.e. 14.6 $\mu g\ s^{-1}$. As a result the concentration calculated by the IIT Area source model was very small i.e. negligible and has therefore not been considered here.

3.4.7 Conclusions

In Chungthang, normally calm winds i.e. wind speeds ≤ 1 m/s occur frequently. As a result the pollutants tend to remain near the ground level only which is an unfavorable condition for dispersal of pollutants at Chungthang. However, the air quality at different places in and near Chungthang is within standards as the number of vehicles is quite low.

3.5 SOUTH AND EAST REGIONS OF SIKKIM

3.5.1 Emission Inventory

Fig. 3.4 shows the South and East region of Sikkim. A gridded source inventory has been developed over an area of (56 x 34) km^2 covering South-East region of Sikkim as shown in Fig. 3.5. The area has been divided into 200 grids of size (2.8 x 3.4) Km^2. The thirteen vulnerable points (receptors) of the east and south regions are Gangtok, Singtam, Rangpo, Rangli, Dikchu, Phodong, Chhangu, Kupup (East district) and Melli Bazar, Damthang, Namchi, Rabangla, Jorethang (South district).

3.5.2 Results

Fig. 3.6 gives the spatial variation of pollutant concentration in East and South region of Sikkim using Caline-3 model. The figure shows that Singtam is the place with the highest concentration (142.35 $\mu g/m^3$) of

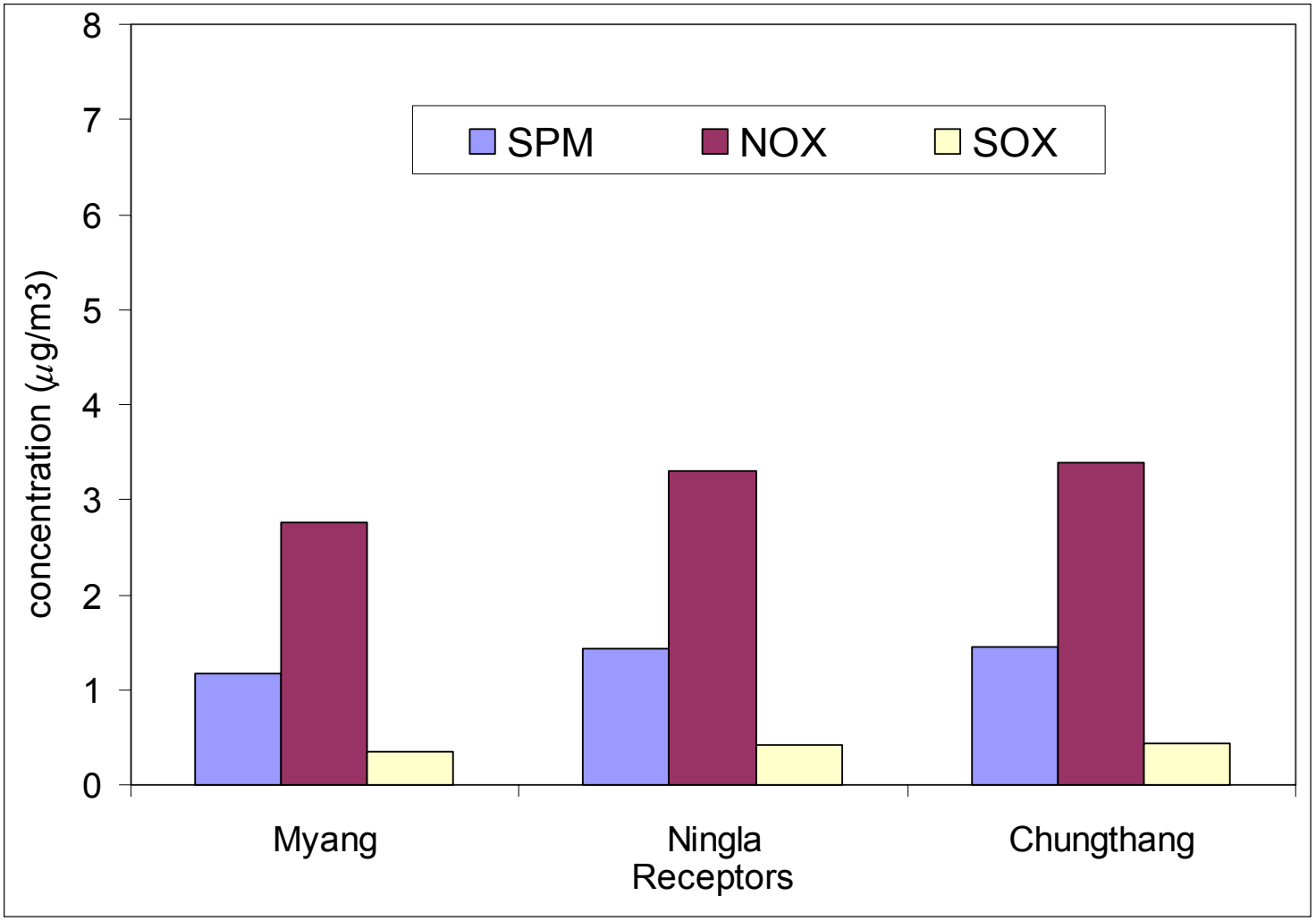

Fig 3.3 Spatial variation of pollutants in North Sikkim

Fig.3.4 Map showing South and East Sikkim districts

Scale-

x-axis: 1unit = 1.4 cms

y-axis: 1unit = 1.7 cms

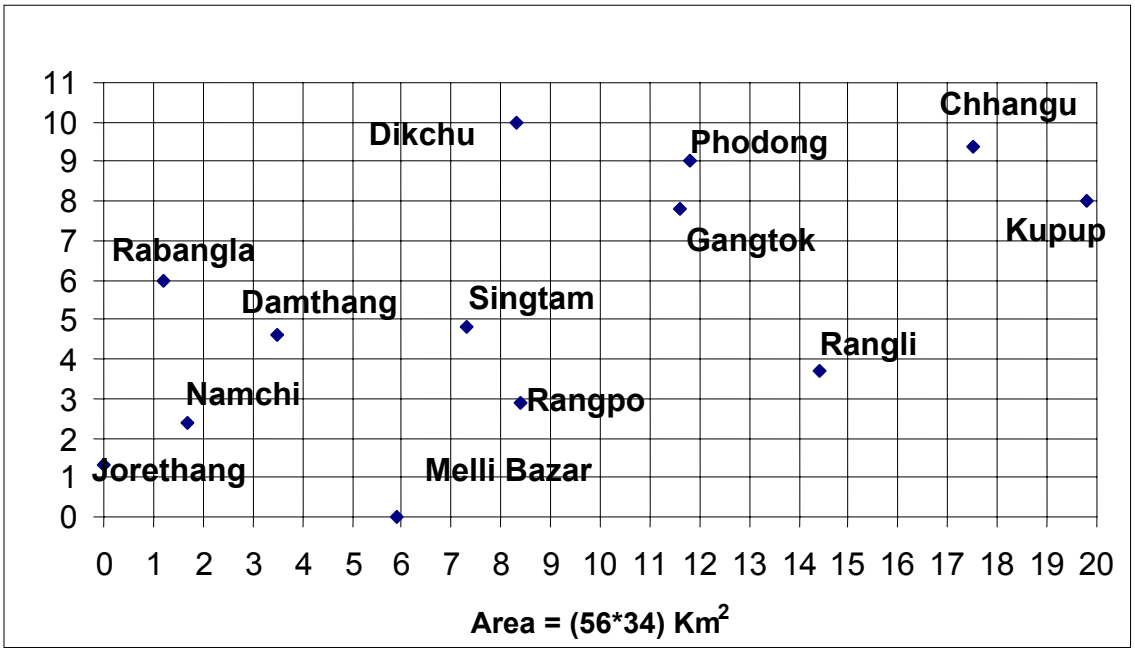

Fig 3.5 Gridded source inventory covering South-East region of Sikkim

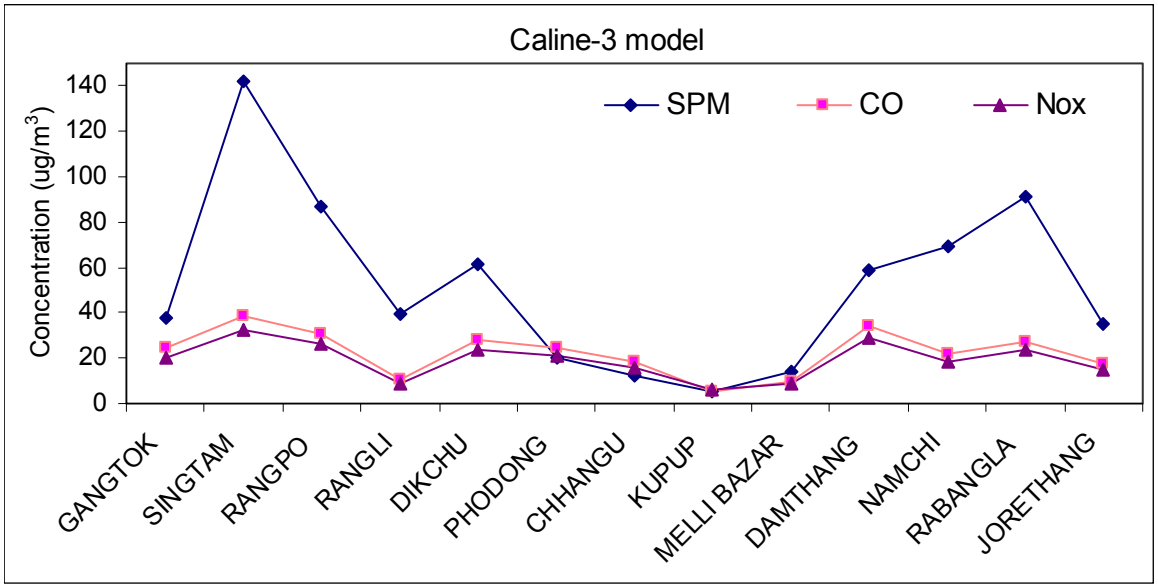

Fig 3.6 Concentration of pollutants in East and South region of Sikkim (Caline-3)

SPM followed by Rabangla (91.53 $\mu g/m^3$), Rangpo (86.81 $\mu g/m^3$) and Namchi (69.24 $\mu g/m^3$) while Kupup (6.9 $\mu g/m^3$) has the lowest SPM concentration. Similar trend can be seen for both CO and NOx. The maximum CO concentration is observed at Singtam (38.45 $\mu g/m^3$) and minimum at Kupup (6.95 $\mu g/m^3$). The maximum NOx concentration at Singtam is (32.6 $\mu g/m^3$) while (5.49 $\mu g/m^3$) at Kupup. At all the other places, the concentration is not very significant. Similarly Fig. 3.7 gives the variation of pollutant concentration in East and South region of Sikkim by using IITLS model. The maximum concentration of SPM (57.38 $\mu g/m^3$) is observed at Singtam followed by Melli Bazar (47.37 $\mu g/m^3$), Rangli (45.13 $\mu g/m^3$) and Rangpo (44.47 $\mu g/m^3$) while Jorethang (36.96 $\mu g/m^3$) has the lowest SPM concentration. The similar trend can be seen for both CO and NOx. The maximum CO concentration is observed at Singtam (29.96 $\mu g/m^3$) and minimum at Jorethang (20.74 $\mu g/m^3$). The maximum NOx concentration at Singtam is (13.94 $\mu g/m3$) while a minimum of (5.69 $\mu g/m3$) is observed at Jorethang. The concentration at Singtam, Rangpo, Melli Bazar and Namchi are high due to the commercial activities.

Similarly Fig. 3.8 shows the temporal variation in East and South region of Sikkim by using Caline-3 model which reveals that the maximum values of the pollutants are at Rangpo in the late evening hours (19 hrs). The IITLS model also predicts a similar trend for all the pollutants in Fig. 3.9, which reveals that evening (19^{th} hour) is the time when most of the carbon monoxide is emitted in the atmosphere and Rangpo is the place having the highest concentration (46.1 $\mu g/m^3$)

followed very closely by Gangtok (40.5 $\mu g/m^3$) and Damthang (39.9 $\mu g/m^3$). At all the other places and at all times the concentration is not very significant. Similarly the maximum concentration of NOx (37 $\mu g/m^3$) is at Rangpo followed by Gangtok (32.5 $\mu g/m^3$) and Dikchu (28.6 $\mu g/m^3$). This peak value is also attained in the evening. The SPM values are however quite low in comparison with CO and NOx but the trend of NOx and SPM are almost the same. The maximum concentration for SPM are again at Rangpo (4.6 $\mu g/m^3$), Gangtok (4.1 $\mu g/m^3$) in 19th hour and Dikchu (3.6 $\mu g/m^3$) in 23rd hour.

The most prominent reason for the above observed trend is the meteorology. During day time because of convective mixing dispersion takes place, while during evening the low mixing height, low wind speed and decreased convective activity of the atmosphere results in increased concentration. The concentration at Rangpo, Gangtok, Dikchu and Damthang indicate their prominence with respect to their commercial location. The above result and discussion reveal that concentration of pollutants or pollution potential due to various sources of pollutants in East and South regions of Sikkim are well within the NAAQS of SPM, CO and NOx.

3.6 GANGTOK

3.6.1 Emission Inventory

A gridded source inventory has been developed over an area of (3.64 x 4.16) km^2 of Gangtok city as shown in Fig. 3.10. The area has

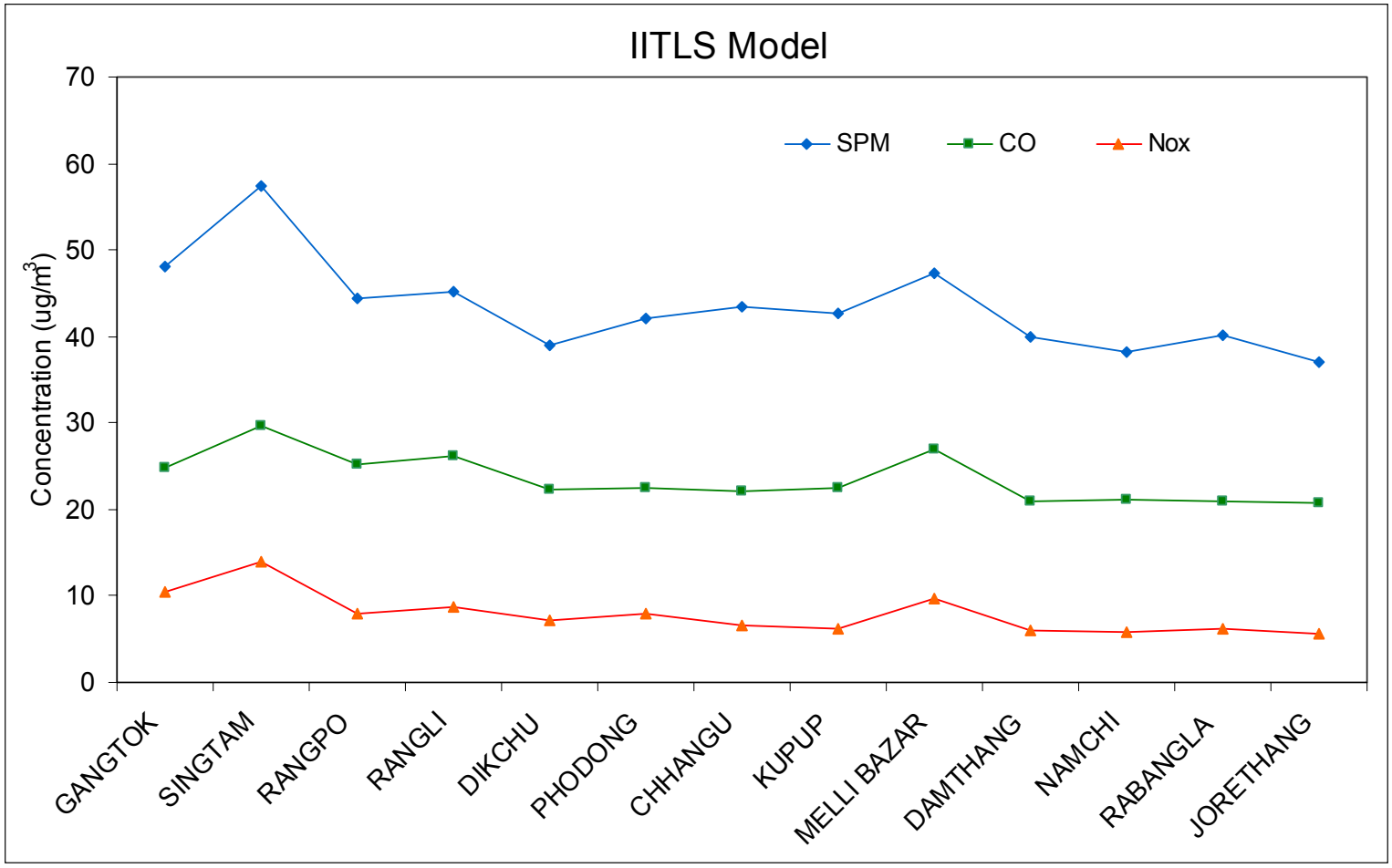

Fig 3.7 Variation of concentration of pollutant in East and South region of Sikkim by using IITLS model

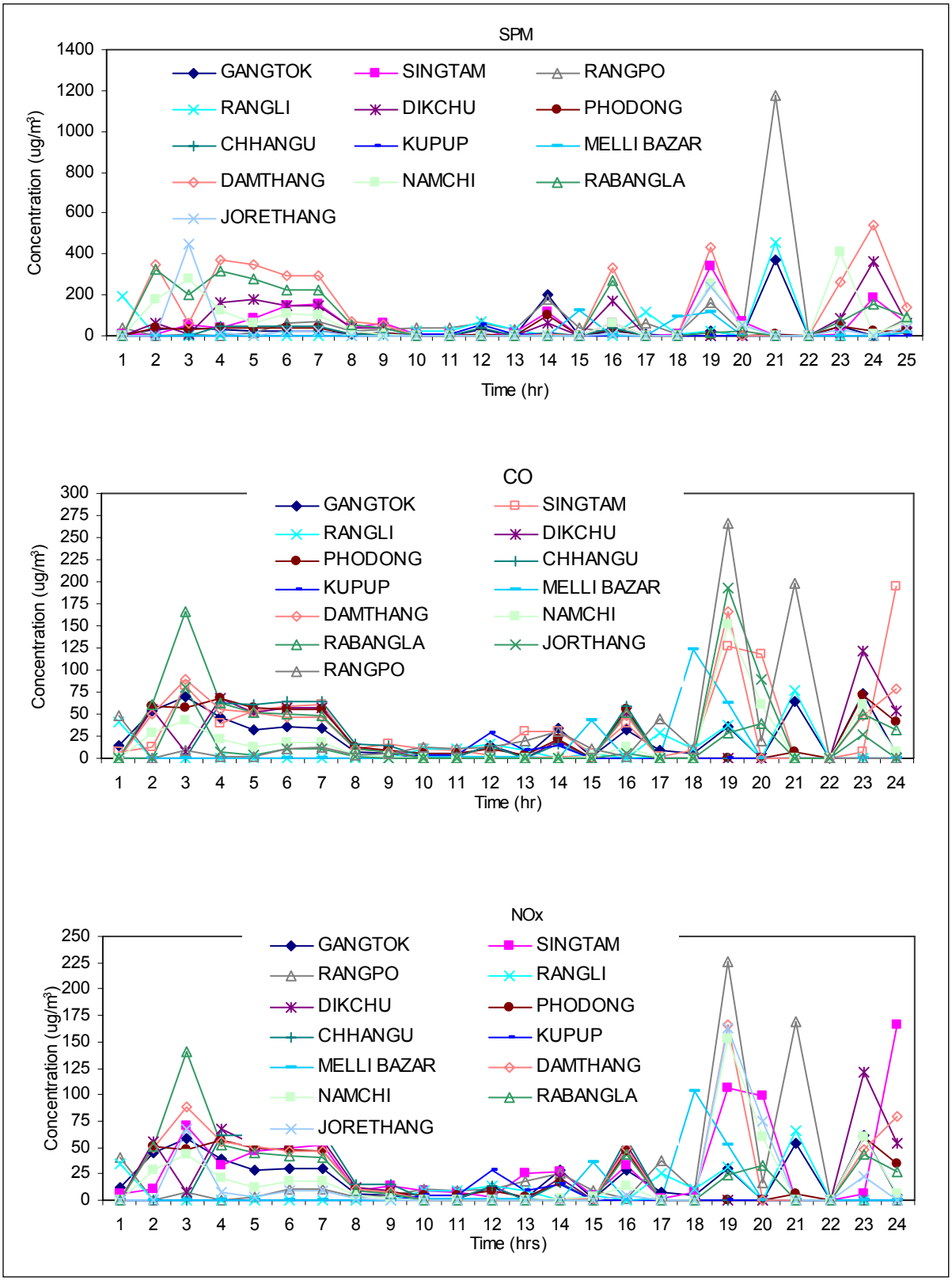

Fig 3.8 Temporal variations of pollutants for East and South Sikkim (Caline-3)

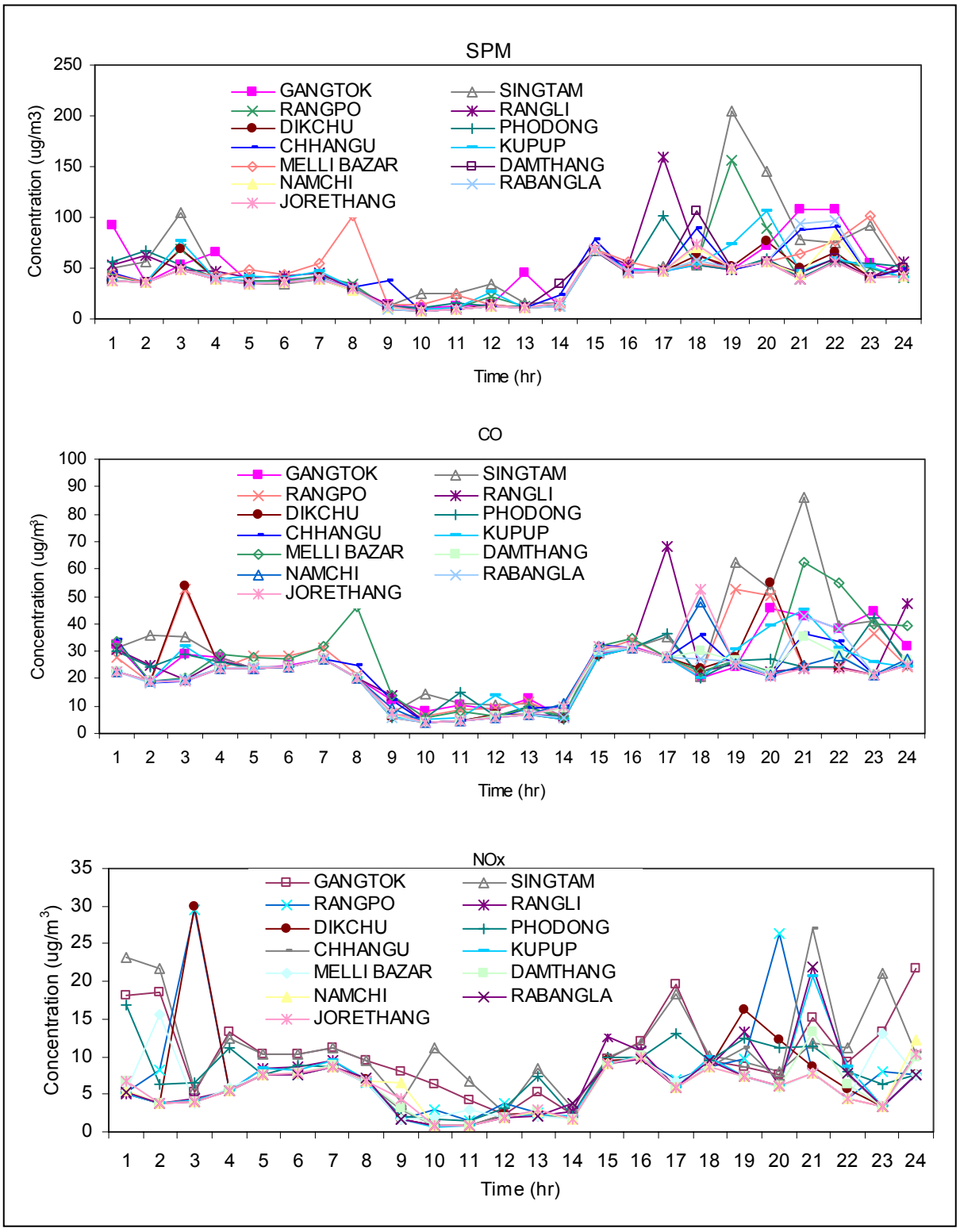

Fig 3.9 Temporal variations of pollutants for East and South Sikkim (IITLS)

been divided into 225 grids of size (0.26 x 0.26) km^2. The locations of six vulnerable points (receptors) of the region namely Metro Point, Deorali, Hospital Point, Indira Bypass, Tadong and Zero Point and the roads (links) connecting them are shown in Fig 3.10. In Gangtok, the number of vehicles increases remarkably in the tourist season and the problem become worst during winter. After analyzing the emissions from various sources, it has been felt that vehicles are the major source of pollution, since there is no major industry in this region. However, due to the absence of observed CO data the study has been done only for SO_2, SPM and NOx.

The emission rate of air pollutants were determined using method-I and the emission factor (g km^{-1} $vehicle^{-1}$) is obtained from IIP (1994) as given in Table-3.6. The emission from automobiles depends not only on the number of vehicles on road but also augmented more intensely due to traffic congestion, driving habits, maintenance and age of vehicles. The increases in the number of vehicles have contributed to increased level of pollution. The number of vehicles registered with Motor Vehicle Division, Gangtok was 6,495 in 1994; 19,014 in 2000; 24,462 in 2002 and 26,035 in 2004 (Fig. 3.11). The vehicles include private cars, taxis, two wheelers, buses and contract carriages. The number of vehicles has increased almost 5 times in just 10 years. Apart from this, there exist thousands of vehicles of Border Road Organization, military forces etc. which is not registered with motor vehicles division. Plenty of vehicles from nearby places like Kalimpong, Darjeeling, Siliguri, New Jalpaiguri, Jaigaon, etc., enter and exit from the town daily. Over the study area

(Gangtok), these vehicles have been assumed to travel an average distance of 25 km daily. On the average a total of 2000 vehicles travel during the normal season and around 2500 vehicles travel during the tourist season. The average speed of the heavy and medium type vehicles is assumed to be 25 km/ hr^{-1} and 30 km/ hr^{-1} respectively. The data obtained from different points during peak hour and non-peak hours is shown in Tables 3.3 and 3.4. This data has been used to estimate the emissions and the traffic density from vehicular sources for all 24 hours in the model. The four monitoring sites in the table witness the maximum number of vehicles in the city. Hence, the frequency of vehicles at these sites is used to estimate the total number of vehicles traveling in and around these sites.

Table 3.3 Vehicular traffic at 4 different points in Gangtok during peak hour (0930– 1030 hrs)

Points	Types of Vehicles	Days of Observation							Mean ± SE
		1st	2nd	3rd	4th	5th	6th	7th	
Zero Point	Two wheeler	18	13	20	17	10	13	17	15± 1
	Light Vehicle	523	521	525	540	526	510	533	525 ± 3
	Medium Vehicle	09	11	09	09	09	10	06	9 ± 1
Hospital Point	Two wheeler	30	23	27	35	33	28	21	28 ± 2
	Light Vehicle	650	629	618	641	622	630	627	631 ± 3.9
	Medium Vehicle	15	17	14	15	12	16	08	14 ± 1.1
Metro Point	Two wheeler	27	34	31	29	38	31	25	31 ± 2
	Light Vehicle	634	628	645	654	641	610	598	630 ± 7
	Medium Vehicle	13	10	10	08	14	12	08	11 ± 1

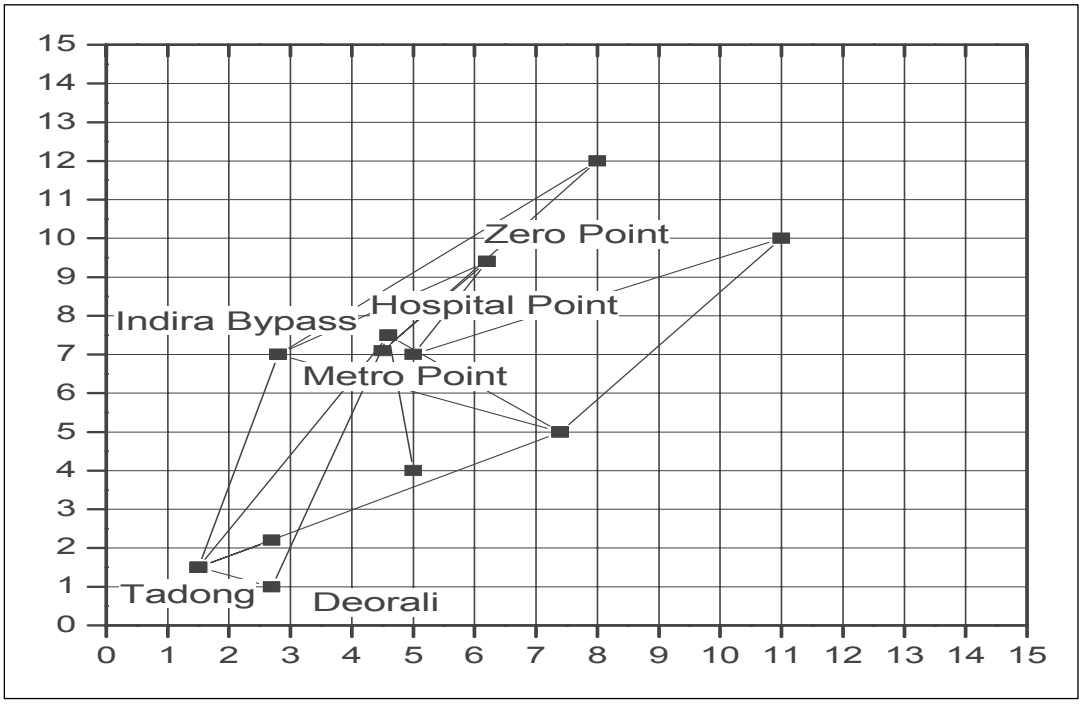

Fig 3.10 Gridded source inventory of Gangtok

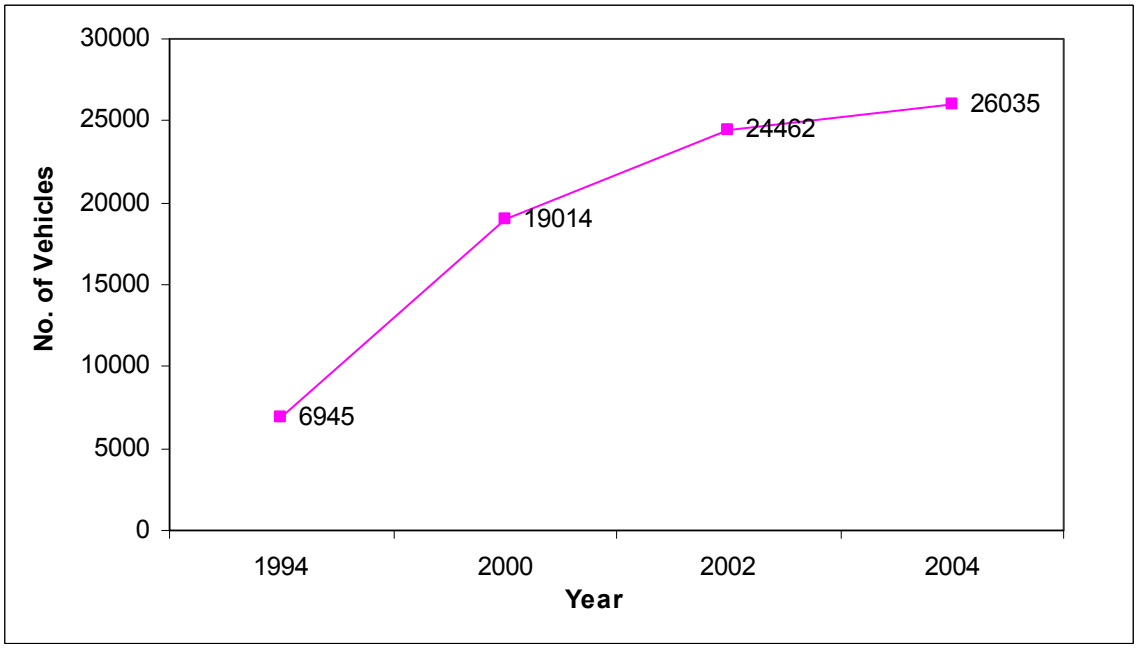

Fig. 3.11 Graph showing increase in the no. of vehicles from 1994 to 2004

Indira Bye	Two wheeler	25	26	21	30	29	27	20	25 ± 1
Pass (NH31A)	Light Vehicle	635	641	620	629	642	615	628	630 ± 4
	Medium Vehicle	16	12	12	15	10	16	16	14 ± 1

Table 3.4 Vehicular traffic at 4 different points in Gangtok during non-peak hour (1300–1400 hrs)

Points	**Types of Vehicles**	**Days of Observation**							**Mean ± SE**
		1st	2nd	3rd	4th	5th	6th	7th	
Zero Point	Two wheeler	07	07	09	05	09	05	05	7 ± 1
	Light Vehicle	201	219	205	207	197	182	182	199 ± 5
	Medium Vehicle	01	03	03	05	05	03	00	3 ± 1
Hospital Point	Two wheeler	12	10	13	13	15	11	14	13 ± 1
	Light Vehicle	299	324	305	297	311	314	421	324 ± 15
	Medium Vehicle	13	11	16	12	12	13	05	12 ± 1
Metro Point	Two wheeler	15	13	16	13	17	12	19	15 ± 1
	Light Vehicle	331	325	298	312	325	301	419	330 ± 14
	Medium Vehicle	13	16	13	12	14	11	04	12 ± 1
Indira Bye	Two wheeler	16	12	10	13	12	18	25	15 ± 2
Pass (NH31A)	Light Vehicle	428	399	411	434	387	405	300	395 ± 16
	Medium Vehicle	06	08	08	10	07	05	05	7 ± 1

3.6.2 Results

Assimilative capacity of air environment of Gangtok has been analyzed for four seasons. But in the present study, two seasons namelyinter and summer have been shown to limit the study to a manageable size. In the modeling approach, the pollution potential is estimated using Caline-3 and IIT Line Source model as vehicular traffic is the major sources of pollution. Fig. 3.12 (a-c) illustrates the

comparison of annually averaged SO_2, SPM and NOx concentration values obtained from Caline-3 and IITLS models and observed data for the year 2003 at Gangtok. Both the models use the same meteorological, emissions and receptor data for this purpose. Both models are used to compute monthly pollutant concentrations using monthly meteorological data at 6 receptors in both the seasons. It is observed that the computed concentrations obtained from IITLS are close to observed values whereas Caline-3 is found to be under-predicting these values (Fig. 3.12a). The SO_2 concentrations obtained by both the models are found to be reasonably in good agreement with observed values at almost all the receptor points except for the over-prediction by IITLS at Zero Point, whereas the SPM prediction by both models are under-predicting the observed concentrations especially at Metro Point and Indira Bypass (Fig. 3.12b). The NOx prediction by IITLS (Fig. 3.12c) is also quite close to the observed values except at Zero Point whereas Caline-3 over-predicts the observed values at most of the places. The trend followed by both the models is nearly the same as the observed values except at Indira Bypass and Zero Point. The reason may be unavailability of accurate emission data at these places. From the above results it is observed that the concentrations predicted by both models are reasonably in good agreement with the observed values. However, IITLS model is performing better than the Caline-3 model. This may be because of the fact that SO_2 is a major pollutant from industrial emissions whereas NOx are the major pollutants emitted by vehicular or mobile sources. In the present study only the influence of vehicular sources is considered

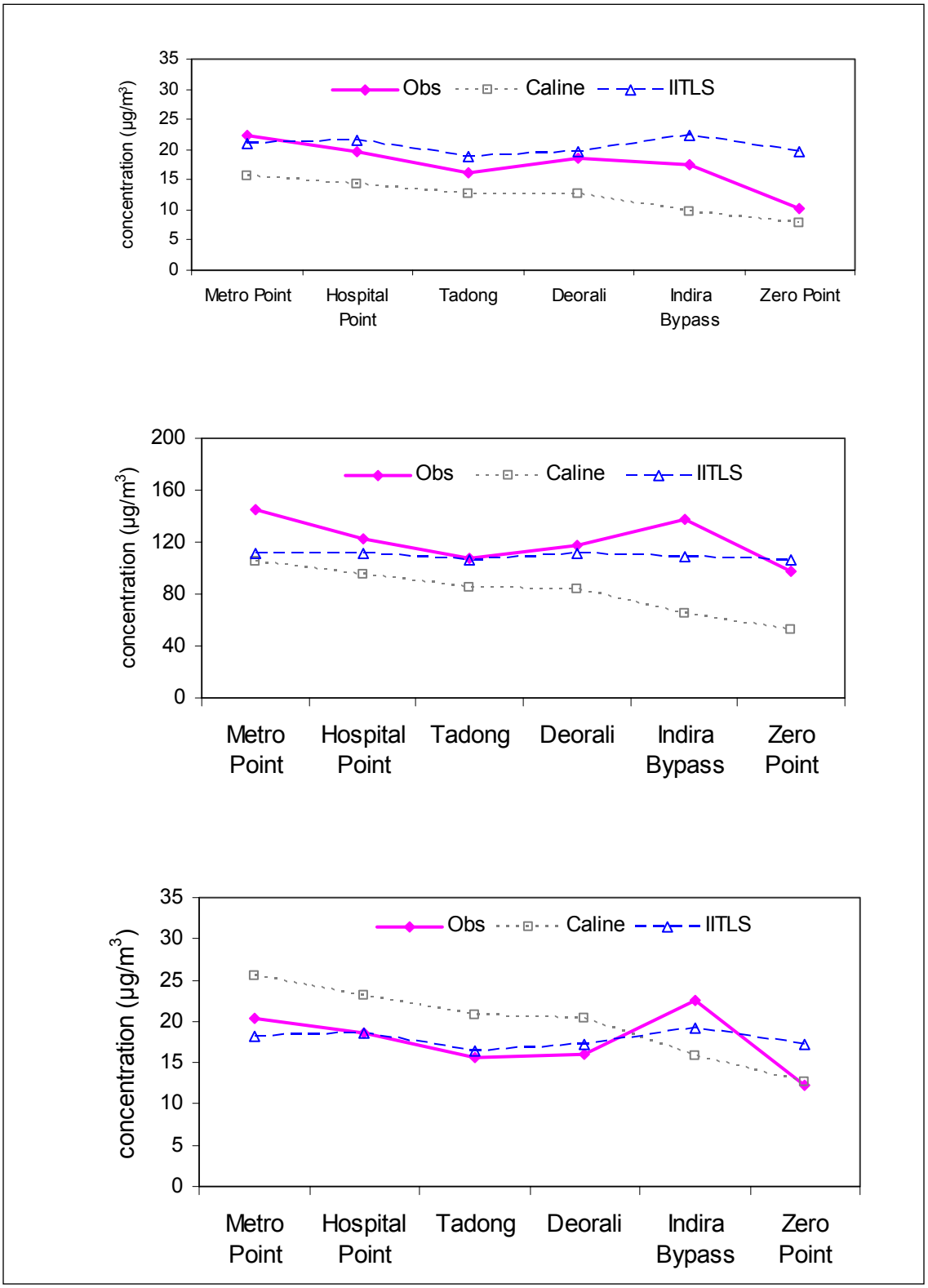

Fig 3.12 Comparison of model evaluated concentration with the observed values

without taking the emissions from the industrial sources as no major industry is present in the study area. The emission inventory for vehicular sources is based upon secondary data indicating that there is a high possibility of approximations in the emissions data which is reflected in the predictions by the models (Table 3.5). The models' validation has been carried out computing several statistical errors *viz*. correlation coefficient (r^2), normalized mean square error (NMSE), factor of two (FA2), fractional bias (FB), fractional variance and index of agreement (IOA). The numerical values of statistical errors are given in Table 3.6. The values of NMSE suggest that IITLS is performing better than Caline-3 model. The NMSE gives information on the strengths of deviations and not on the over or under-prediction thus, always giving positive values. From the values of FA_2, it is seen that IITLS slightly over-predicts the SO_2 and NOx concentrations while it under-predicts the SPM concentrations, whereas Caline-3 under-predicts SO_2 and SPM concentrations and over-predicts NOx concentration. The FB indicates how well the computation produces the average values around the average values of observed variable. The ideal value of this measure is zero, but it can range from -2 to +2; and absolute value 0.67 corresponds to a prediction within a factor of two of the observations (Arya, 1999). The value of FB indicates better performance of both the models. The values representing IOA reveal that the performance of both models is satisfactory. From these errors (see Table 3.6) performance of both models is reasonably good as majority of their predictions are within a factor of two (Hanna et al., 1982).

Table 3.5 Secondary data of emission factor for vehicular source

Type of vehicle	Emission factors (g per vehicle km)		
	SO_2	SPM	NO_x
Scooter/M.Cycles	0.5	0.05	0.1
Car/Jeep	0.6	1.0	1.4
Bus/Truck	2.0	2.0	21.0

(Source: IIP, 1994)

Table 3.6 Statistical Errors computed for both the models IITLS and Caline- 3

Error	Ideal value	SO_2		SPM		NOx	
		Caline-3	IITLS	Caline-3	IITLS	Caline-3	IITLS
FB	0	-0.35	0.16	-0.39	-0.10	0.10	0.009
NMSE	Least value	0.14	0.06	0.20	0.02	0.09	0.04
R^2	1	0.79	0.71	0.62	0.67	0.54	0.80
IOA	1	0.61	0.48	0.38	0.47	0.42	0.20
FA_2	≥0.8	0.7	1.3	0.8	0.9	1.3	1.6

Fig. 3.13 show the temporal variation of pollutant concentration obtained from IITLS model at Gangtok for the two seasons i.e., winter and summer represented by December and April. The figures have low concentrations during afternoon hours and high values in the early morning and late evening hours. The peaks of concentration in morning

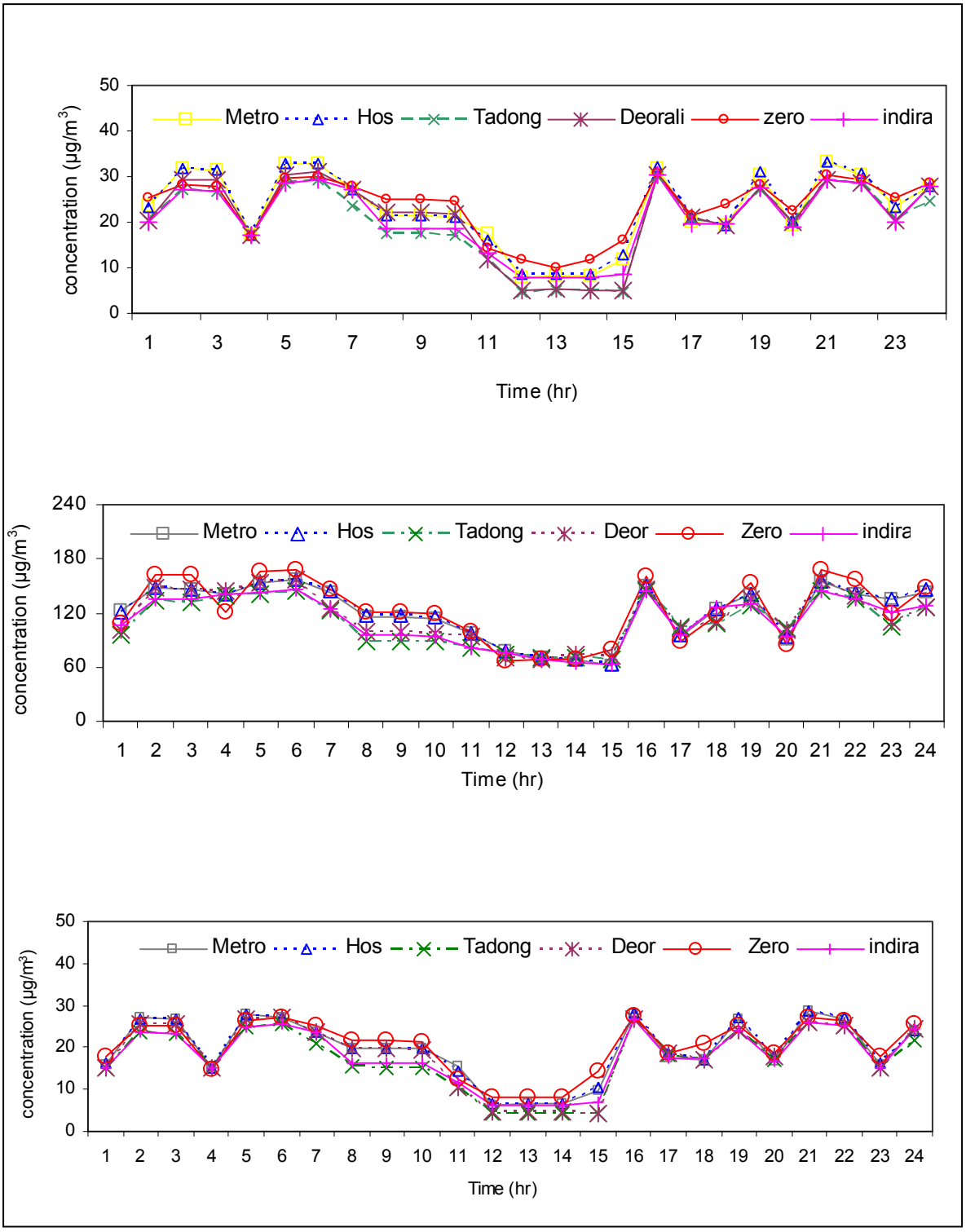

Fig 3.13 Temporal variations of pollutants by using IITLS Model at Gangtok in December

and evening hours can be justified through variation in traffic flow (source strength) and meteorological conditions. It is quite obvious to have higher concentrations in the morning and evening hours as the peak office hours add extra emissions of pollutants into diminishing mixing layer and declining wind speed.

It can also be observed that concentrations of pollutants during day hours, in both the seasons, are lower compared to morning and evening hours. The concentration of SO_2 as predicted by IITLS in December varies from 5 to 33 μg/ m^{-3} and in April it is recorded between 4 to 31 μg/ m^{-3}. Similarly the variation of SPM in December is from 45 to v168 μg/ m^{-3} while in April it reduces to a range of 40 to 161 μg/ m^{-3}. The NOx values ranges from 4 to 29 μg/ m^{-3} in December and 3 to 27 μg/ m^{-3} in April. It can also be seen that the lower value of concentration occur in afternoon hours while higher values during early morning and evening in both the seasons. This when correlated with the meteorology of these seasons was found that the above values corresponds to the values of ventilation coefficient which is higher during afternoon hours in April and December while low during early morning and evening time. This is certainly due to the fact that during late evening hours mixing height is quite low disallowing the dispersion of pollutants. The above result and discussion however, reveals that the pollution potential due to various sources of pollutants in Gangtok are showing lower concentration of pollutants during day hours compared to morning and evening hours.

3.6.3 Conclusions

The computed pollutant concentrations obtained from the models IITLS and Caline-3 have been compared with the monitored concentrations at different receptors in both the seasons. The results indicate that both the models are well in agreement with the observed concentrations in the study area. However, models estimate high pollution potential i.e., low assimilative capacity during winter season whereas summer season has different result. It is noticeable at this juncture that results of both the approaches correlate well for winter as well as summer seasons. The statistics however, shows that IITLS model is performing better than the Caline-3 which is possibly due to the more realistic emission data which is input to the model and its ability to incorporate calm winds. In the present study the influence of topographical features and other complex terrain related forcing have not been considered in the models. However, consideration of these effects is expected to improve the models predictions. The study finds that the commercial place like Metro Point, Zero point and Hospital Point are the places where the level of pollution is high hence decongestion of traffic is required at these places.

3.7 WEST SIKKIM

The Western district of Sikkim has a total area of 116 km^2 and population of about 1.2 lakhs (Census 2001). The district has two main towns Gyalsing (Gyalzing) and Nayabazar. The distance between

Nayabazar and Gyalzing is approx. 37-38 km. River Rangit separates the west from the south district of the State. The district starts from Nayabazar.

3.7.1 Sources of Pollution in West Sikkim

Automobile is the major source of pollution. Except a cheese factory in Dentam, there are no industries in West Sikkim. There are around 2,500 vehicles present in West Sikkim, which constitute 9.5% of the total automobiles present in Sikkim.

3.7.2 Emission Inventory

A gridded source inventory has been developed over an area of (18.0 x 18.0) km^2 as shown in Fig. 3.15. This area has been divided into 324 grids of size (3.0 x 3.0) km^2. Since, the major road network covers only the eastern and southern part of this district only three receptors were chosen. The receptors are Gyalzing, Nayabazar and Soreng. The roads (links) connecting them are shown in Fig 3.15. The emission rate of air pollutants were determined using method-I. Since, these receptors lie very close to south Sikkim some of its places (like Namchi, Jorethang) are also included in evaluating the concentration at these receptors.

According to the statistics available about 1500 vehicles commute daily in west Sikkim. Hence, the distribution of these vehicles is obtained in 10 links between Gyalzing, Nayabazar and Namchi. The largest

source was found between Nayabazar and Legship of approximately 10 km. However, the maximum number of vehicles (600 approximately) was found between Namchi and Nayabazar as these are well connected from all other places in this area. The vehicular movement was monitored twice a day in a week between Nayabazar - Gyalzing and Nayabazar - Soreng from 9.30 to 10.30 am for peak traffic hour in the morning and 1.00 to 2.00 pm for non-peak traffic hour in the afternoon. The traffic monitoring revealed that about 60% of the vehicles plying on these roads are Light vehicles. The same ratio was used to distribute the vehicles in different links.

3.7.3 Results

A comparative study of two different year's air quality has been done for this region to estimate the air quality status of this region. The present work has been done in a similar way as has been done for Gangtok city. The study has been done for April and December months which are representatives of summer and winter season respectively. The pollutants studied are carbon monoxide (CO), suspended particulate matter (SPM), oxide of nitrogen (NOx) and sulpur dioxide (SO_2). Fig. 3.16 gives the variation of concentration during summer and winter season in the years 2001 and 2004 for CO, SO_2, SPM and NOx. Fig. 3.16a shows that the concentration of all pollutants increases in 2004, though very slightly, from 2001. This is observed at all receptor points. The concentration of NOx is maximum followed by CO at all the receptor points in both the years. However, winter (January)

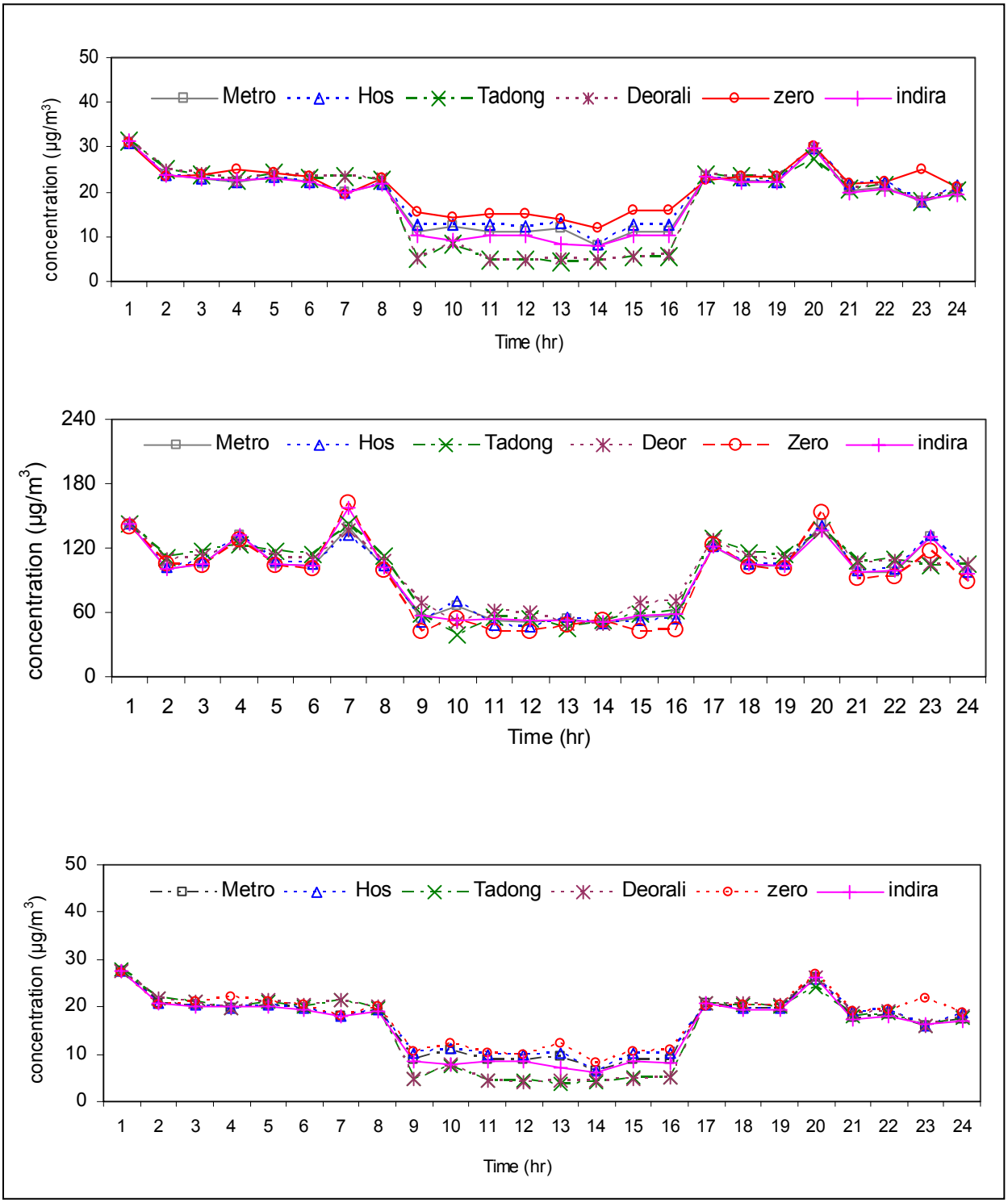

Fig 3.14 Temporal variations of pollutants by using IITLS Model at Gangtok in April

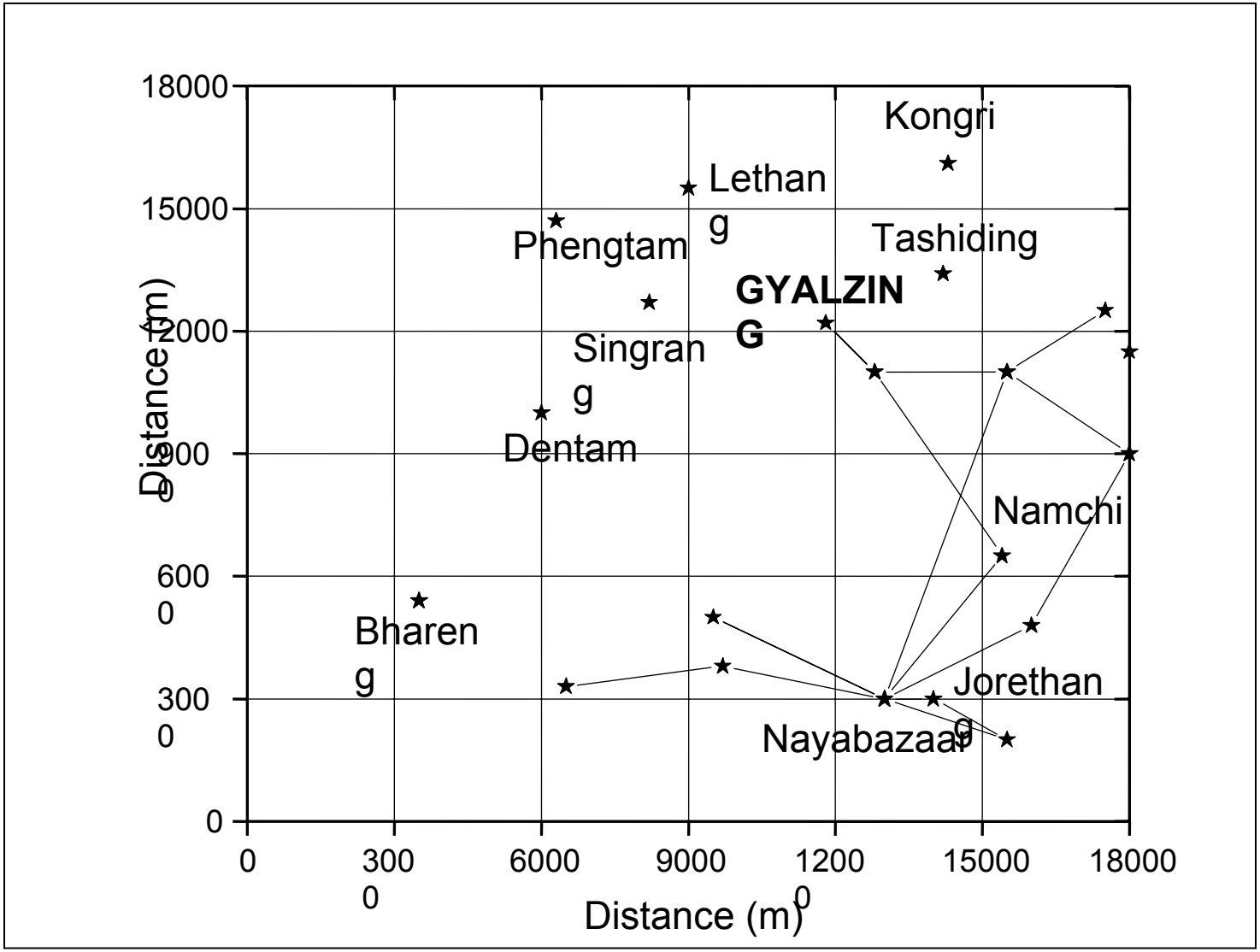

Fig 3.15 West Sikkim: Sources (Links) and Receptors

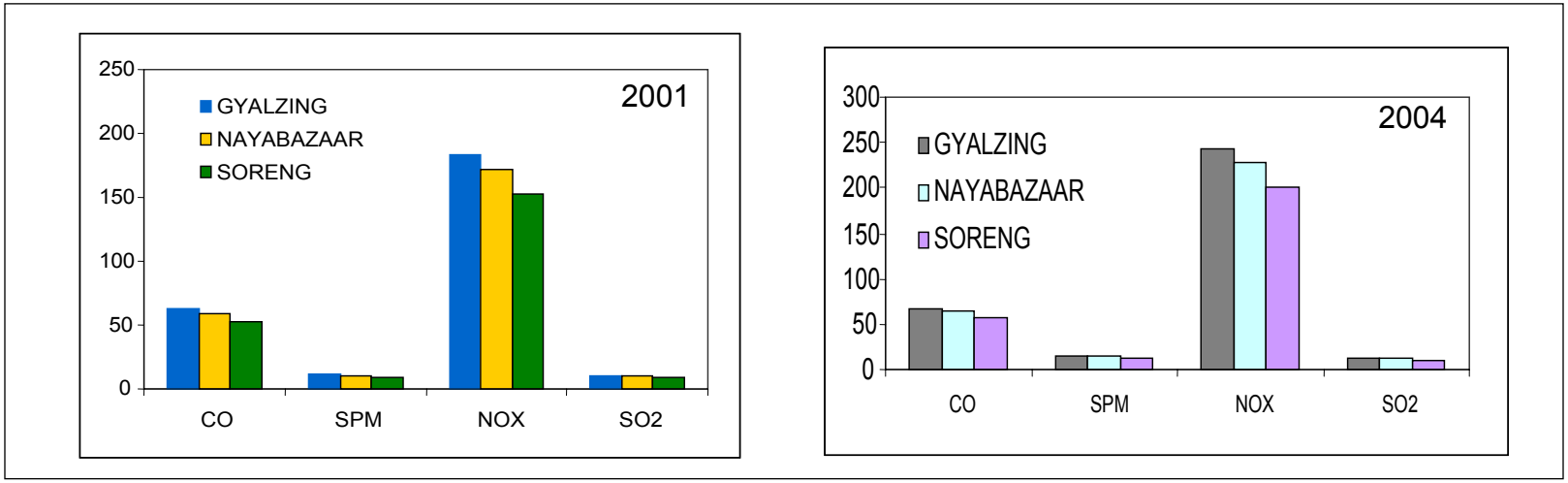

Fig 3.16a Variation of pollutants concentration during summer

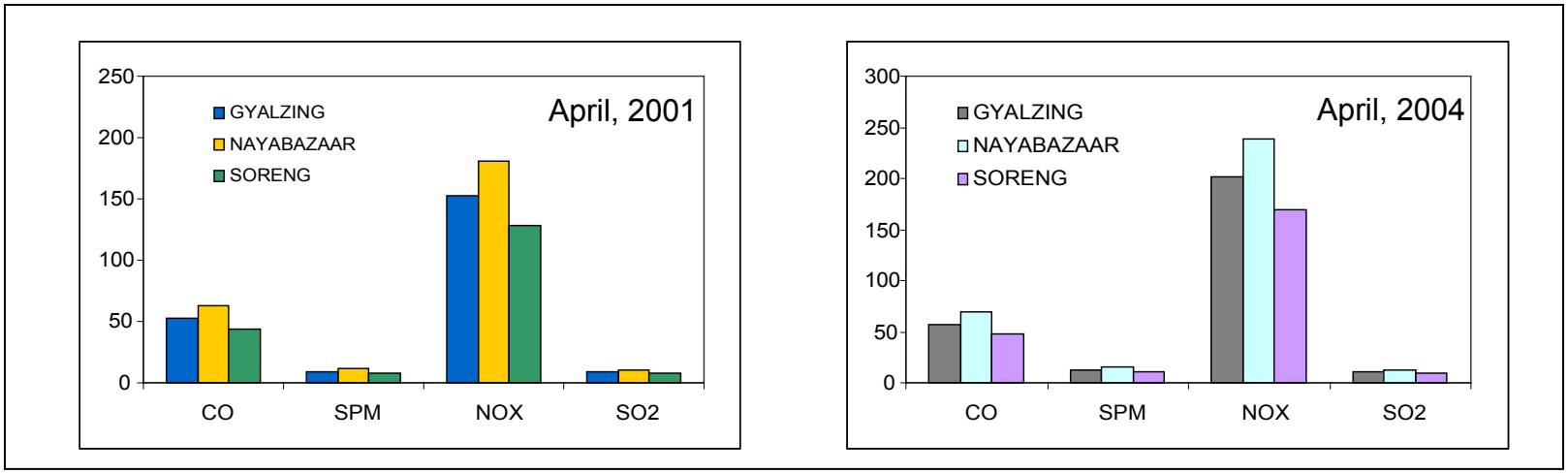

Fig 3.16b Variation of pollutants concentration during winter

concentration is slightly higher than that of summer (April) for both the years. Fig. 3.16 reveals that, in winter (January) the highest concentration of pollutants is observed at Gyalzing followed by Nayabazar and Soreng. In summer season, however, Nayabazar has highest concentration followed by Gyalzing and Soreng.

Figures 3.17-3.20 gives the temporal variation of pollutants during 2001 and 2004 obtained using IILS model. Fig. 3.17 reveals that the winter 2001 concentration is quite low during the morning afternoon hours (9 am to 16 pm) for all pollutants. This is due to the mixing height values that help in dispersion of pollutants during that time. Gyalzing has maximum SPM concentration of 11.5 μg m^{-3} followed by Nayabazar (10 μg m^{-3}) and Soreng (9.5 μg m^{-3}). The model evaluated values for winter 2001 gives the concentration of NOx at Gyalzing (183 μg m^{-3}) followed by Nayabazar (171 μg m^{-3}) and Soreng (152 μg m^{-3}) which is highest among all pollutants. The SO_2 concentration also follows the similar trend having the maximum concentration at Gyalzing (10 μg m^{-3}) followed by Nayabazar (9.5 μg m^{-3}) and Soreng (8.5 μg m^{-3}). These values however, increase in the year 2004. The maximum NOx concentration in winter 2004 is observed at Gyalzing (242 μg m^{-3}) followed by Nayabazar (227 μg m^{-3}) and Soreng (201 μg m^{-3}). The model evaluated concentration for summer 2001 gives the highest SPM concentration at Nayabazar (11.4 μg m^{-3}) followed by Gyalzing (9.6 μg m^{-3}) and Soreng (8 μg m^{-3}). The maximum NOx concentration in this season is observed at Nayabazar (181 μg m^{-3}) followed by Gyalzing (152 μg m^{-3}) and Soreng (127 μg m^{-3}). The same trend is observed in 2004. There is however an increase in the concentration values in 2004.

The maximum SPM concentration in summer is observed at Nayabazar (15 μg m^{-3}) followed by Gyalzing (12.6 μg m^{-3}) and Soreng (10.6 μg m^{-3}). Similarly Nayabazar gets the maximum NOx concentration (239 μg m^{-3}) followed by Gyalzing (201 μg m^{-3}) and Soreng (168.8 μg m^{-3}).

Form the above results it is clear that though the concentrations of SPM, SO_2 and NOx have increased in 2004 they are well within the limits. Among the seasons, winter is a more critical month than summer because of low wind speeds and low mixing/inversion height.

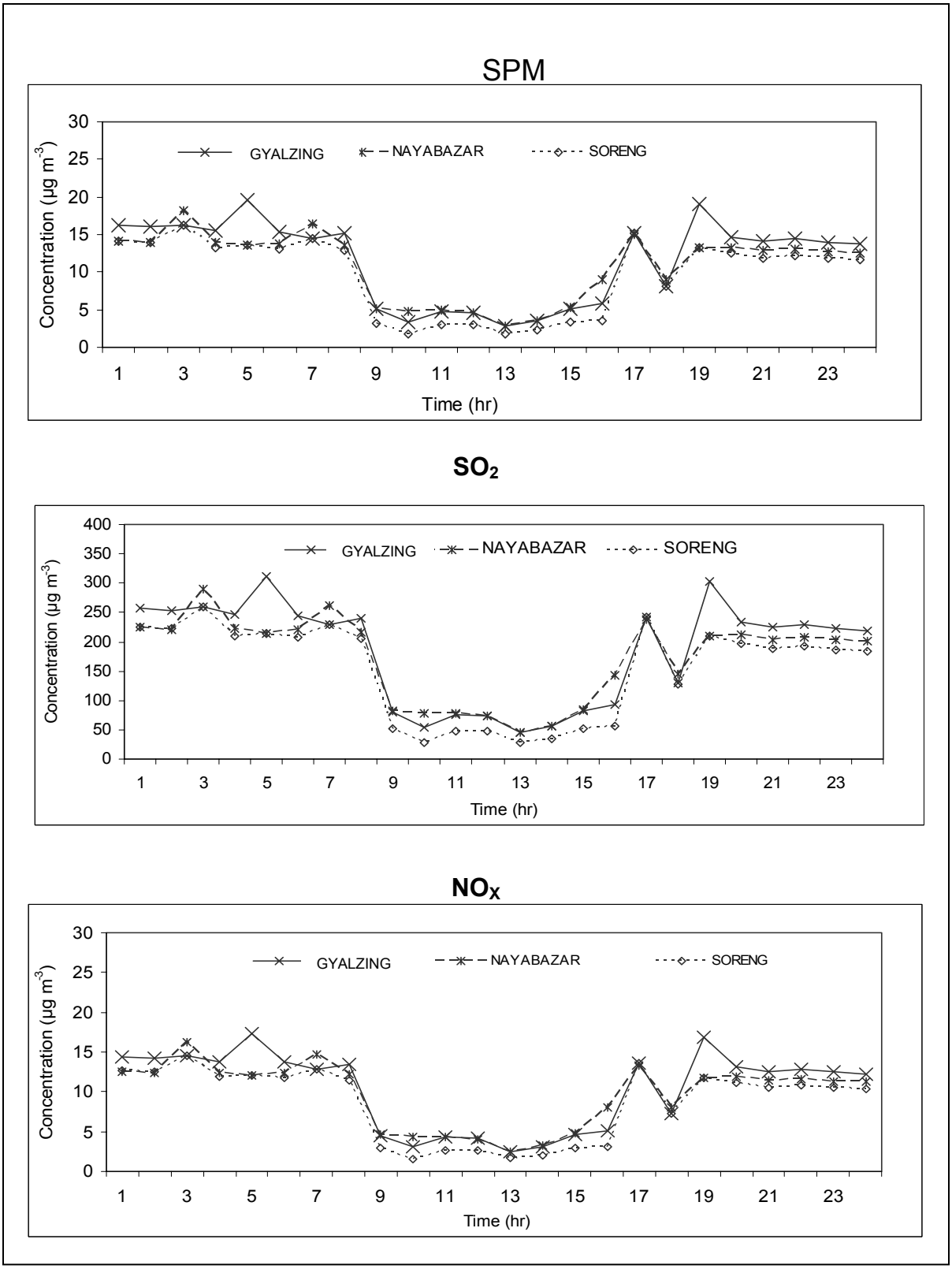

Fig. 3.17 Temporal variation of concentration in West Sikkim in January 2001

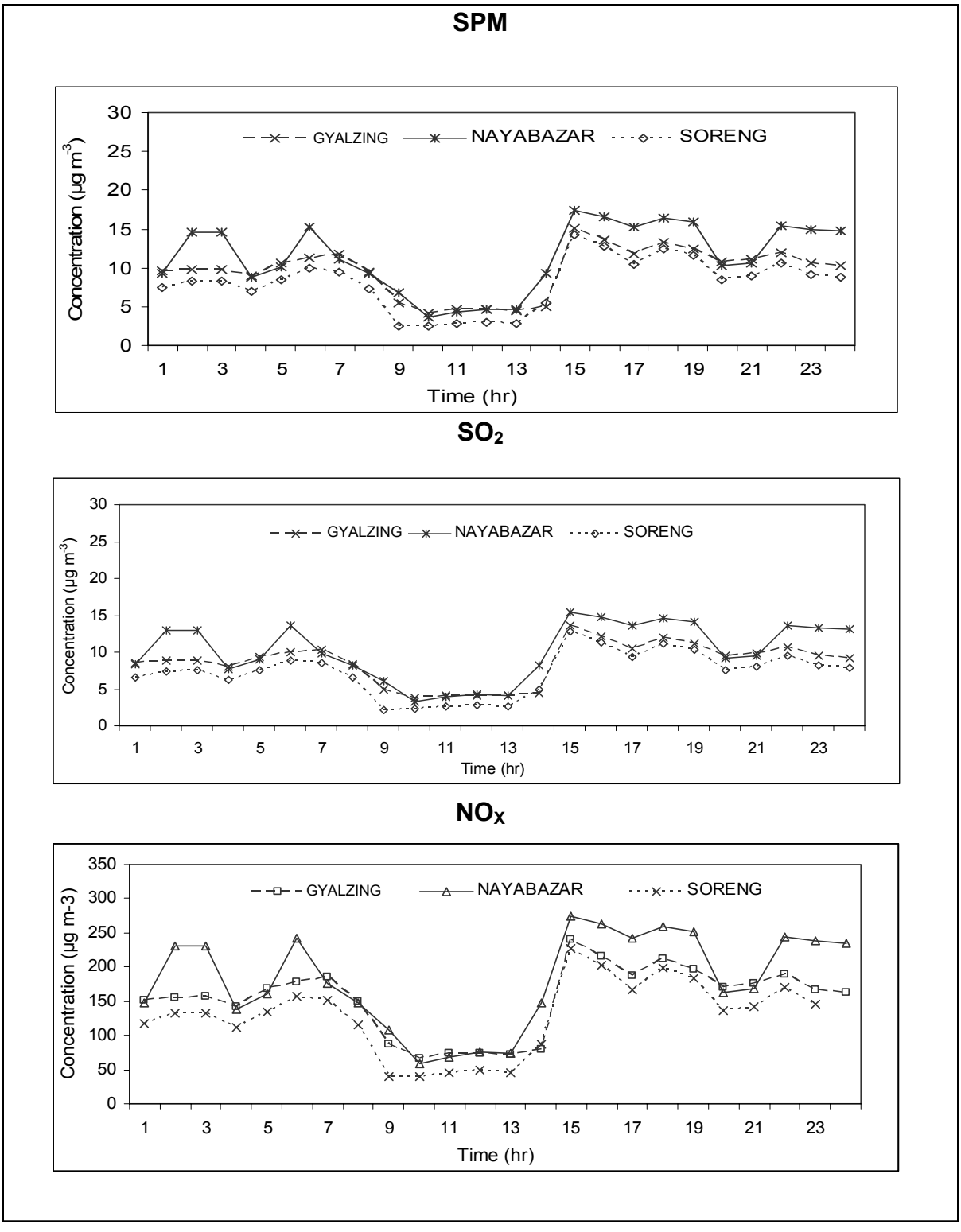

Fig. 3.18 Temporal variation of concentration in West Sikkim in April 2001

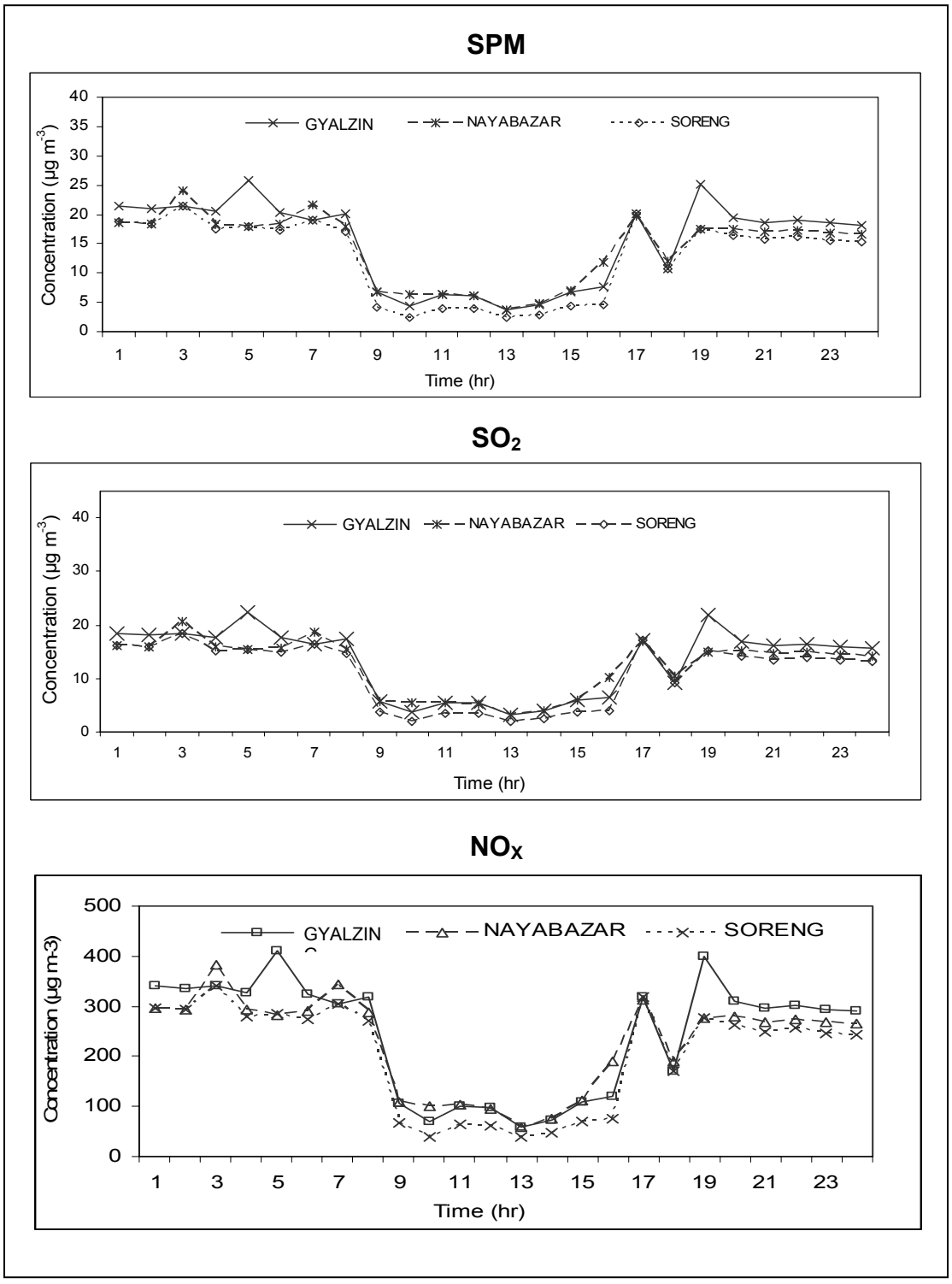

Fig. 3.19 Temporal variation of concentration in West Sikkim in April 2004

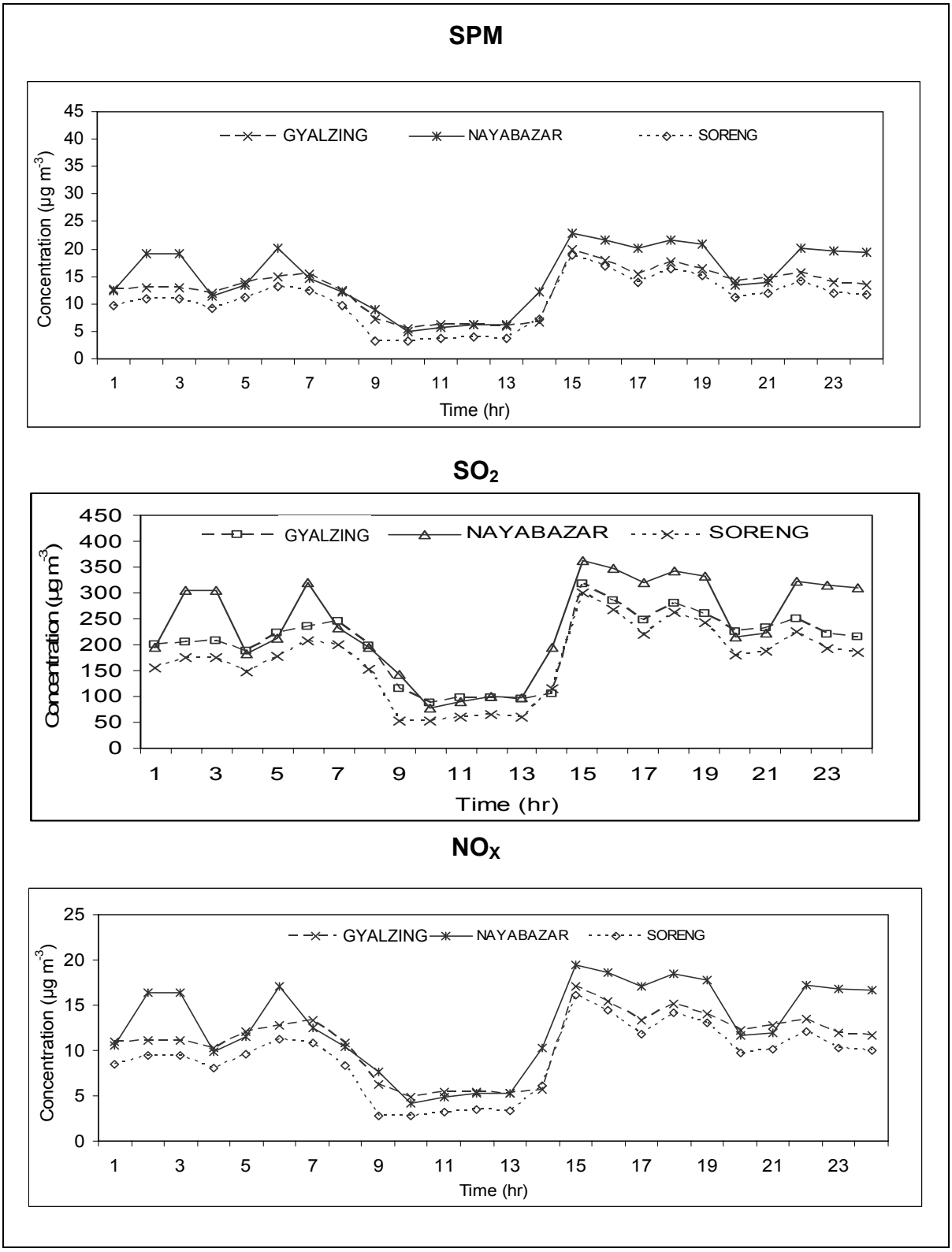

Fig. 3.20 Temporal variation of concentration in West Sikkim in January 2004

CHAPTER - 4

AIR QUALITY ASSESSMENT OF TEESTA RIVER BASIN IN SIKKIM

4.1 INTRODUCTION

Air quality index is a flexible approach based on detailed air quality data of the concerned region. It is an important task for general public to understand easily that how bad or good the air quality is and to assist in data interpretation for decision making process related to pollution mitigation measures and environmental management. It is primarily a health related index with the following descriptor words:

- Excellent – <20,
- Good – 20-39,
- Satisfactory – 40-59,
- Poor – 60-79,
- Bad – 80-100 and
- Dangerous – >100.

In the present study air quality assessment of Sikkim region, which is environmentally very fragile, has been chosen. The three pollutants SO_2, SPM and NOx, recognized as major pollutants of various sources in Sikkim, have been studied. Unplanned urbanization and industrialization in many urban cities are causing deterioration of the environment and quality of life. It is essential to assess the spatial distribution of air quality and its impact on human beings. Thus, a vast amount of ambient air quality data is to be generated to know the quality

of air environment and to take appropriate corrective actions wherever necessary. Such an endeavor would result in large volumes of data which may neither give clear picture to the decision- maker nor to a common man who simply wants to know how good or bad is the air quality. One way to describe the air quality is to report the concentrations of all the pollutants with acceptable levels i.e., National Ambient Air Quality Standards (NAAQS) to protect public health. Rating of the air quality into broad descriptive groups or using numerals to denote the quality of air are the most commonly used methods across the world and are known as air quality indices. Since all the pollutants are not measured under the NAAQS it is proposed that a minimum three pollutants (SO2, SPM and NOx) concentrations must be available to calculate and report the AQI.

4.2 METHODOLOGY

In the present study the air quality of Sikkim is determined using the Oak Ridge Air Quality Index (1976) formula given by-

$$AQI = \left[39.02 \left\{ \left(\frac{SPM}{200} \right) + \left(\frac{SO_2}{80} \right) + \left(\frac{NO_2}{80} \right) \right\} \right]$$

The air quality is considered to be excellent when AQI is less than 20; good, when AQI is between 20 to 39; satisfactory, when it is between 40-59; poor, when it is between 60-79; bad when it is between 80-100; dangerous when its value is above 100.

4.3 RESULTS

Figs. 4.1- 4.3 show the isopleths of SO_2, SPM and NOx for Sikkim during 2001 and 2005. Fig.4.1 shows the variation of SO_2 concentration during 2001 and 2005. The figure shows two critical points in the whole Sikkim area. These points are located near Phudong in East district and near Namchi in South district. The SO_2 values increases from a maximum concentration of 7 to 9 μg m^{-3} in the gap of 4 years i.e., 2001-2005. Similarly, SPM values increases from 55 to 70 μg m^{-3}. The NOx values, however, show an increase from 70 μg m^{-3} to 90 μg m^{-3}. The investigations into 2001-2005 data (Fig. 4.4) *vis*-à-*vis* the air quality index for Sikkim shows that air quality did not significantly deteriorate during this period. Among the individual places the air quality near Gangtok and Phodong is found critical, crossing the danger level from poor. The Northern and Western district are found to be the safest as the vehicular population is restricted by the terrain. The Eastern and Southern district which has higher vehicular population, has been found to be critical. Among the pollutants NOx is the critical pollutant (having the highest value of the sub-index) at all places in Sikkim in both the years. The air quality levels of SO_2 and SPM are within standards.

4.4 CONCLUSIONS

Ambient Air Quality (AAQ) is attractive as the starting point for an urban air pollution index because it lies along the environmental pathway between sources/emissions, which are the points of control and people's treating zones, which are the locations to be protected. AQI is a

useful technique for its application to any urban city. It is mainly based on sparse of ambient air quality data and NAAQS of a particular region. The overall analysis of Sikkim particularly at points near the Teesta River Basin has been found to be well within the limits except for a point near Gangtok where NOx values are found to be critical.

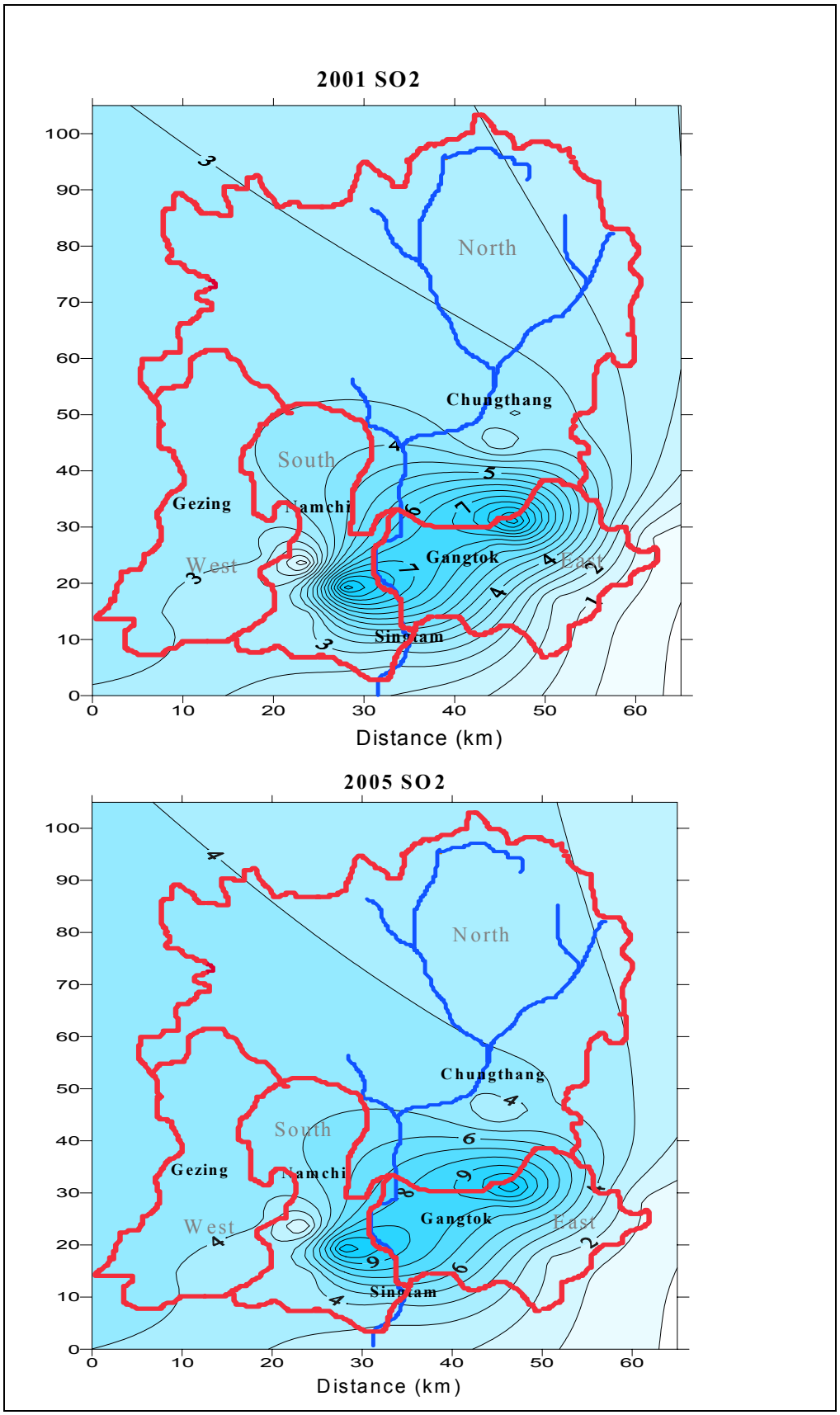

Fig. 4.1 Isopleths of Sikkim

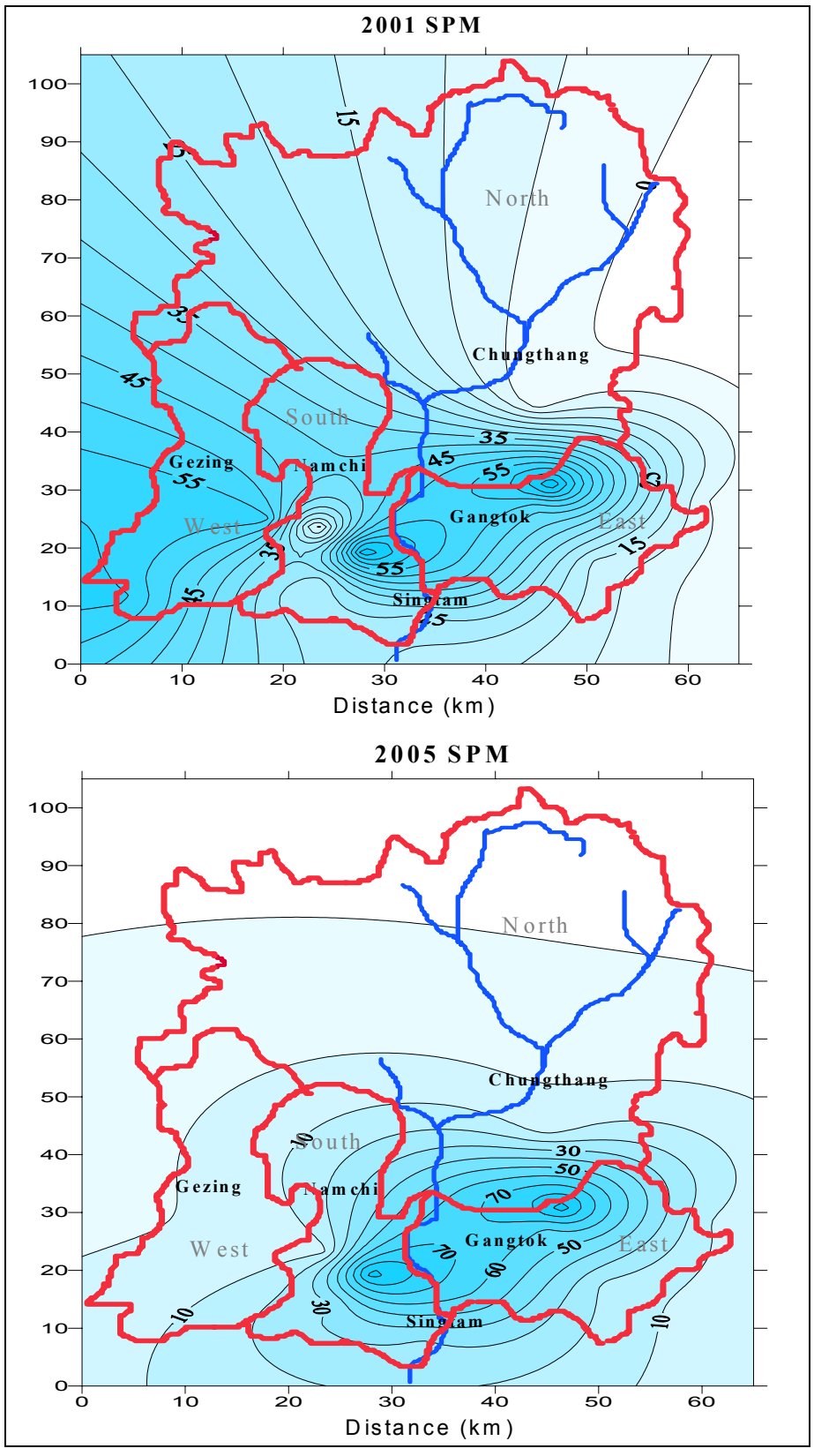

Fig. 4.2 Isopleths of Sikkim

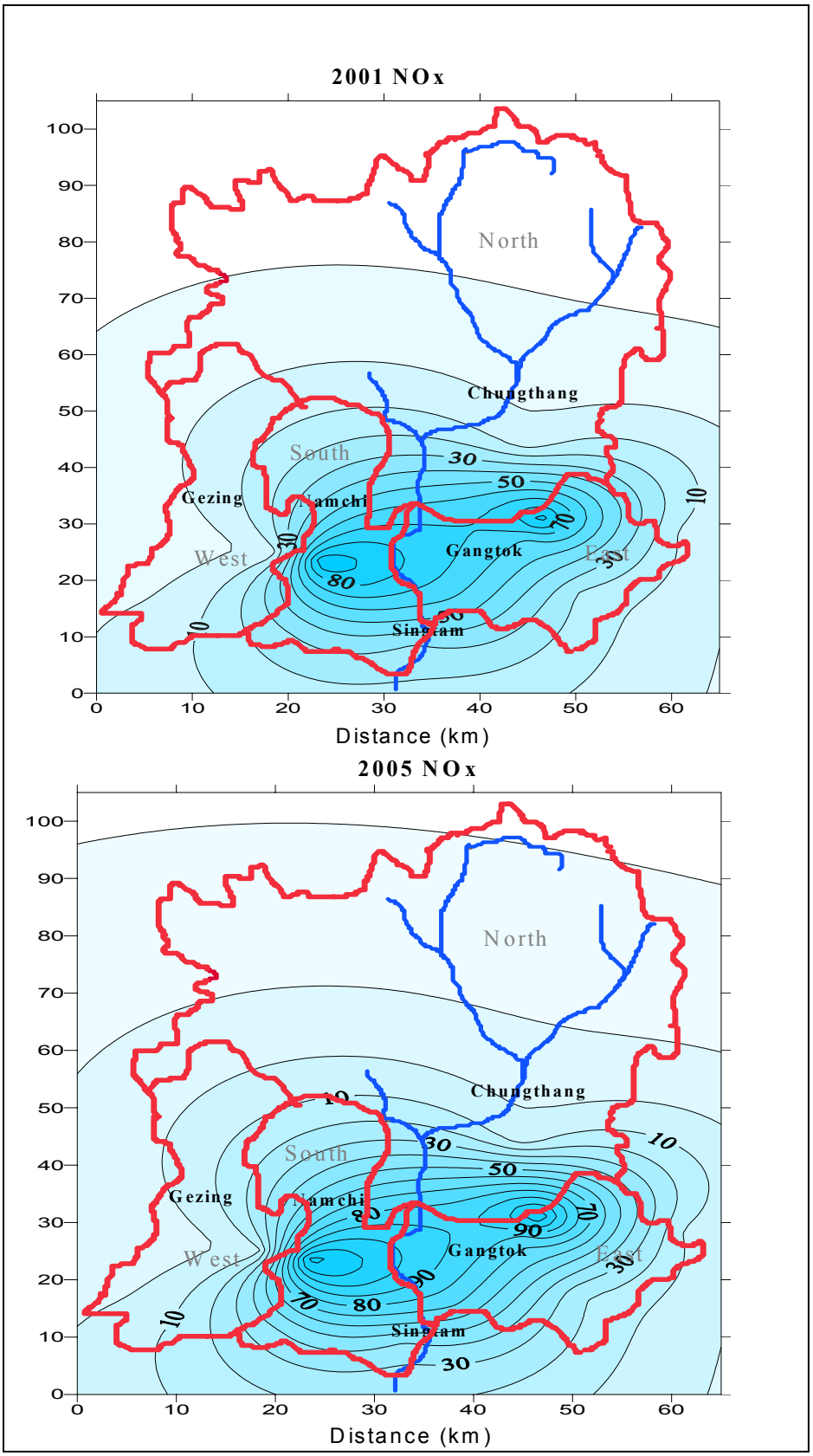

Fig. 4.3 Isopleths of Sikkim

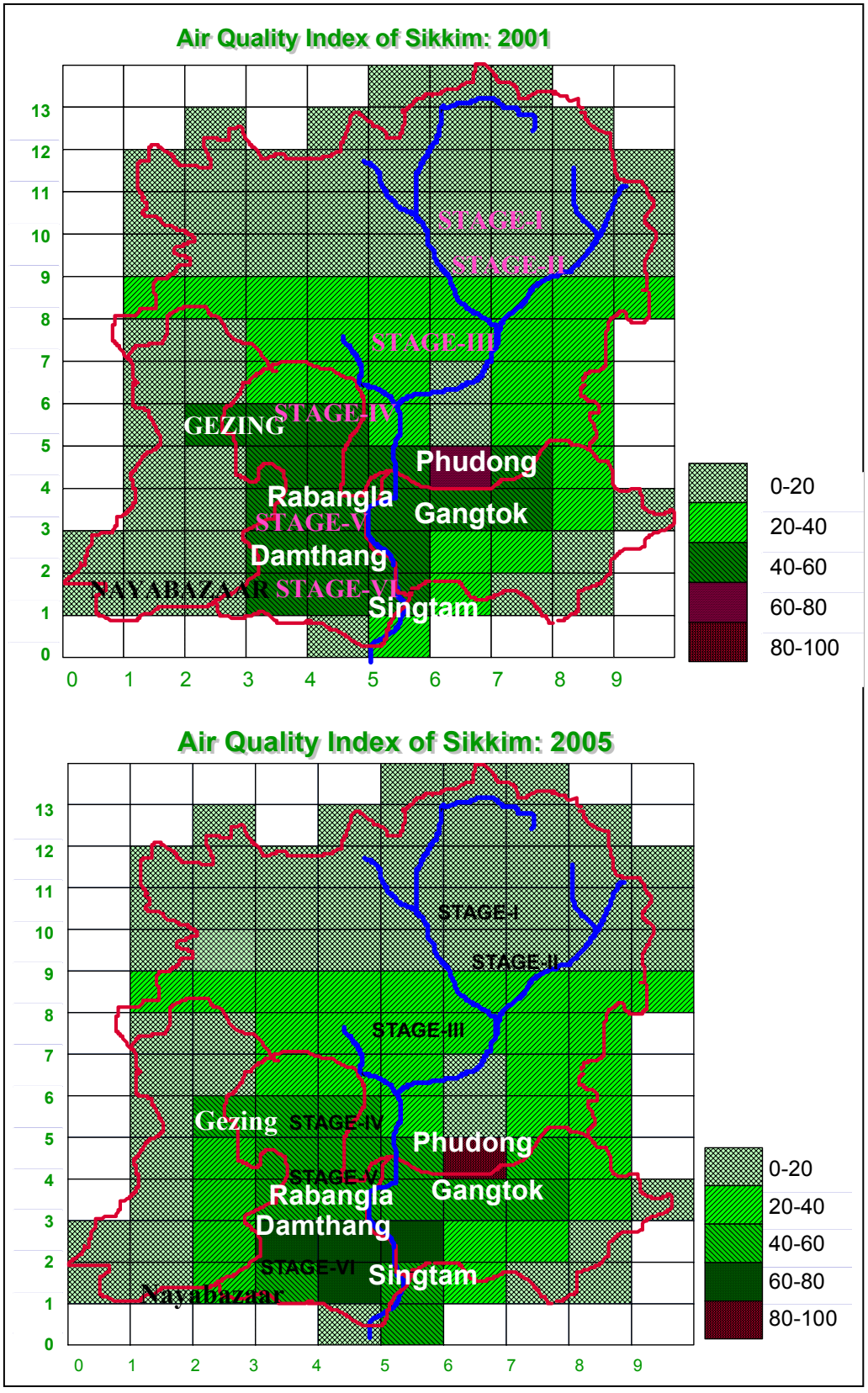

Fig. 4.4 AQI of Sikkim

BIBLIOGRAPHY

BIBLIOGRAPHY

Benson, Paul E. (1979). CALINE3 - A versatile dispersion model for predicting air pollutant levels near highways and arterial streets. Office of Transportation Laboratory, California Department of Transportation, Report No. FWWA/CA/TL-79/23.

Briggs, G.A. (1973). Diffusion Estimation for Small Emissions. ATDL contribution file No. 79, Atmospheric Turbulence and Diffusion Laboratory.

Faiz, A. (1993). Automotive emissions in developing countries-relative implications for global warming, acidification and urban air quality. *Transportation Research* 27A, 167-186.

Goyal, P., Rama Krishna, T.V.B.P.S. (1995). Various Methods of Emission Estimation of Vehicular Traffic in Delhi. *Atmospheric Environment* 3, 309-317.

Gross, E. (1970). *The national air pollution forecast programme*. ESSA Technical Memorandum, WBTM-NMC 47, National Meteorological Center, Suiteland, MD.

Hanna, S.R., Briggs, G.A. and Hosker Jr., R.P. (1982). *Handbook on atmospheric diffusion*. DOE/TIC-11223 (DE82-002045). NTIS/USDOC, Springfield, VA.

IIP, Indian Institute of Petroleum. (1995)**.** Vehicle emissions and control perspectives in India- A state of the art report. Engines Lab, Dehradun.

Kono, H., Ito, S. (1990). A microscale dispersion model for motor vehicle exhaust gas in urban areas–OMG volume source model. *Atmospheric Environment*, 24B, 243–251.

Okamoto, S., Shiozawa, K. (1978). Validation of an air pollution model for the Keihin area. *Atmospheric Environment* 12, 2139–2149.

Ott, W.R., Thons, G.C. (1976). Oak Ridge Air Quality Index: Air pollution Indices, A Compendium and Assessment of Indices used in the United States and Canada. *Ann. Arbor Science*, 43-46.

Pradhan, K.C., Sharma, E., Pradhan., Gopal, Chettri, A.B. (2004). Sikkim Study Series. *Geography and Environment* 1.

Singal, S.P., Gera, B.S. (1982). Acoustic remote sensing of the boundary layer. *Proceedings of Indian Academy of Science* (Engg. Sec.) 5, 131-157.

Singh, M.P., Goyal, P., Panwar, T.S., Agarwal, P., Nigam, S., Bagchi, N. (1990). Predicted and observed concentrations of SO_2, SPM and NOx over Delhi. *Atmospheric Environment* 24A, 783-788.

Stack Pole, J.D. (1967). The Air pollution potential forecast programme. ESSA Technical Memorandum, WBTM-NMC 43, National Meteorological Center, Washington, DC.

Sturm, P., Almbauer, R., Sudy, C., Pucher, K. (1997). Application of computational methods for the determination of traffic emissions. *Air & Waste Management Association* 47, 1204–1210.

Wark, K., Warner, C. (1981). Air Pollution – Its origin and control. Addison-Wesley Longman Inc., Reading, MA.

World Health Organization/United Nations Environment Program (WHO/UNEP). (1992). *Urban air pollution in megacities of the world*. United Nations Environment Program, Blackwell, Oxford, UK, 230.

ANNEXURE

REPORT
ON
INVERSION / MIXING HEIGHT STUDIES
AT
G.B. PANT INSTITUTE OF HIMALAYAN ENVIRONMENT & DEVELOPMENT, GANGTOK (SIKKIM)

NATIONAL PHYSICAL LABORATORY
Dr. K.S. Krishnan Road,
New Delhi-110 012

REPORT
ON
INVERSION / MIXING HEIGHT STUDIES
AT
G.B. PANT INSTITUTE OF HIMALAYAN ENVIRONMENT & DEVELOPMENT, GANGTOK (SIKKIM)

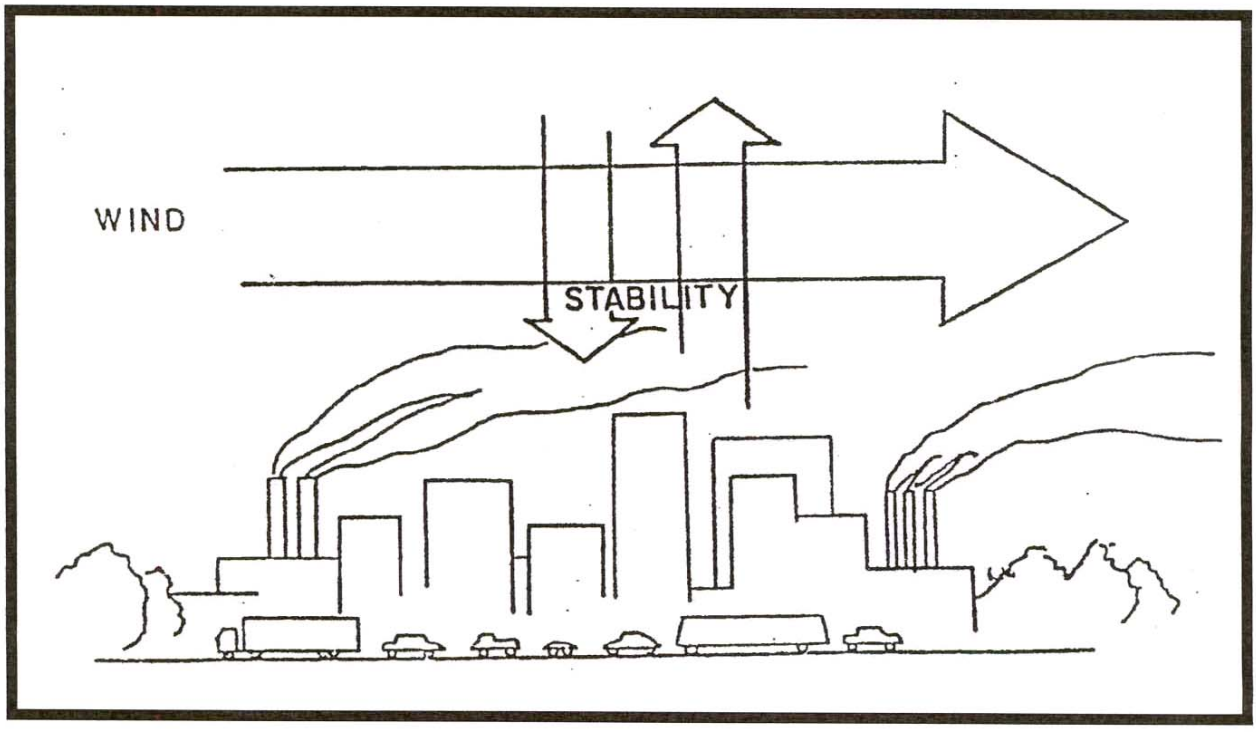

NATIONAL PHYSICAL LABORATORY
Dr. K.S. Krishnan Road,
New Delhi-110 012

CONTENTS

LIST OF TABLES

LIST OF FIGURES

1. INTRODUCTION

Increasing population, mechanization, transportation, urbanization conurbation and the human activities hit the fragile ecology and often the damages are irreversible. Pollution of the air that sustains life on the planet is one of the direct fallout of industrialization, human activities etc. In fact, nature through the inherent dispersive character of the atmosphere provides control measures to a large but finite extent.

The pollutants released in the atmosphere are carried aloft due to vertical mixing of the atmosphere during daytime under the action of solar heating of the ground and there from they are migrated to distant places by the prevailing winds. In the absence of such natural ventilation factors one can well realize that the situation will become unbearable for us to live. It is important to note that the said natural mechanism works and regulates its action in accordance with our own (human) activities on a diurnal scale.

However, one can not bank solely upon these natural meteorological factors or mechanisms to take care of the environment. We also need to exercise checks on our activities and resolve not to pollute the atmosphere beyond its natural cleansing or the carrying capacity. As otherwise pollution hazards may take place due to excessive accumulation of pollutants, particularly so, under conditions of poor dispersion and low level vertical mixing for transportation / migration of the pollutants.

Thus studies aiming at carrying capacity of the atmosphere on a regional scale are important in planning and phasing out of pollution concerned industrial units and other such activities. In pursuit of the same cause carrying capacity study of the Teesta basin in Sikkim (Fig.1) has been undertaken by IIT, Delhi.

The subject calls for sub domain studies of meteorological processes concerned with the transport and diffusion of pollutants or the dilution of the emissions in the atmosphere. The various meteorological parameters which govern such meteorological processes and on which depends the level of pollution in an urban environment, are the low level vertical temperature structures, mesoscale flow pattern, wind, cloud cover, vertical transfer of heat, momentum and moisture- flux etc. The interaction and inter-dependence of these parameters in conjunction with meteorological conditions and under lying topographical features is reflected in the evolution characteristics of inversion topography, depth of turbulence (mixing height) and low level atmospheric stability

The inversion which is characterized by increase in temperature with height is known to play a significant role in characterizing dispersion conditions.

The illustrative downwind stack plume behavior under different dispersive conditions of the atmosphere as determined by the temperature lapse rate is shown in Fig 2. It clearly demonstrates the significance and importance to have the knowledge of stack height with respect to ground based and elevated inversions for air quality studies.

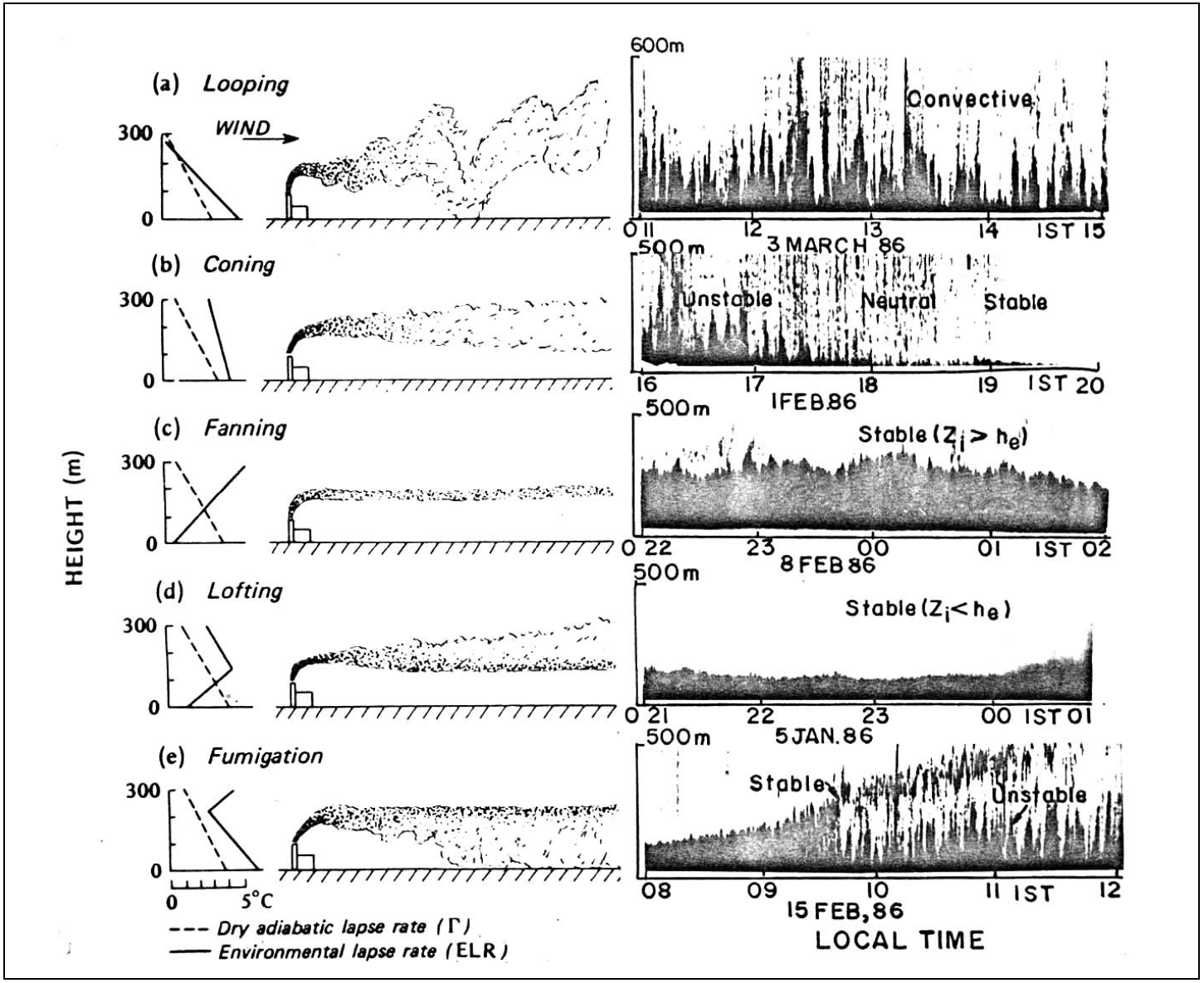

Fig. 2 Stack Plume behavior in relation to Sodar Echograms

As the local micro-meteorological conditions, topographical features and the synoptic weather conditions have bearing on the development and evolution characteristics of inversion, it is reasonably more scientific to use site specific data of ABL mixing height and stability class in real time dispersion models for environmental impact assessments (EIA) and carrying capacity studies. In this context, Sodar is an internationally recognized and proven cost effective technique to provide continuous real time data such as mixing / inversion height, ABL stability and wind profile.

In view of the said considerations, a Sodar was used to monitor site specific air pollution meteorological parameters of mixing / inversion heights required for the carrying capacity studies of Teesta basin. A monostatic Sodar was set up at the G. B. Pant institute of Himalayan Environment & Development, Gangtok by the National Physical Laboratory, New Delhi. The system was set up in October, 2003.

The data obtained over a year long period during October, 2003-September, 2004 has been analyzed for evaluation and studies of monthly diurnal variation of average mixing / inversion height and ABL stabilities.

This report presents an overview of Sodar technique and the results of data analysis.

2. Sodar Potential

Often, conventional weather forecasting *in situ* techniques like radio-sonde, instrumented tower, tethered balloon and instrument aircraft *etc.* are employed to monitor the essential air quality related meteorological parameters. However, it has been found that these techniques, though good and give reliable direct information of the relevant parameters, have several limitations. These are very expensive to operate for real time continuous data requirements. Radio-sonde provides data of temperature, humidity and wind profile (twice daily) which serve as inputs to forecast synoptic scale motions. This is although adequate for mesoscale urban forecasts but have own limitations and are costly to operate on a continuous basis. The information on mixing height, inversion height and stability class can be derived but it involves indirect techniques and data interpolations.

The need to study the fine scale structure of the atmospheric boundary layer and the necessity to use economical methods of obtaining a continuous data have resulted in a growing effort to use remote sensing techniques. Considering the overall operational cost of the system, stage of development and reliability of measurements related to air pollution monitoring situations, it has been seen that acoustic remote sensing by SODAR (Little 1969, Brown & Hall 1978, Singal 1988) is a best compromise. It is relatively simple, inexpensive, rich in information and effective technique for remote probing of the lower atmosphere. It uses natural tracers of temperature, wind and moisture fluctuations available in the turbulent boundary layer. Thus, it has a very large potential for air quality applications.

2.1 Operational Principle

SODAR (also called Acoustic Radar) functions like an active sonar or a pulsed radar system (Fig.3). Highly directional short bursts of sound energy of fixed frequency (in the audio frequency range 1500 to 5000 Hz) are radiated into the atmosphere. These waves during the course of propagation in the atmospheric air get scattered from regions of fluctuations in temperature, wind speed and humidity of eddy sizes within the inertial sub-range (0.1–10 m). The scattered signals are received either by the same antenna (in mono static or back-scattering Sodar mode) or by another antenna (bi-static or forward scattering Sodar mode).

The information contained in the received signals is processed to produce the facsimile display of the dynamics of ABL thermal structure in real time. The Sodar echograms deliver useful qualitative and semi-quantitative information about the ground based thermal activity, nocturnal inversions and symmetric phenomenon *e.g.* waves, subsidence, cold out flow of thunderstorm, dust storm etc.

Qualitatively, the prevailing meteorological phenomenon and the atmospheric stability (stable, unstable or neutral atmosphere) can be immediately recognized just by looking at the echogram. While quantitative information about velocity and temperature structure parameters, turbulence intensity and wind field in the scattering volume at various heights in the atmospheric boundary layer can be computed by measuring the amplitude and frequency of the received scattered

signal. The mixing/inversion height is computed from the intensity profile of received signals.

2.2 Sodar Components

The various Sodar components (Fig. 4) include electronic blocks for a tone burst generator, power amplifier, filters, preamplifiers , data acquisition system, facsimile recorder, acoustic antenna etc. The detailed discussions and the circuit description of each component are beyond the scope of present report and is, therefore, not discussed here.

However, it may be mentioned that the Sodar antenna forms a most sensitive component as it works in bi-directional mode to transmit high energy sound burst and receive the very weak sound signals. It needs special design considerations as it has to work in an open environment wherein interference of ambient noise is a serious problem. Thus Sodar installation calls for a suitable site selection based on site specific noise survey and analysis.

The basic Sodar antenna, most commonly in use all over the world, consists of a parabolic dish with the acoustic transducer fitted at its focus and a built over acoustic shield (Fig.5).

The shield is basically an acoustic absorbing conical cuff. It is made up of fiberglass, impregnated with lead powder. The walls of the conical cuff act as insulation and shield the antenna from the interfering

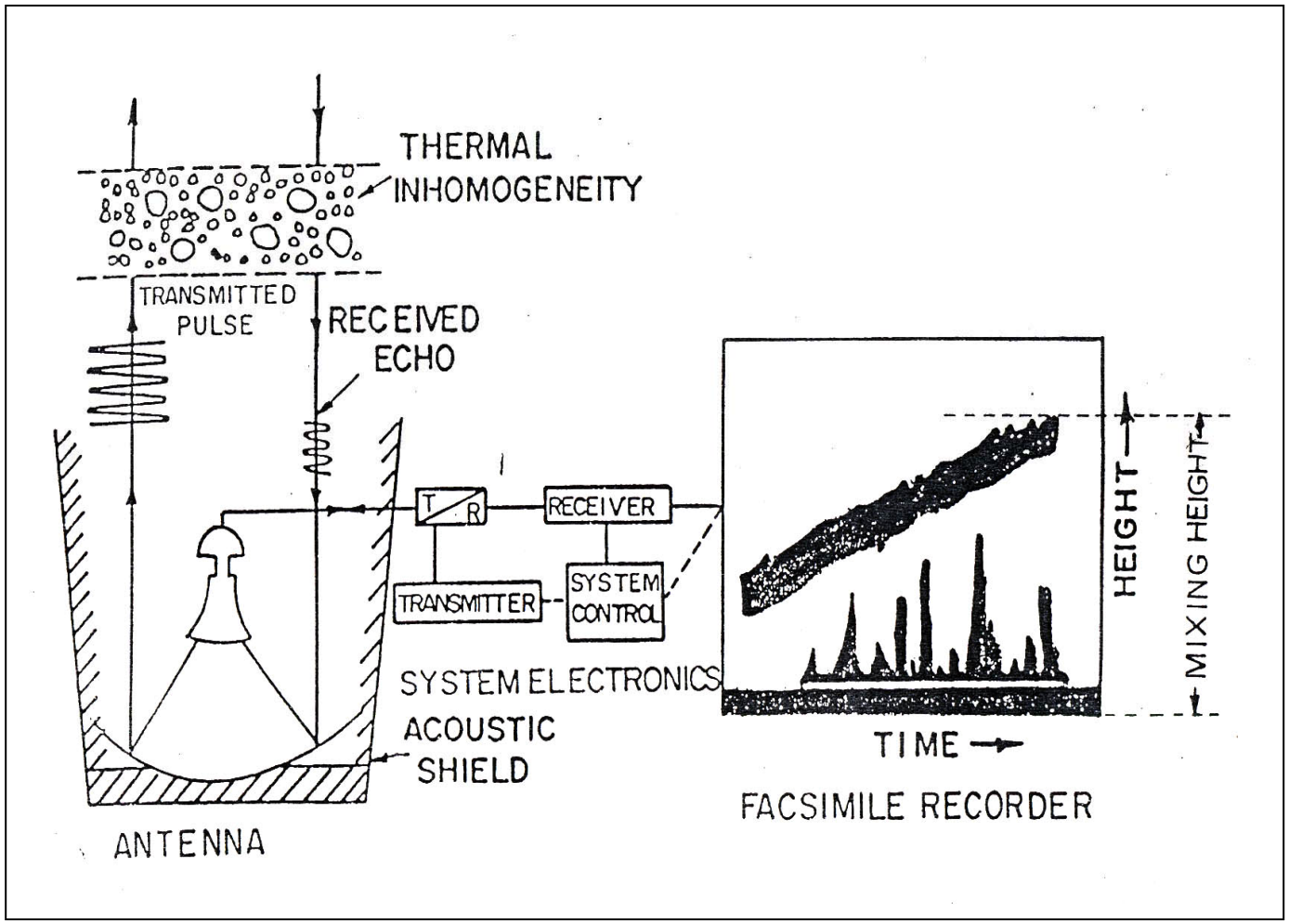

Fig. 3 Monostatic Sodar System

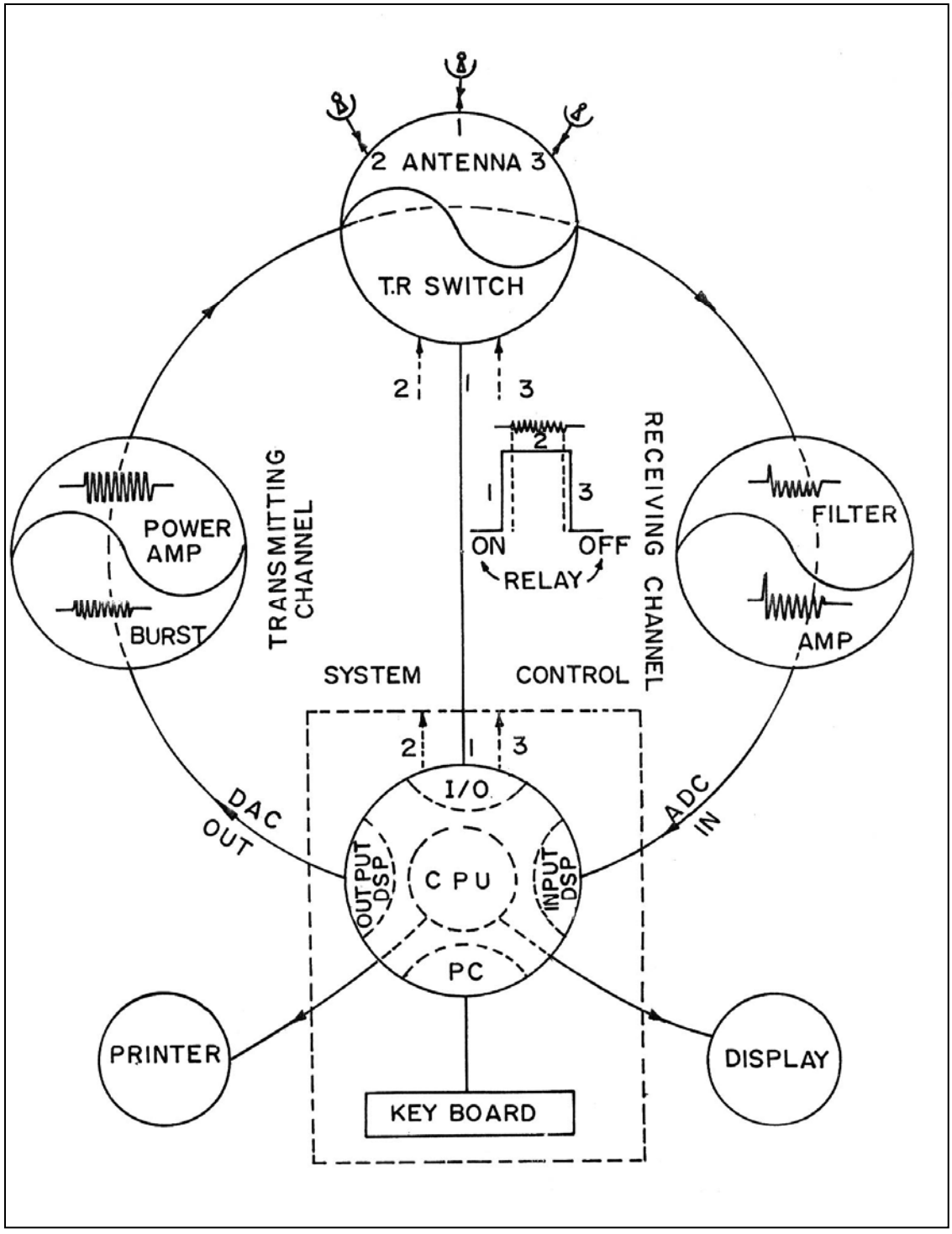

Fig.4 Schematic diagram of NPL Sodar system

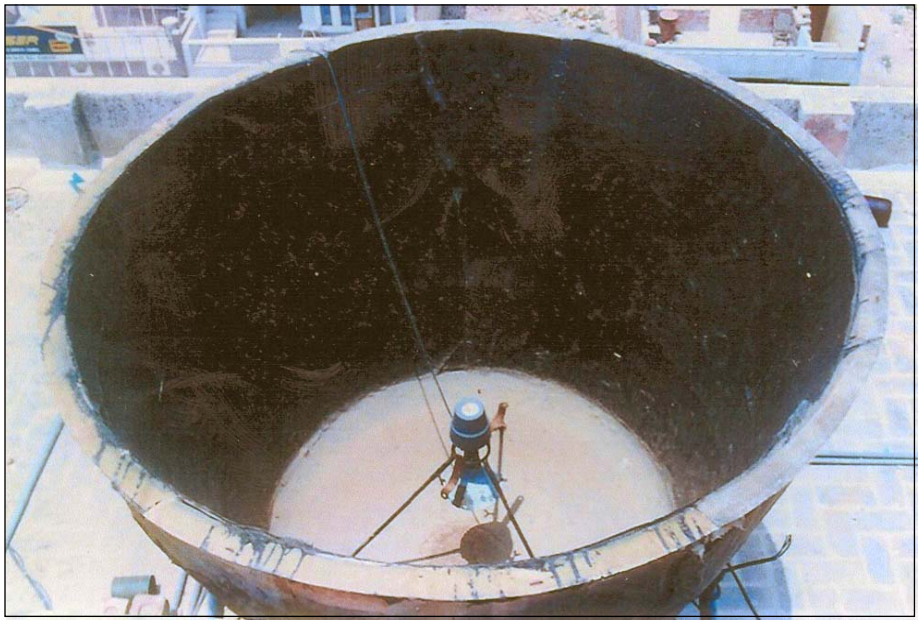

Top View

Fig.5 Sodar antenna

ambient noise. It also absorbs side lobes of the transmitted acoustic tone burst. Such a simple transportable antenna has shown fairly acceptable results for its worldwide acceptability. However, a fixed structure of hexagonal shield consisting of iron planks, sloping outwards, lined inside with acoustic absorbing material is equally good and can also be used if required.

The entire system operation for data acquisition is controlled through user friendly software. The prevailing meteorological phenomenon can be seen online while the data for mixing height is processed using offline programs.

3. SODAR SIGNATURES OF AIR POLLUTION METEOROLOGY

3.1 Sodar Structures

The various Sodar structures are broadly classified as thermal echoes and shear echoes in accordance with associated meteorological conditions. They are specifically named after the physical appearance of their echograms structural details. The commonly observed echograms, at any site and also observed at Gangtok (Fig.6), include thermal plumes, ground based stable layer with flat top, short spiky / tall spiky top layer, elevated layer, multiple layers, wavy layers, dot echoes etc.

The different Sodar structures are manifestations of prevailing spatially distributed turbulent conditions in the atmosphere. They portray the pictorial view of the thermodynamics of the associated

meteorological phenomenon. Each individual thermal structure portrayed on the echograms reflects a varied (simple to complex) turbulent phenomenon perpetually going on in the atmospheric boundary layer. Since turbulence is main mechanism for dispersion of pollutants, these structures are considered to be replete with information which is of immediate relevance to air pollution studies, even without going into the finer meteorological conditions behind the structures.

3.1.1 Significance in Air Pollution

With reference to significance in air pollution, it is important to understand that the different Sodar structures refer to the turbulence superimposed on the background lapse rate conditions. Thus, the pictorial view of a Sodar structure serves as an indicator of the online quality index of occurring lapse rate profile in the ABL. The information about pictorial view of Sodar structures can be used to infer lapse rate dependent atmospheric stability and thereby the dispersion characteristics as depicted in (see Fig.2).

With reference to Figure 6, the typical structures occurring at any site on a diurnal scale (discussed later) include:

(a) Thermal plumes indicate unstable atmospheric condition with free convection occurring in the atmospheric boundary layer due to solar heating of the ground. The Plumes look like vertical orientations with broad base and tapered columns. They are responsible for vertical mixing of pollutants. The structural

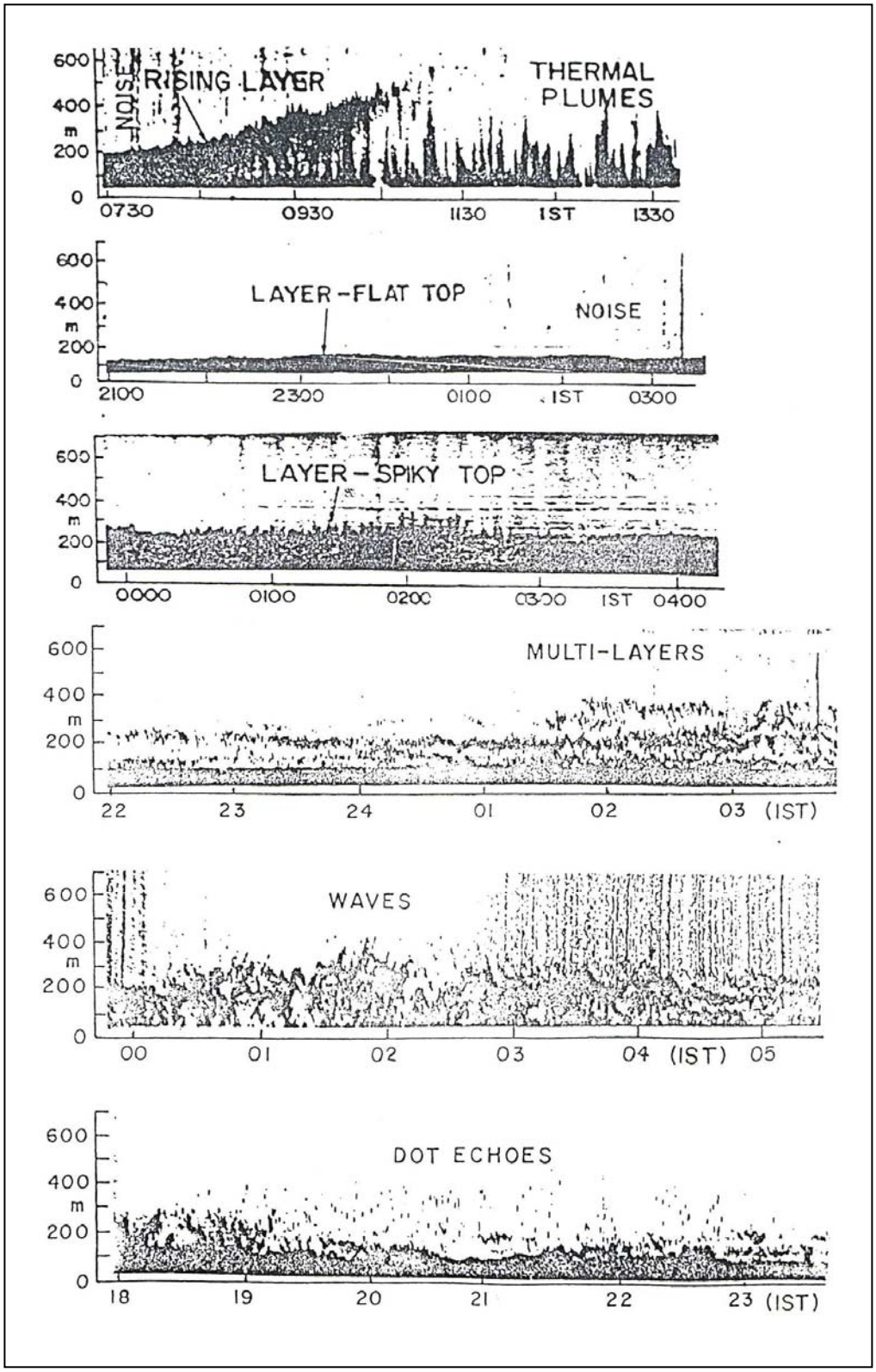

Fig.6a Various Sodar Echograms

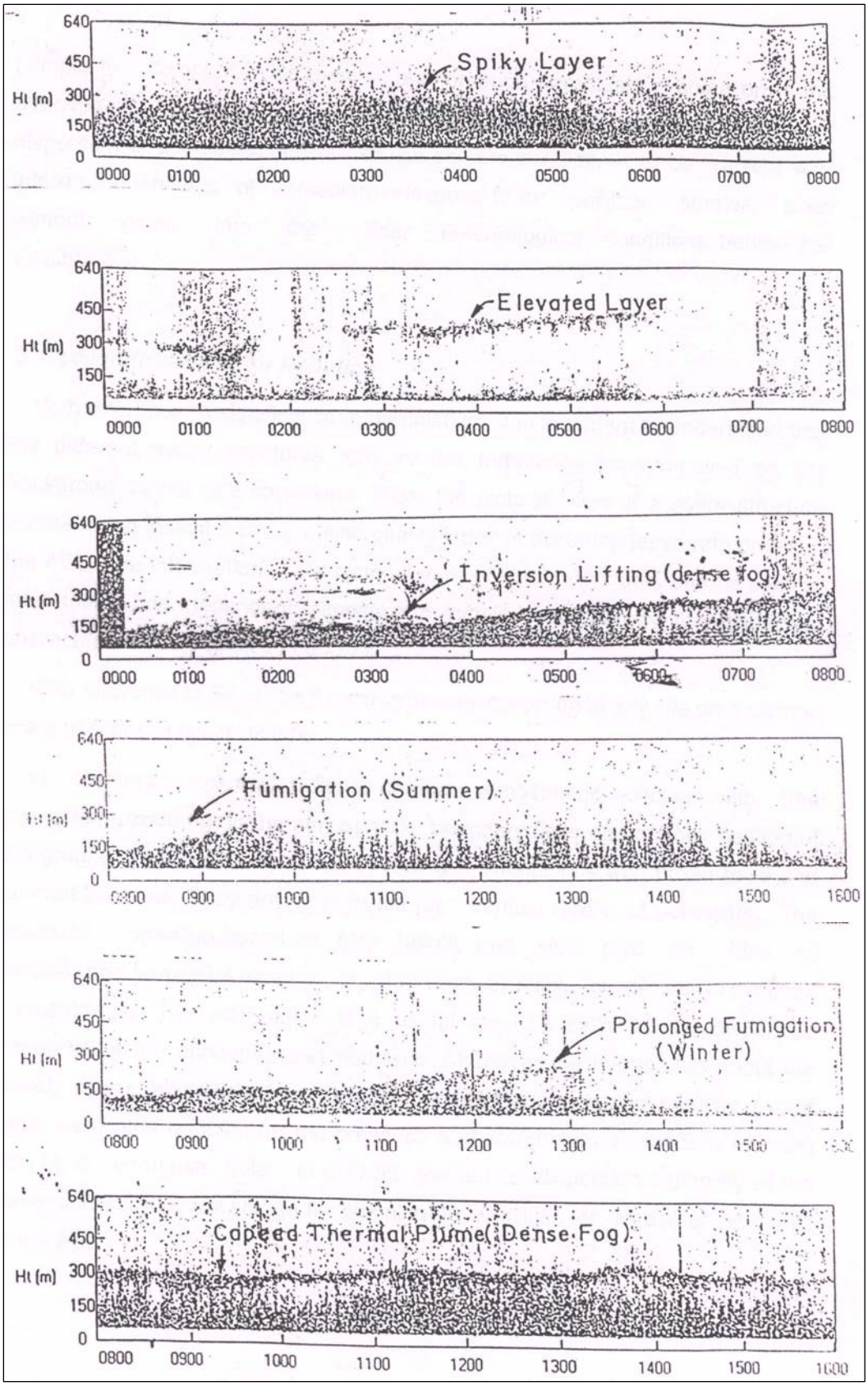

Fig.6b Various Sodar Echogrammes

information based on their height and width give an idea of vertical and horizontal extents of the room available for dilution of pollution concentration. The information is a useful input to estimate the dispersion capability of the atmosphere in real time. Moreover the information about the onset, decay and (there from) the duration of the convective activity (or in other words the duration for the presence of thermal plumes on Sodar records) can be of immense help in utilizing the natural dispersion capability of the atmosphere to our advantage for planning our activities for release of pollutants in the ABL.

(b) Nocturnal stable boundary layer (inversion) is commonly known as flat / spiky top layer in Sodar terminology. It looks like a horizontal band of ground based echo layer on the Sodar echograms. The top of this layer defines a boundary line from where above there are no echo returns. The height of this layer, for most practical purposes, gives an idea of the inversion height. This height is the vertical limit for mechanical mixing of the pollutants released within the inversion.

Knowledge of the inversion height has a direct application in the fixation of industrial stack heights. As shown in Figure 2, it is the relative position of the stack with respect to inversion height which governs the outflow characteristics of pollutants and their possible impact on inhabitants on ground. Furthermore, the information is of much significance in selecting the model equations in real time dispersion modeling for EIA.

Since the inversion top has a stable regime below, it tends to arrest the vertical dispersion and thereby leads to accumulation (or the increased concentration) of pollutants. The longer the inversion persists more is the degree of threat to life due to pollution effects. Thus, the study of the persistence of inversions, in relation to climatology and topography of a place, is of immense importance for regional industrial planning with reference to environmental impact assessment (EIA) and carrying capacity studies.

(c) The rising layer (or the eroding inversion in meteorology) characterizes the transition phase from stable to unstable atmosphere due to solar heating (insulation) of the ground, shortly after sunrise. During this period, meteorological conditions leads to fumigation of pollutants trapped overnight. During this period the effluents trapped overnight start mixing downward towards the ground. As a consequence, ground level concentrations become much higher because upward dispersal is dissuaded by inversion aloft. This transitional phase of the meteorological phenomenon, in the ABL, appears as a rising layer on the echograms.

Information about the onset of the said fumigation phenomenon and the onset of full scale convective activity (that follows) is useful to regulate the operational hours of smoke spewing industrial units and even plan the traffic transit to avert adverse impact of pollutants during morning hours of the day.

The above considerations clearly reveal the significance of real time Sodar information about the dynamics of ABL thermal structures and the tremendous scope of parameterizing the same to derive air pollution meteorological data for EIA.

It may be mentioned that the climatalogical and topographical elements do play an important role in shaping ABL thermal structures or in other words the dispersion conditions to the extent that they cannot be ignored. In this context, separate studies by Fanaki (1986) at two sites with different elevations and by Singal *et al*. (1984) at sites 10 km apart have shown perceptible difference (due to topographical variation) in the simultaneous Sodar observations. The studies stress upon the need to use site specific data for air quality studies.

However, it may be mentioned that most of the air pollution scientists, in practice, ignore the topographical influence on the ABL mixing height. Radiosonde data collected twice a day and that too belonging to a distant place or airports is commonly being used by involving interpolations and extrapolations to evaluate diurnal trends in ABL mixing height for air pollution problems. In view of such situations, Sodar offers a key potential to deliver site-specific data of air pollution meteorology.

3.1.2 Diurnal Cycle of Thermal Structures on Sodar Scale

The above mentioned ABL thermal structures form a repeatable pattern of Sodar structures on a diurnal scale. The cycle is visualized as

the occurrence of thermal plumes during sun shine hours of the day and the development of a ground based stable layer (inversion) during nocturnal cooling period of the ground at night time. The inversion gets eroded within couple of hours after sunrise on the following morning. The eroding inversion appears as a rising layer with thermal plumes beneath it. The schematic features are shown in Fig.7. The diurnal pattern of Sodar structures is seen every where in accordance with solar heating and nocturnal cooling of the ground as depicted through diurnal trends of ground temperature.

The deviations from the conventional diurnal cycle in terms of superimposition of additional thermal structures, complexities in observed structures (Fig.8) or the delays in onset / dissipation of prevailing structure are possible due to changes in local meteorological factors, topographical features, occurrence of synoptic weather phenomenon etc.

From the air quality point of view, the thermal plumes occurring during the day provide a considerable mixing height for vertical dilution of pollutants released near the ground. However, the occurrence of inversion under stable atmospheric conditions and the complexities therein need careful considerations for dispersion related studies.

3.2 Meteorological Background

Confining ourselves to the night time structures, strong short range echoes having abrupt but almost uniform upper limit exhibiting nearly flat

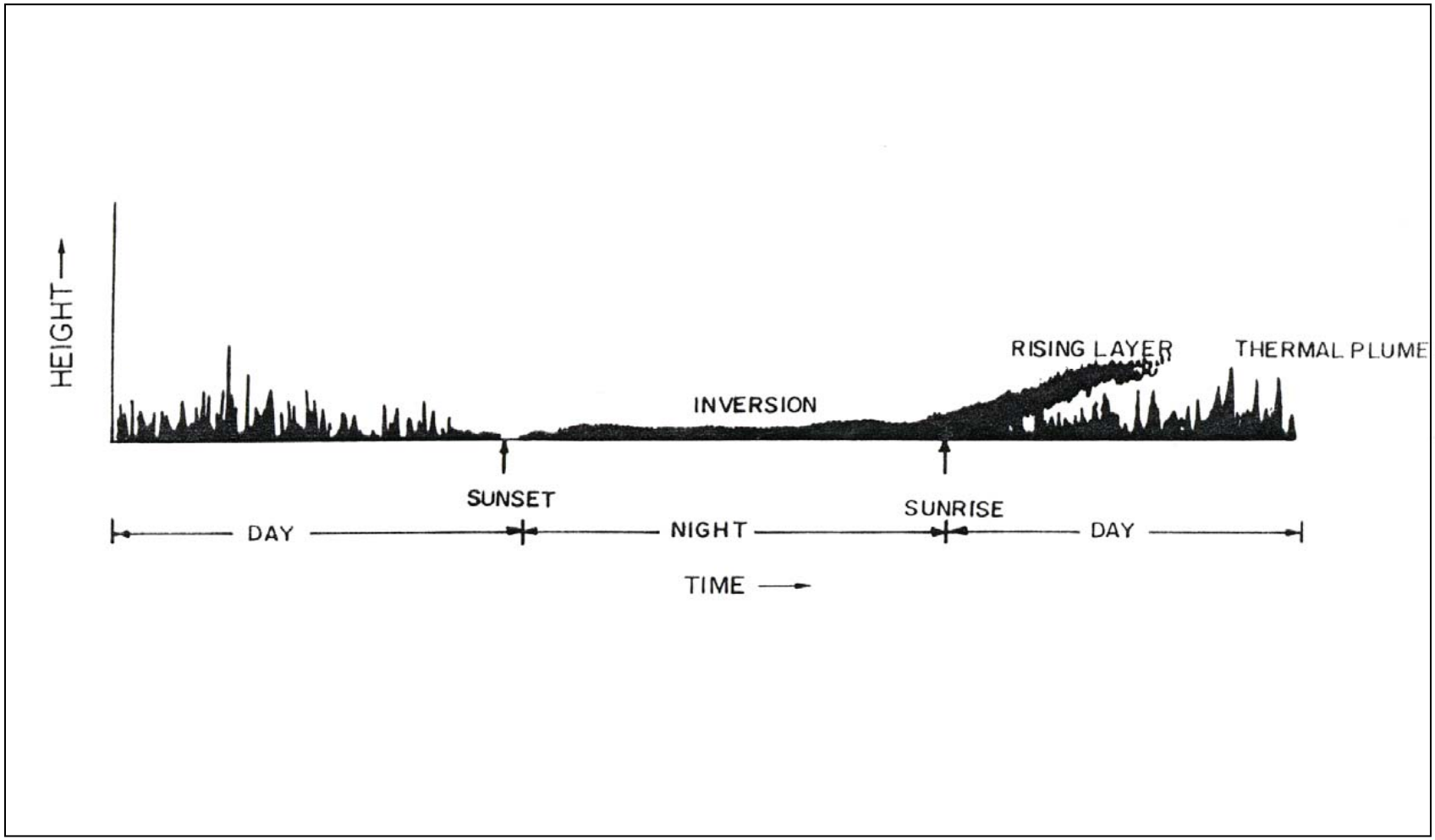

Fig.7 Diurnal cycle of Sodar structures (schematic)

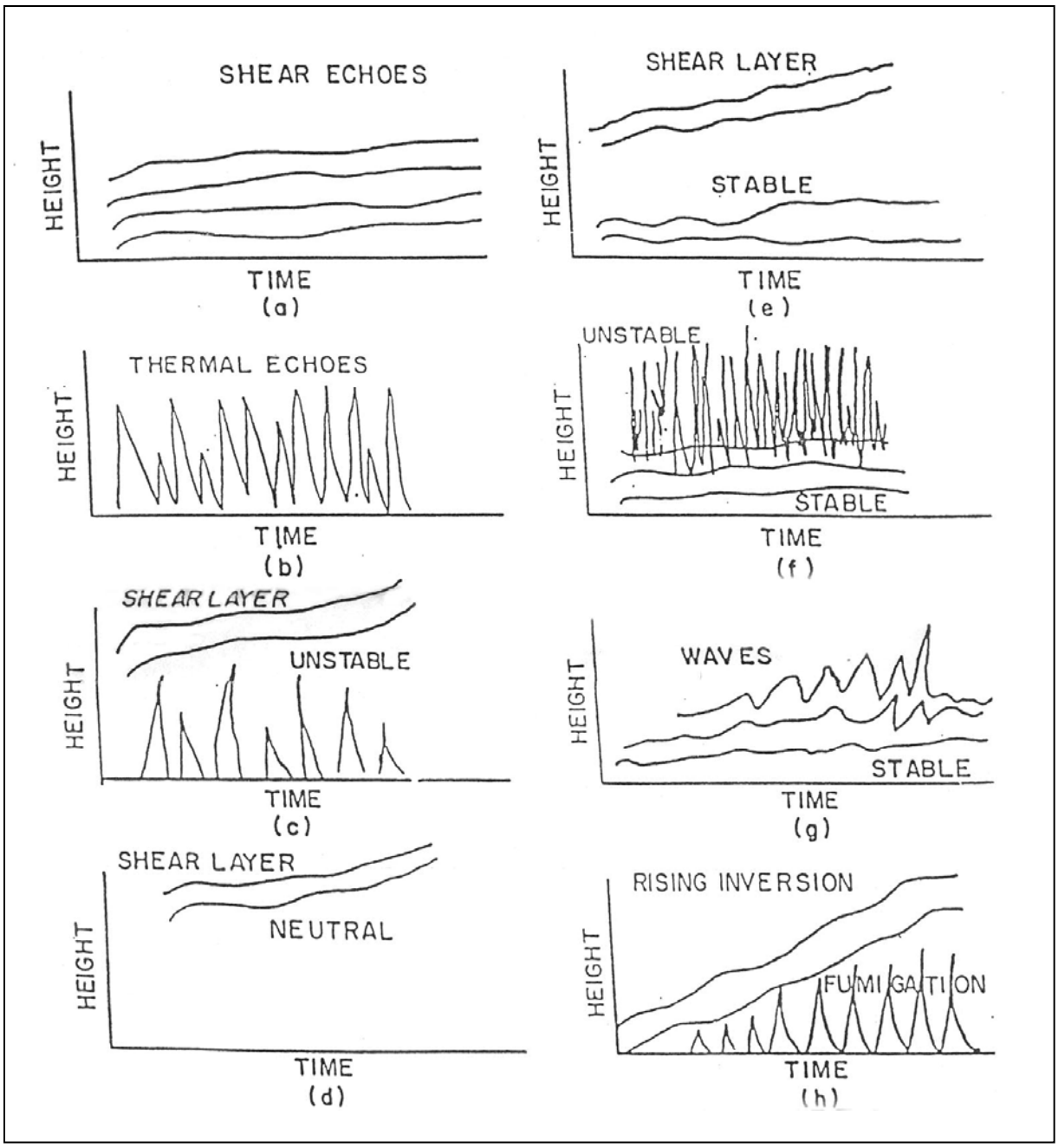

Fig.8 Complexities of Sodar structures

top layer are formed due to nocturnal cooling of the ground under slight or no wind conditions. Thickness of these layers may slightly increase with advance of time due to increased nocturnal cooling of the ground. Such a structure is characteristic of stable atmospheric conditions and is called ground based layer with flat top or simply the ground inversion (see Fig. 6).

Medium to strong surface winds bring in mixing within the ground based stable layer resulting in random spikes at the top of the structure. Thus the structure is associated with mechanical mixing due to winds and is called spiky layer (see Fig.6). Such spiky inversion signifies relatively weaker ABL stability as compared to the stability under flat top inversion of same depth.

Turbulent weather conditions associated with wind shear under clear sky conditions are mostly responsible to develop, sometimes, a stratified/multi layer or elevated layer structure with or without undulations superimposed over them. Multiple layers normally represent the wind shear structure under light wind and highly stable conditions of the atmosphere. The ABL stability is relatively more as compared to the stability under inversion with flat top.

At times, multiple layers structures may also be associated to the advection of super-imposed flow representing some mesoscale weather phenomena. However, the occurrence of a well defined distinct thick elevated layer (see Fig.6) represents either of the presence of fog layer, subsidence layer, marine boundary layer, the approaching or persisting

turbulent weather conditions. It may be mentioned that very frequent and the prolonged duration of elevated layers in an industrial area is not desirable as it leads to limit the vertical dispersion of pollutants which at times may cause pollution hazards under conditions of accidental release.

Undulations or the wavy structures are seen under calm to medium wind conditions. They are also seen before and after the occurrence of thunder storm and dust storm. The undulating structures may either exhibit features of symmetric sinusoidal wave motion under clear weather conditions or they may show slightly asymmetric rounded saw tooth type wave motion under turbulent weather conditions.

These waves are found to have periods of the order of few minutes and amplitude in the range of 100 m peak to peak (Aggarwal *et al*. 1980). It is considered that these undulations represent gravity waves developed in the regions separating two air masses of different density and wind vector. At other times they are also associated either with convective stability during fumigation period or with wind shear variations under stable conditions. However, such structures are manifestations of still higher stable atmospheric conditions.

4. PARAMETERISATION OF AIR POLLUTION METEOROLOGY

The air pollution meteorological parameters of interest for air quality studies include wind vector profile, turbulence intensity,

atmospheric stability class, mixing/inversion height and the diffusion parameters. The researchers have shown that a Doppler Sodar has the potential to deliver all these parameters to fairly good accuracy. While, a monostatic Sodar can provides good estimates of the mixing height and the stability class at very economical cost. In pursuit of the same cause the present work is focused on studies of the mixing / inversion height and stability classes of the ABL.

4.1 Mixing Height

4.1.1 Unstable Atmospheric Boundary Layer

The turbulence in the lower atmosphere is responsible for dispersion of the emissions and it also serves as tracers for generating Sodar signals. Therefore, a measure of the vertical height of the turbulent region of ABL or the thermal plumes (on Sodar echograms) during day time and of the shear echoes during night time (Fig. 9a) gives a direct measure of the mixing depth for the emissions. However, it may be pointed out that a measurement of the height of the thermal plumes during day time by Sodar gives an under-estimate value as it is a function of the Sodar sensitivity in relation to the prevailing ambient noise which is high enough during day time as compared to night time. A true measure of the unstable mixing depth can only be made in case thermal plumes are capped by a shear echo layer (Fig. 9b).

The observed height of the thermal plumes is the most active mixing height during day time. Based on the correlation studies of the Sodar observed height of the thermal plumes and the actual mixing

height of the convective boundary layer (CBL) using the Holzworth model in radiosonde data (using the simultaneous Sodar and radiosonde observations made at IMD, Aya Nagar, Delhi) an empirical relationship has been worked out (Singal and Gera, 1982) to determine the actual mixing height of CBL using the Sodar observed height of the thermal plumes. The said relationship, given below, is used in the present work.

$$\text{Mixing Height, MH} = \lambda - ½ (4.24\ Ph + 95) \text{ meters}$$

Where Ph is the plume height (in meters) as observed on the Sodar echograms and λ is the topographical correction factor given by the following expression

$$\lambda = zi/z0$$

zi being the roughness length for the site under consideration (G.B. Pant Institute of Himalayan Environment & Development, Gangtok) and z0 is the roughness length for the site where the above relation was developed (IMD, Ayanagar, Delhi). It may be mentioned that the Sodar echoes, at any site, are the manifestations of the resultant of turbulent conditions caused by interaction of topographical features and several prevailing meteorological factors viz: wind, vertical transfer of heat, mass, momentum, moisture etc. As such the said empirical relationship may be assumed to be valid for different topographical sites, including the present site under consideration

Further more, the relationship has been re- examined through

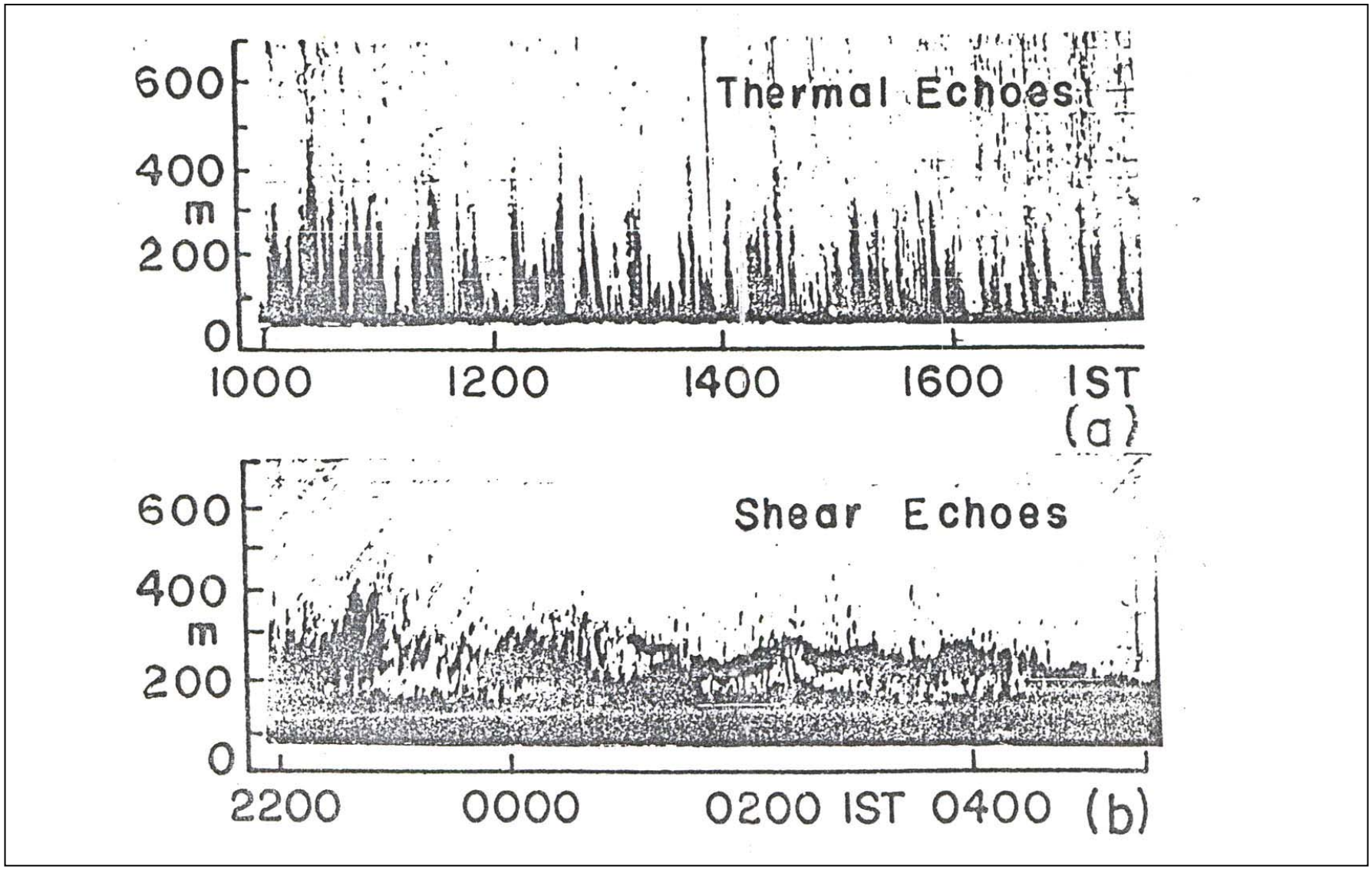

Fig. 9a The two types of characteristic Sodar structures-thermal echoes and shear echoes

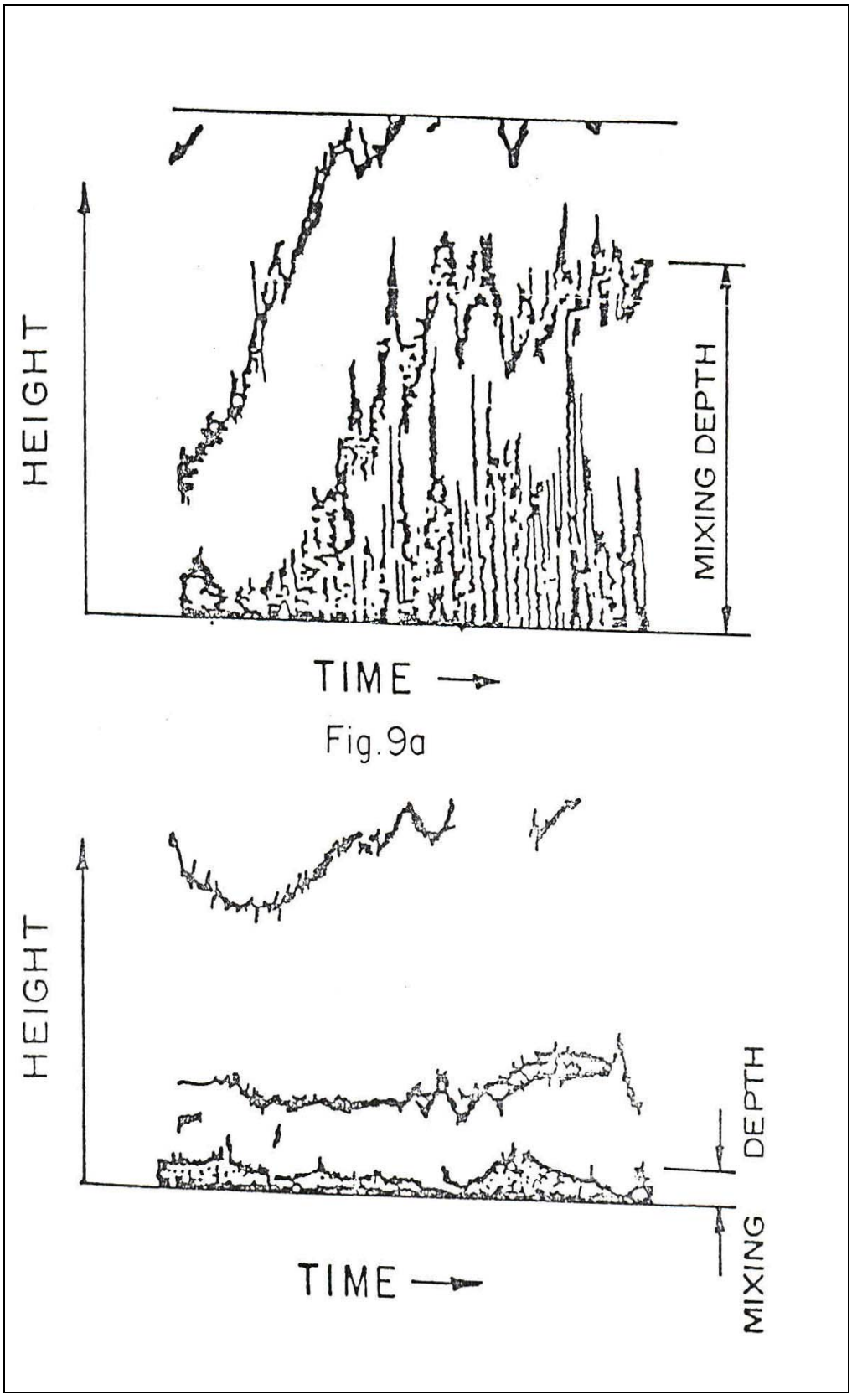

Fig. 9b Criteria for determining mixing depth

another experimental observations made in the hilly area of complex terrain in Guwahati (Singal and Kumar, 1998). The relationship has been found to hold good. Therefore, it is reasonable to assume the validity of relationship for the present work too. In the present case, the Sodar site (Gangtok) is also hilly and topographical features are similar to that of Guwahati, therefore the correction factor in the empirical relationship is taken as unity (assuming the roughness length for two sites is nearly same).

4.1.2 Stable Atmospheric Boundary Layer

Under stable ABL conditions, the height of ground based shear echoes or the flat / spiky top layer gives a fairly good estimate of the mixing height (see Fig. 9b). The precise height of shear echoes is determined from the intensity profile of Sodar returns of each sweep, using an off line program.

In the present case, the Sodar probes the ABL at sweep rate of 4 sec. The received signal (or the digital data) is processed, online, to produce echograms showing pictorial view of the dynamics of the meteorological phenomenon prevailing in ABL.

An offline computer program, based on Sodar pattern recognition and the criterion (Beyrich, 1993, Coulter, 1979, and Twang, 1978) laid down for mixing height determination under different meteorological conditions, is used to derive mixing height values using the digital data file. The program computes one value of the mixing height from each

sweep of received signals. Confining ourselves to the requirement of hourly mixing height studies, 900 values of mixing height are obtained in each hour of the day. These 900 values are averaged to obtain one hourly mean value of mixing height. The hourly mean data, obtained on different days of observations during the month, is further processed to compute monthly mean diurnal variation of mixing height.

4.2 Atmospheric Stability Class

Atmospheric stability is a measure of the prevailing turbulence strength which ranges over a broad spectrum. It ranges from vigorous turbulence (extremely unstable ABL) to nearly no turbulence (extremely stable ABL) conditions. Since Sodar echoes represent the turbulent regions of the atmosphere, the nature and extend of the Sodar echoes have been used (Clark, 1977) to broadly characterize the general state of the atmospheric stability *viz.* stable, unstable and neutral However, practical application for air quality studies requires the estimation of Pasquill stability class rather than knowledge of stable or unstable condition only.

In this context, several attempts have been made (Singal *et al.* 1984, Singal *et al*.1989, Balser and Netterville,1981, Thomas,1986, Best *et al*. 1986) to correlate Sodar structural details and the Pasquill stability classes which are derived by the standard methods using simultaneous measurements of meteorological parameters of wind speed, wind direction, temperature gradient, bulk Richardson number, standard deviation of vertical and horizontal wind speed and direction, solar

radiation, cloud cover etc. It has been shown (Singal *et al*.1984) that Sodar derived stability classes are in fairly good agreement with those derived by conventional methods for practical purposes. In pursuit of the same, based on correlation studies of the site specific observed echoes, at Gangtok, and the Sodar derived variance of vertical wind velocity, a scheme has been worked out to derive stability class using Sodar structural details.

Based on the present correlation studies and the studies reported earlier, it has been seen that on normal clear days, the stable category of the ABL exists mostly during night time and the unstable category exists during day time However, the neutral stability can exist both during day and night time depending upon the prevailing meteorological conditions. It is seen to occur, more specifically, around sunset hours in the evening, when the transition from unstable to stable ABL takes place. This transitional period or the neutral stability is marked as a blank record showing no structure on Sodar record. Besides, the strong surface winds which make the facsimile record totally dark all through its height also depict the duration of near neutral conditions. The details of the classification scheme are given in Table 1.

It may be mentioned that the Sodar based classification scheme for stability class A, B and C (pertaining to the unstable ABL) is plume height dependent. The height to which plume echoes are visible on a sounder facsimile record depends on the background noise level, the sensitivity and acoustic power of the sounder. Moreover, the true height to which thermal plumes would rise depends on temperature gradient

and the intensity of turbulent temperature fluctuations within these plumes. Therefore, one would not necessarily expect a scheme developed at one site with a particular type of sounder to be totally applicable for a second site with a different make of sounder. Thus, a little modified scheme, based on correlation of plume height and variance of vertical velocity has been used in the present case. For stable ABL (stability E and F) the scheme stands valid for different sites, provided the acoustic sounder of the same specification is used. This is true in the present case.

Table 1. Sodar based stability classification scheme

Local Time	Sodar structure	Stability Class
0500-1000	Stable layer (>150m)	E
	Stable layer (<150m)	F
	Rising layer	C
	Elevated layer/or multi-layers/or waves	F
	(200m) ≥ Convective plumes (≥125m)	B
	Convective plumes(<125m)	C
	No structure	D
1000-1800	Rising layer	C
	Convective plumes (≥200m)	A
	Convective plumes (125-200m)	B
	Convective plumes (≤125m)	C
	No structure	D
	Stable layer	E
	Stable layer with elevated layer /waves	F
	Elevated layer with plumes below	C
	Stable l	

1800-2100	No structure	D
	Stable layer with flat top/short spikes	E
	Stable layer with tall spikes (≥300m)	D
	Stable layer with wavy top	F
	Elevated layer/waves	F
2100-0500	No structure	D
	Stable layer with flat top (<125m)	F
	Stable layer with flat top (≥125m)	E
	Stable layer with spikes (≥300m)	D
	Stable layer with wavy top	F
	Elevated layer	F

Broad features of the classification scheme can be summarized as follows:

i) Category A, representing strongly unstable conditions, is marked on the Sodar echograms by well-defined families of tall thermal plumes.

ii) Category B, representing moderately unstable conditions, is marked on the Sodar echograms by thermal plumes of moderate height.

iii) Category C, representing slightly unstable conditions, is marked on the Sodar echograms by very shallow plumes formed during the early morning and late afternoon hours.

iv) Category D, representing near neutral conditions, is marked on the Sodar echograms either by no structure or by dark bands due to strong wind induced noise.

v) Category E, representing slightly / moderately stable conditions, is

marked on the echograms either by a ground based horizontal layer of higher depth or by the tall spiky layer structures during the night time

vi) Category F, representing highly stable conditions, is depicted on Sodar echograms either by shallow and flat top ground based layer or by shallow stratified layer structure or presence of elevated and wavy layers in addition to ground inversion.

5. GANGTOK SODAR AND SITE CHARACTERISTICS

The Sodar system installed at G.B. Pant Institute, Gangtok is shown in Fig.10. The whole system has been indigenously designed, developed and fabricated at the National Physical Laboratory, New Delhi.

The Sodar antenna was set up on the terrace of water tank outside main building while the electronic and recording system was housed side by, in the meteorological laboratory located a little down below.

The system characteristics are given in Table 2.

The system operates at the fixed audio frequency of 2250 Hz. High power audible tone bursts of 100 ms duration are transmitted every 4 seconds which offer a probing range of about 700 m of the lower atmosphere.

A parabolic dish of aperture 1.2 m is used as the acoustic

antenna. At the focus of the dish a transducer fitted with an exponential horn assembly is placed. The antenna dish is surrounded by the 2 m high conical apex acoustic shield.

The operational frequency, duration of the tone burst and pulse repetition rate (determining the probing range) are selectable through user friendly software of the system.

The system was installed at Gangtok during October 2003. Data collected during the year long period (October, 2003-September, 2004) has been analyzed and presented in this report.

5.1 Site characteristics

Sikkim is subject to the Indian monsoon that sweeps up from the Bay of Bengal, bringing heavy rainfall from early June until the end of September. The post-monsoon months of October and November provide settled conditions with clear views of the mountains. The nighttime temperatures above 3,500 m frequently fall below freezing.

The Sodar location is more or less on the sloping edge of deep valley on one side and hills on the other side. Since mixing height characteristics are manifestations of the upward transfer of heat, momentum and moisture flux in the ABL, the micrometeorological factors associated with topographical features of mountain characteristics, winds, frequent clouds, etc. are likely to induce

modifications in the normal characteristics of mixing height on a diurnal scale. Sodar echograms (or the facsimile records) provide pictorial view of the occurrence of such modifications in real time.

Table 2. Characteristics of Gangtok Sodar

Transmitted power electrical	40 Watts
Transmitted power acoustical	10 Watts
Pulse width	100 ms
Pulse repetition period	4 sec
Operational range	700 m
Receiver bandwidth	50 Hz
Frequency of operation	2250 Hz
Acoustic velocity	340 m/s (average)
Receiver gain	80 Db
Transmit –receive antenna	Parabolic reflector dish surrounded by Conical acoustic cuff
Receiver area	2.5 sq. m
Pre amplifier sensitivity	Fraction of a micro-Volt
Recorder	Facsimile/ dot matrix/ laser printer

6. RESULTS

Sodar observations made during the period October 2003 to September 2004 have been examined and analyzed to work out the monthly mean diurnal variation of mixing height and Pasquill stability classes of the ABL.

6.1 Physical Characteristics

The examination of Sodar echograms has revealed that ABL phenomenon such as free / forced convection, inversions, fumigation, elevated shear layers/waves etc. are occurring, at the observational site in Gangtok, in accordance with prevailing meteorological conditions.

Typical Sodar records of ABL, observed at Gangtok, representing different meteorological phenomenon are shown in Fig.10. Based on examination of facsimile records, following characteristic features of ABL thermal structures have been observed:

It is seen that the clear thermal plumes [Fig.10a(1)], representing free thermal convection during the day under solar heating of the ground, have been seen during September and October while the diffused thermal plumes [Fig.10a(2)] under conditions of poor incoming solar radiation, cloud cover and superimposed induced mechanical mixing due to combined action of ambient and mountain winds are seen during other months .

Ground based inversion with more or less flat top [Fig.10a(3)], representing stable atmospheric conditions and/or spiky inversion layers [see Fig.10a(3)], representing wind induced mechanical mixing within the stable ABL, are seen during night time on all the days of observations.

Eroding inversion [Fig.10a(4)], representing inversion breakup

under the transition phase of the stable to unstable ABL after sunrise, is distinctly seen under calm and clear atmospheric conditions during the post monsoon (September and October) months and on clear days of winter. However, it is seen to be prolonged till afternoon during the winter months November to January. The observation is similar to what is normally observed during winter over the plain land areas.

Elevated wavy/ descending layers [Fig.10e(5)] generally associated with the occurrence of wind shear, subsidence; frontal passage, thunderstorm etc. are seen on several days of observations. However, the occurrence of elevated structures is seen to be more confined to the winter period. Such layers have been seen (Singal *et al*. 1984) to be associated with the outburst of dust storm/ thunderstorm at NPL, New Delhi.

6.2 Mixing Height Studies

The month wise hourly averaged values of mixing height are given in Table 3 and the plot of diurnal variation of mixing height is shown in Fig.11.

The studies aiming to evaluate the characteristics of the diurnal variation of mixing height shows that the mixing height of unstable atmospheric boundary layer under sunshine hours during the day is fairly good. The maximum mixing height of about 2 Km is seen during the post monsoon month of October while a maximum height of about 800 m is seen during the winter month of December. It is seen to vary between

Fig.10 Sodar experiment set-up at G.B. Pant Institute, Gangtok

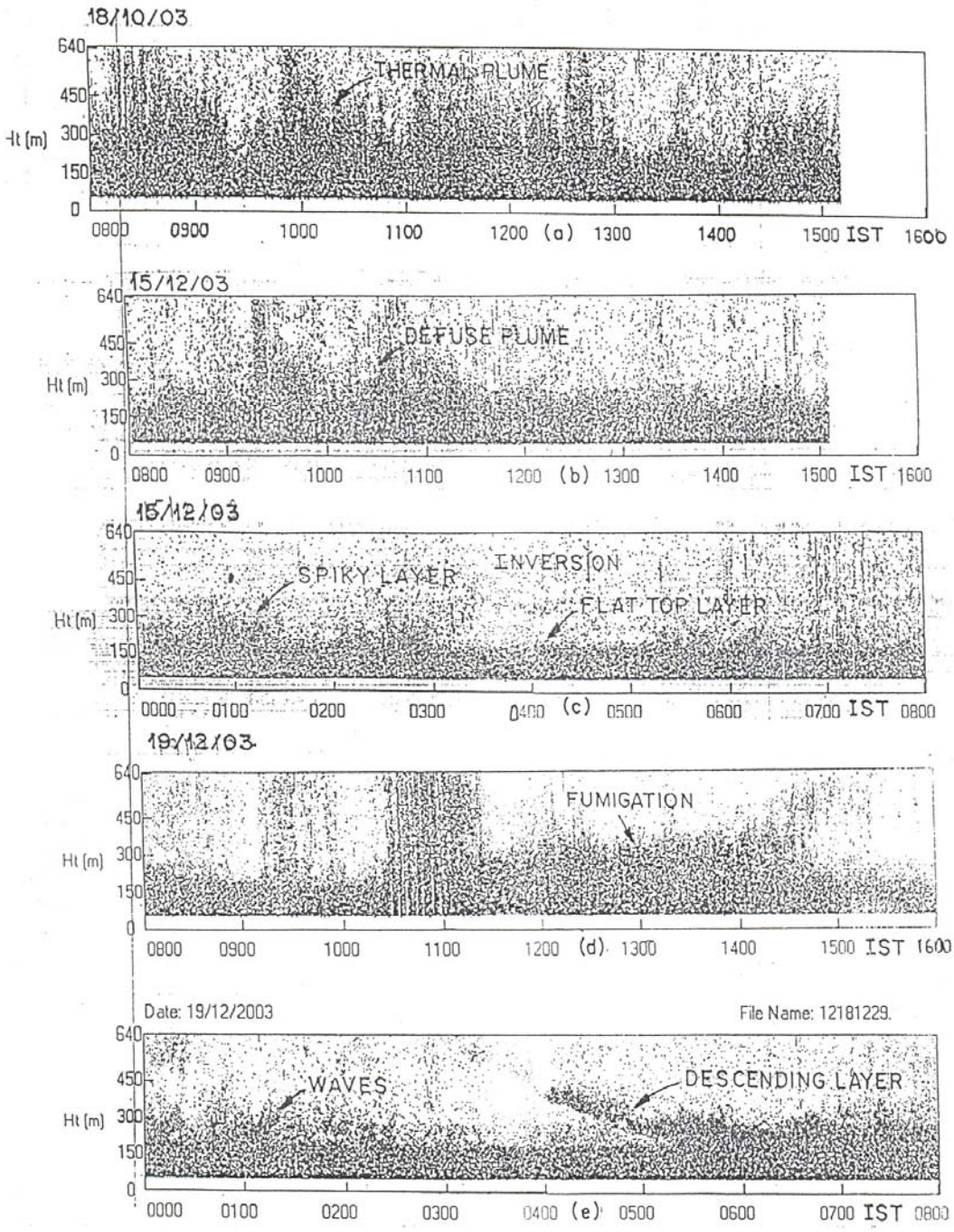

Fig.10a Various Sodar structure observed at G.B. Pant Institute, Gangtok

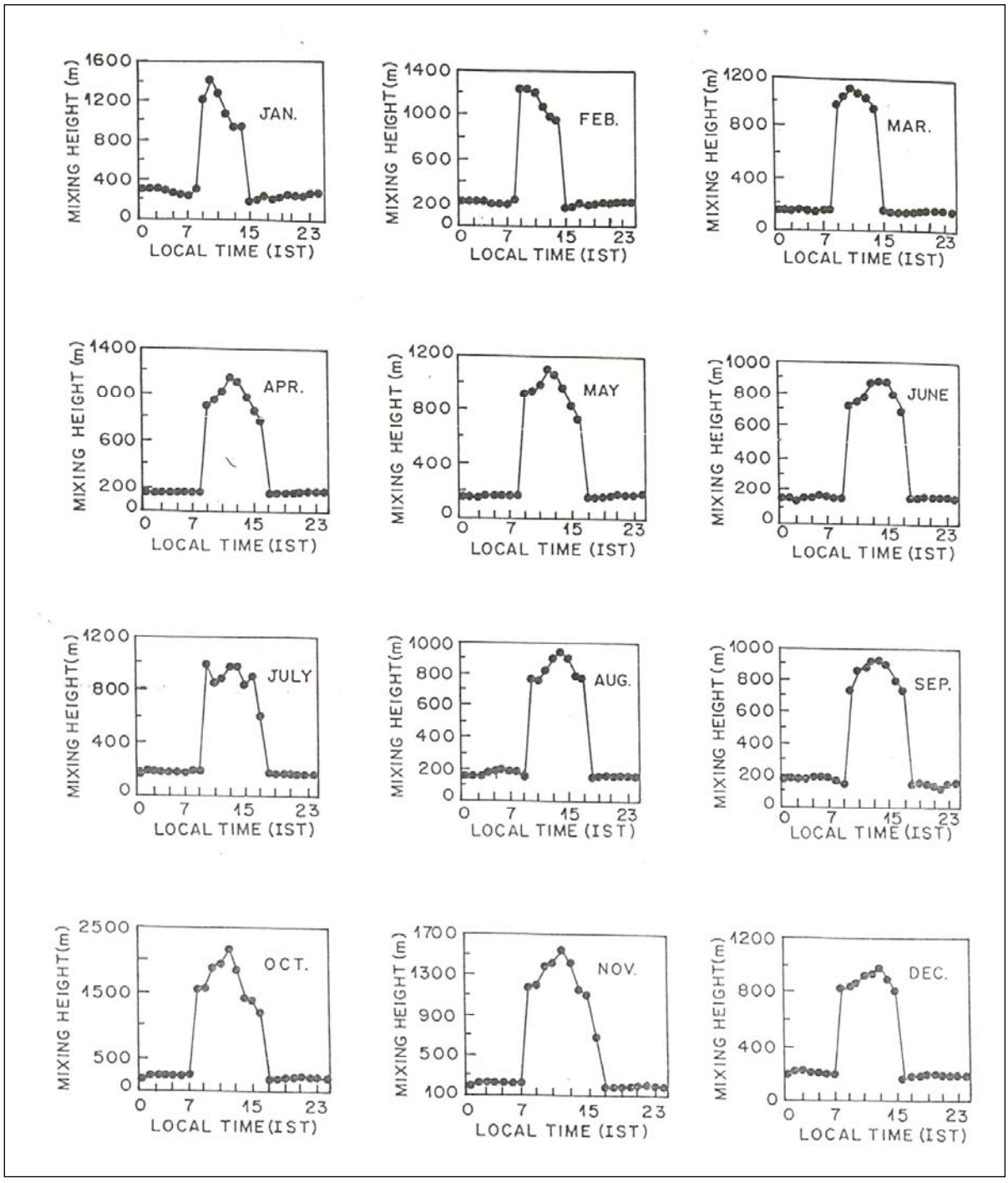

Fig. 11 Monthly diurnal variation of averaged mixing height at G.B. Pant Institute, Gangtok, during Oct. 2003 to Sep. 2004

these limits during course of the day and seasonal conditions in accordance with incoming solar radiation, prevailing meteorological conditions and time of the day. The observed maximum of mixing height is comparatively more as compared to maximum mixing height of about 1.6 Km observed in the plane areas of Delhi. However, Singal and Kumar (1998) have reported similar results of observing a mixing height of about 1.7 km for the unstable ABL at Guwahati in the hilly area Assam.

Table 3. Hourly averaged mixing height at Gangtok, during October 2003 to September 2004

Time	Jan	Feb	Mar	Apr	May	Jun	Jul	Aug	Sep	Oct	Nov	Dec
0	298	225	153	148	148	148	152	157	178	183	188	194
1	306	230	156	150	155	149	188	150	180	233	226	219
2	305	230	153	156	140	135	187	153	177	250	230	223
3	285	225	163	160	158	154	184	177	173	250	230	202
4	260	200	151	155	162	157	183	190	190	246	230	202
5	247	200	151	162	170	165	178	200	190	243	220	196
6	228	191	154	160	160	158	177	190	190	250	230	196
7	302	235	170	165	175	156	193	183	160	1540	1180	822
8	1220	1250	990	900	925	151	190	157	150	1582	1200	834
9	1422	1235	1053	950	930	720	996	775	733	1901	1380	868
10	1282	1200	1130	1020	980	741	847	758	860	1943	1420	919
11	1083	1080	1083	1150	1100	775	894	830	869	2156	146	936
12	926	990	1049	1100	1050	864	966	903	920	1850	1420	983
13	935	950	968	970	960	873	966	945	924	1421	1155	894
14	178	170	170	860	830	873	843	903	890	1412	1100	805
15	200	170	147	775	733	796	911	788	796	1212	690	170
16	243	200	145	152	150	690	618	775	733	190	190	180

17	**204**	**185**	**146**	**160**	**155**	**148**	**173**	**152**	**147**	**190**	**190**	**185**
18	**221**	**200**	**150**	**162**	**160**	**158**	**174**	**155**	**157**	**206**	**200**	**198**
19	**256**	**210**	**156**	**171**	**165**	**163**	**172**	**160**	**147**	**216**	**200**	**189**
20	**243**	**200**	**179**	**180**	**182**	**157**	**173**	**160**	**135**	**226**	**210**	**193**
21	**239**	**220**	**166**	**175**	**170**	**161**	**173**	**160**	**120**	**216**	**210**	**185**
22	**279**	**220**	**169**	**182**	**175**	**165**	**167**	**160**	**160**	**216**	**200**	**194**
23	**289**	**220**	**163**	**185**	**180**	**150**	**173**	**152**	**170**	**190**	**200**	**190**

The height of stable boundary layer (inversion) is seen to vary between the minimum of 145 m to maximum of about 300 m. The minimum height is seen during month of March while maximum is observed in the winter month of January. The height of the stable ABL is also higher as compared with height of stable ABL for an urban plane site like Delhi.

Normally the stable ABL or the ground based radiation inversion height is height up to which the effect of radiational cooling of the ground is transmitted. However, in a hilly area with valley topography, there is an additional superimposed contribution of mountain winds or the katabatic winds. These winds carry cold air mass from higher heights down to the slopes and pile the same on to the top of ground based radiation inversion. The effect is more pronounced in winter due to strong inversions. This is considered as the probable cause of, presently, observing increased inversion height (at high altitudes in Gangtok) during the extreme winter period. However, the extent of increase in height will depend upon the altitude and slope of the hill. The present studies have shown a significant contribution for the increase in inversion depth (about 100%) as we advance from summer to winter.

The monthly variation of minimum/ maximum inversion /mixing height heights are shown in Fig.12. The inversion height pertains to the maximum cooling period (0000-0200 hr) for stable ABL and the mixing height pertaining maximum heating period (1200-1400 hr) for unstable ABL It is seen that minimum inversion height is observed during the post winter periods (March - April) while the maximum inversion depth is seen during the winter period (December - January). The observations of relatively more inversion depth in winter are attributed to the role of katabatic winds.

The maximum in mixing height for the unstable boundary layer is seen during the post monsoon period in October when the sky conditions are clear.

The visual inspection of the individual facsimile charts in addition to examination of evolution characteristics of ABL on diurnal scale (see Fig.11) has revealed that the onset of transition from stable to unstable ABL (or the onset of fumigation or the eroding inversion) in general takes place around 0800-0900 hr on normal clear days while the transition from unstable to stable (or the onset of inversion formation) occurs around 1500 hr during winter and around 1600-1700 hours during other months. The studies reveal that the convectively unstable atmospheric conditions or the favorable dispersion conditions are available, on an average for about 8 hours during the day The morning transition period, that normally starts shortly after sunrise, is seen to be comparable with the observations made over plane urban area at NPL (Gera *et al*., 2004).

However, the onset of the evening transition is advanced by an hour as compared with the similar observations for an urban area like Delhi. In fact this transitions takes place around (shortly before) sunset when near neutral conditions develop due to absence of incoming solar radiations and the outgoing radiations from the earth. The observation of advanced evening transition is a characteristic of present site under study and it supports the consideration that the higher altitudes experience faster cooling and the near neutral conditions, at high altitudes, may develop at any time due to rigorous mechanical mixing caused by the strong wind, persistence of clouds etc. Such conditions have been frequently observed, at Gangtok, during the present studies.

The month wise diurnal variation of mixing height is shown in Fig.11. It further shows that maximum in mixing height is observed around noon hours during all the months. This is in agreement with the commonly observed feature, of ABL, associated with maximum of surface temperature at around noon hours.

Another notable feature is that the growth of inversion depth is comparatively more during the winter (December-January) and summer months (April-May) as compared with growth of inversion during other months. During summer it is normal to observe such a feature of ABL due to the availability of excessive heat flux, at source (earth) for cooling at night and other meteorological factors responsible for faster cooling of ground at higher altitudes. However, during winter besides nocturnal cooling, it is the additional contribution of drainage flow of cold air mass down the hill slope that is responsible for the more inversion depth. During other months the growth of inversion is gradual as normally

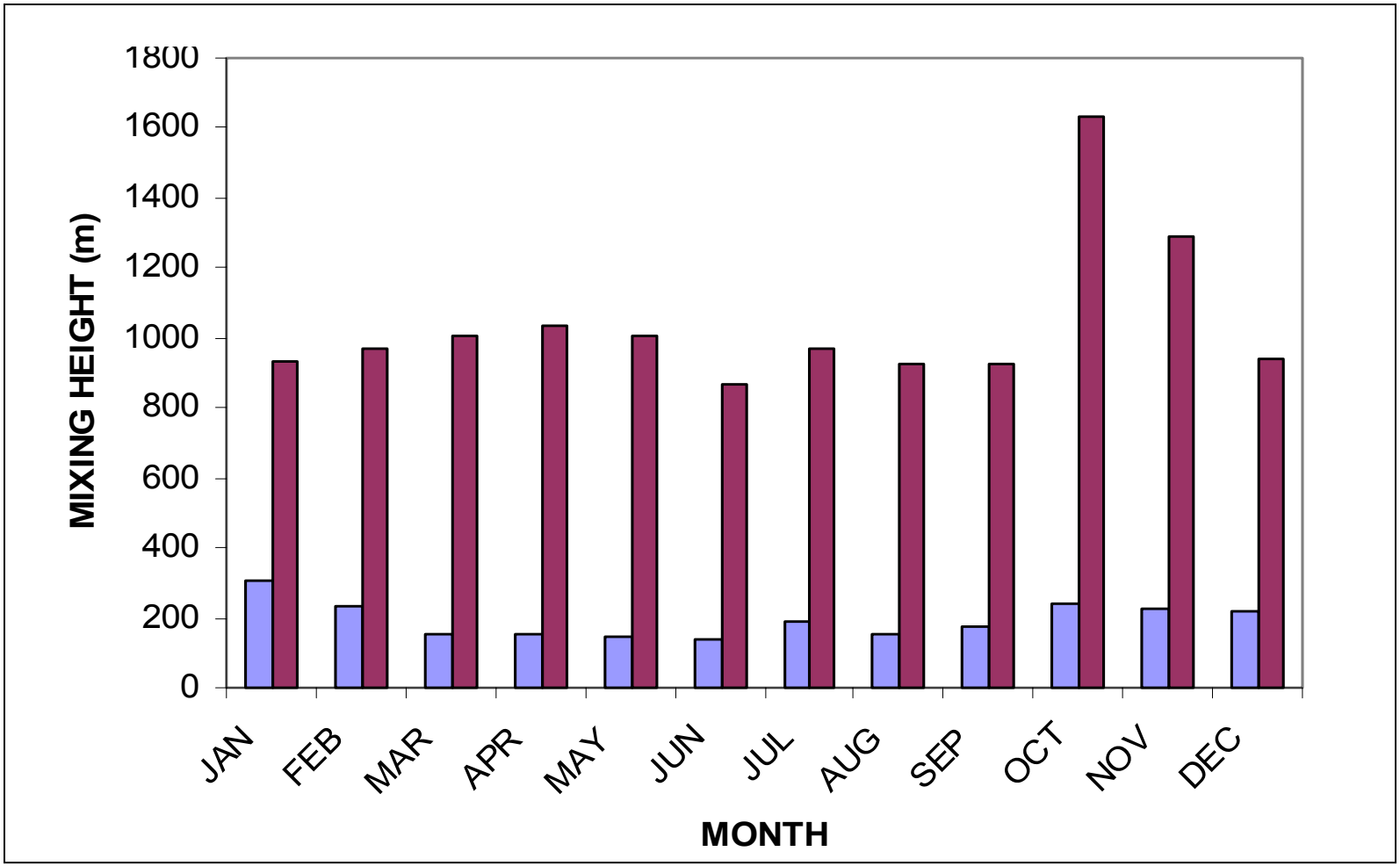

Fig.12 Monthly variation of maximum and minimum inversion/ mixing height (averaged) observed during the periods of maximum cooling (0100-0300 hr) and heating of the ground (1200-1400 hr)

observed, at any site, in accordance with the increased cooling of the ground with the passage of time.

Month wise the cumulative occurrence frequency of inversion depth and mixing height is shown in the Fig.13a, b. and Fig.14a, b. These have been further used to study the monthly inversion height for different three significant occurrence probabilities (Fig.15). It is seen that the inversion height is always more than about 125 m through out the year. Except for the winter months, the inversion depth is around 200 m for the occurrence probability of 75%. There is 50% of occurrence probability for height of the stable ABL (inversion) being around 225 m. The monthly occurrence probabilities shown in Fig.14a, b reveal the inversion depth reaching even more than equal to 300 m. However, such a occurrence probability is les than 10%.

The annual cumulative occurrence frequency for the height of stable and unstable ABL (Fig.16a) further supports the above results. It reveals that the inversion depth up to 150 m is seen for about 90% of the total time of observations. It is up to 200 m for about 75% of the time and more equal to 300 for occurrence probability of less than 10%.

Similar analysis for the unstable ABL shows that the height of the convective boundary layer (CBL) is up to 1.0 Km for about 70% of the total observations. The mixing height is 1.5 Km for about 10% of the time and it is around 2 Km for about 5% of the time.

6.3 Stability Class Studies

Following the stability classification scheme given in Table 1, we have studied the month-wise diurnal variation for the occurrence of Pasquill stability classes at the operational site in Gangtok. It may be mentioned that the occurrence of stability class for a particular hour may very from day to day in accordance with prevailing meteorological conditions. However, the occurrence for a particular stability for a particular hour for more than 75% of the total observations for that particular hour is taken as the significant occurrence or the most probable occurrence of stability for that hour. The significant occurring stabilities are considered for the monthly diurnal variation of stability class.

The month wise diurnal variation of Pasquill stability classes is shown in Figs 16b, c.

The atmosphere becomes near neutral (stability class D) during the sunset hours (1600 -1800 hr) in the evening when the transition from unstable to stable ABL takes place. The occurrence of stability class D is mainly confined to the pre monsoon and post monsoon periods (March, April, September and October). Subsequently, the atmosphere becomes stable by 1800 hr in the evening and it remains stable (stability class E or F) upto about 0800 hr on the following morning. Further, that the stability class F (stronger inversion) is generally seen around midnight hours to early morning hours (2200 hr to 0200 hr) while stability class E

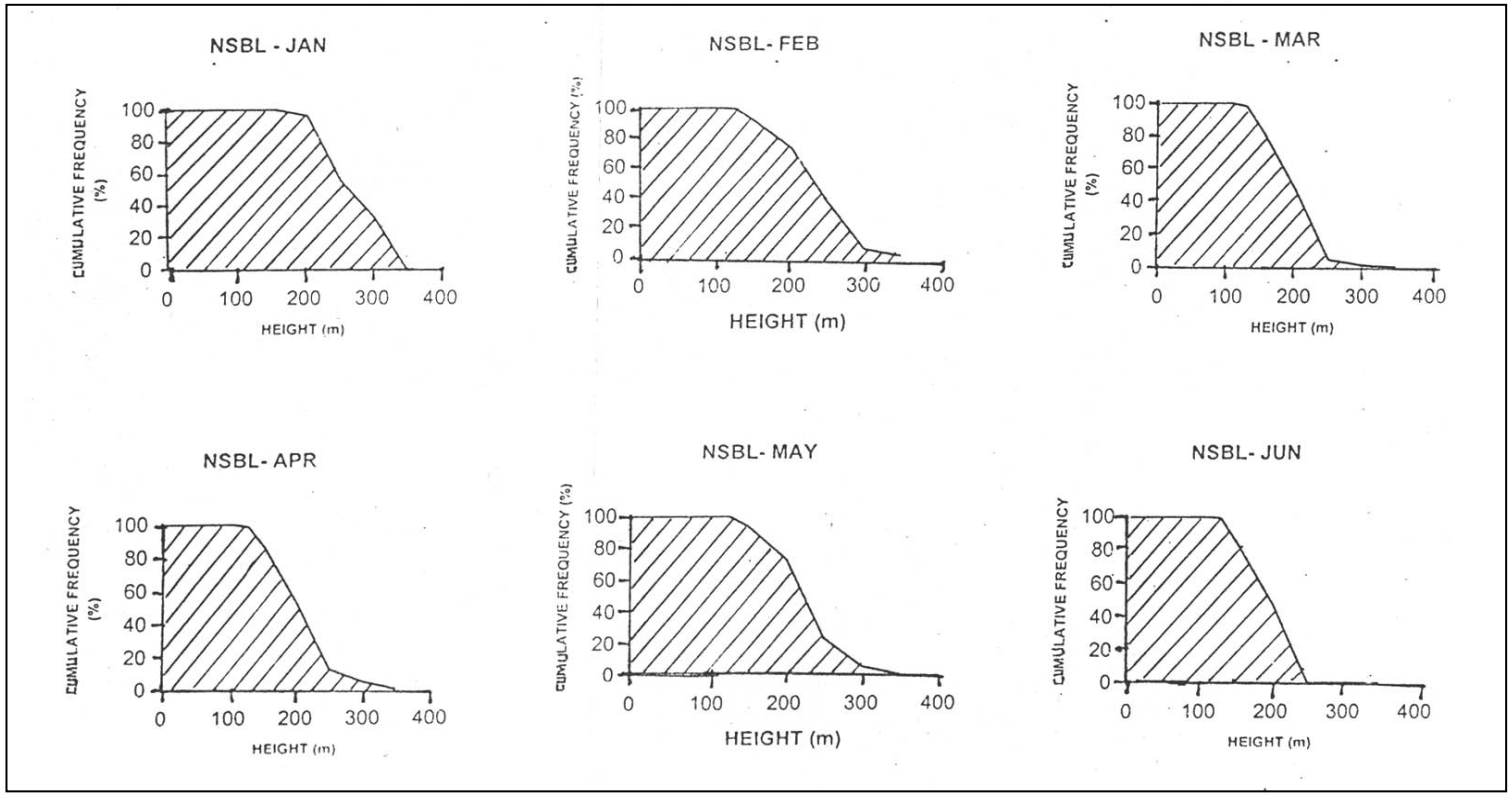

Fig.13a Cumulative occurrence percentage of the mixing height under state atmospheric conditions. (1800-0600 hr) at G.B. Pant Institute, Gangtok

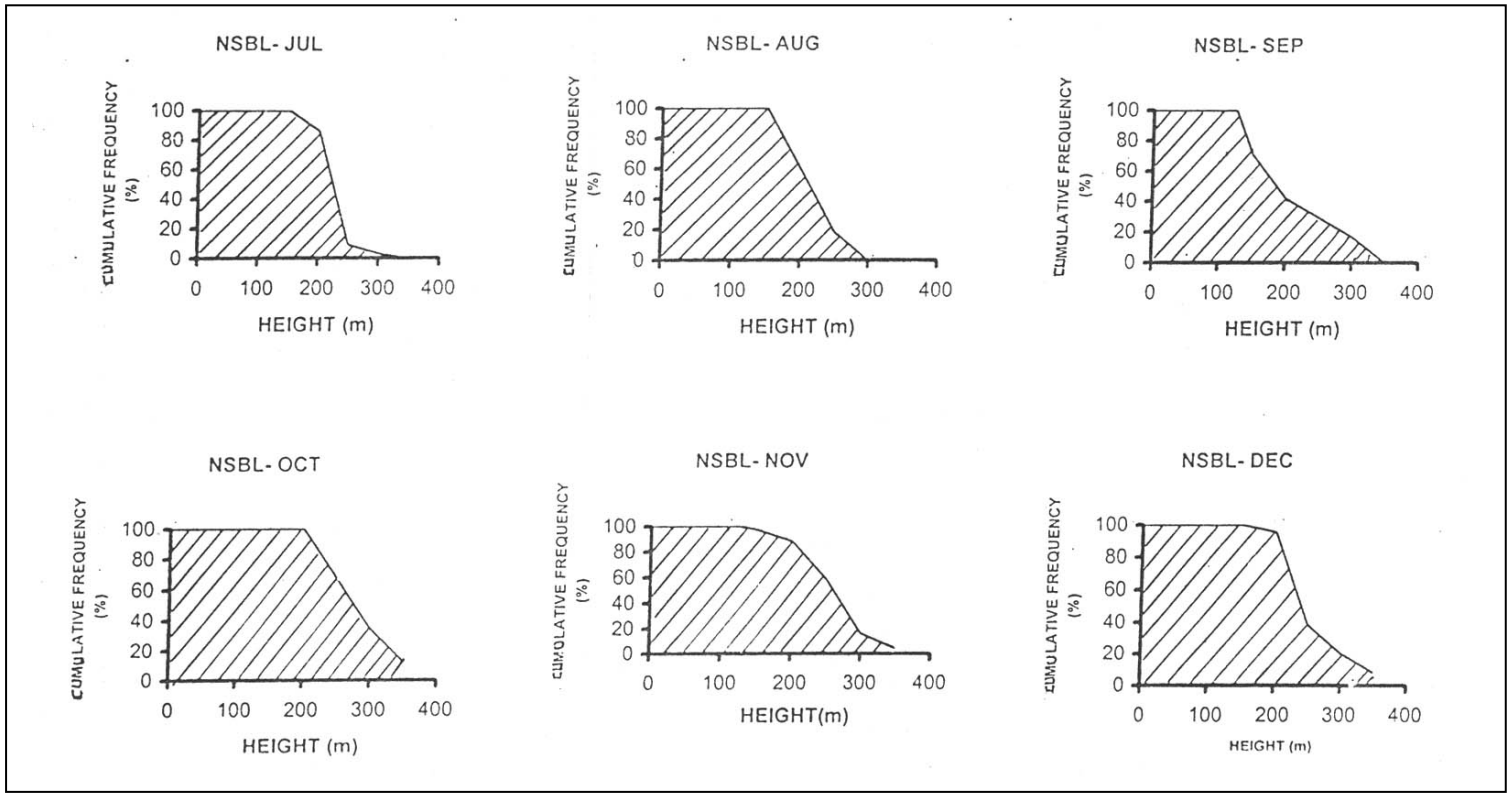

Fig.13b Cumulative occurrence percentage of the mixing height under stable atmospheric conditions. (1800-0600 hr) at G.B. Pant Institute, Gangtok

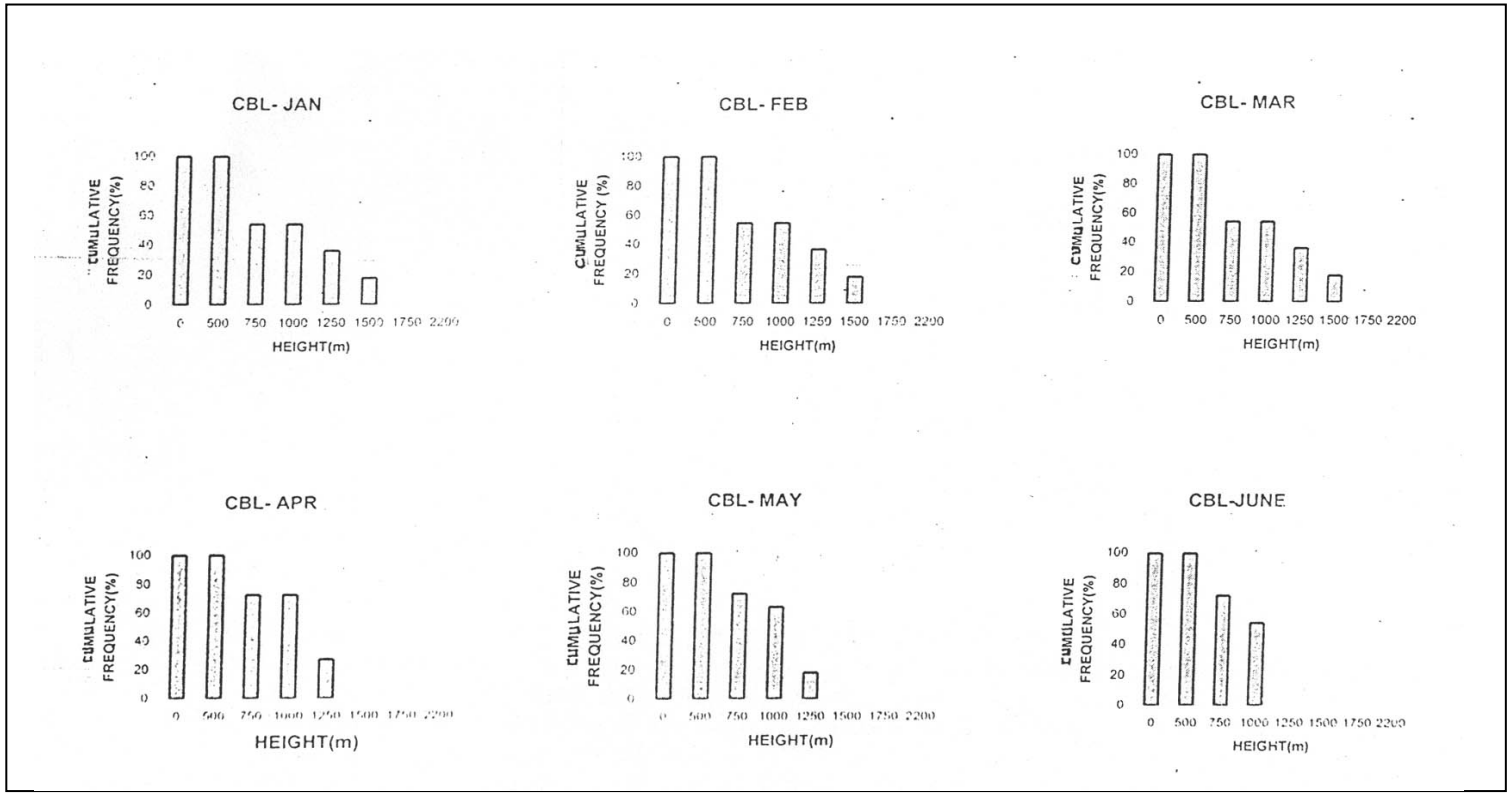

Fig.14a Cumulative occurrence percentage of the mixing height under unstable atmospheric conditions. (0700-1700 hr) at G.B. Pant Institute, Gangtok

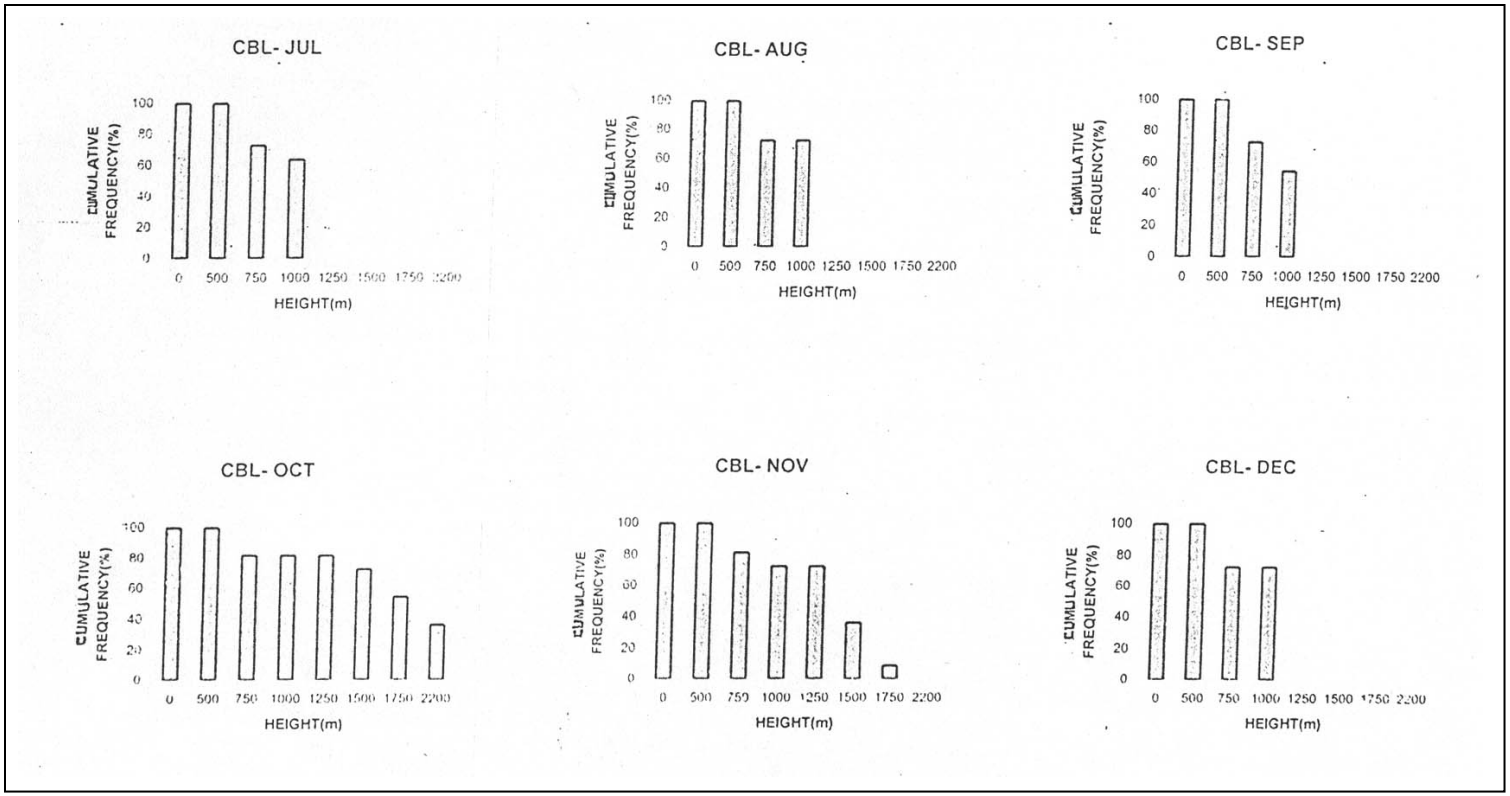

Fig.14b Cumulative occurrence percentage of the mixing height under unstable atmospheric conditions (0700-1700 hr) at G.B. Pant Institute, Gangtok

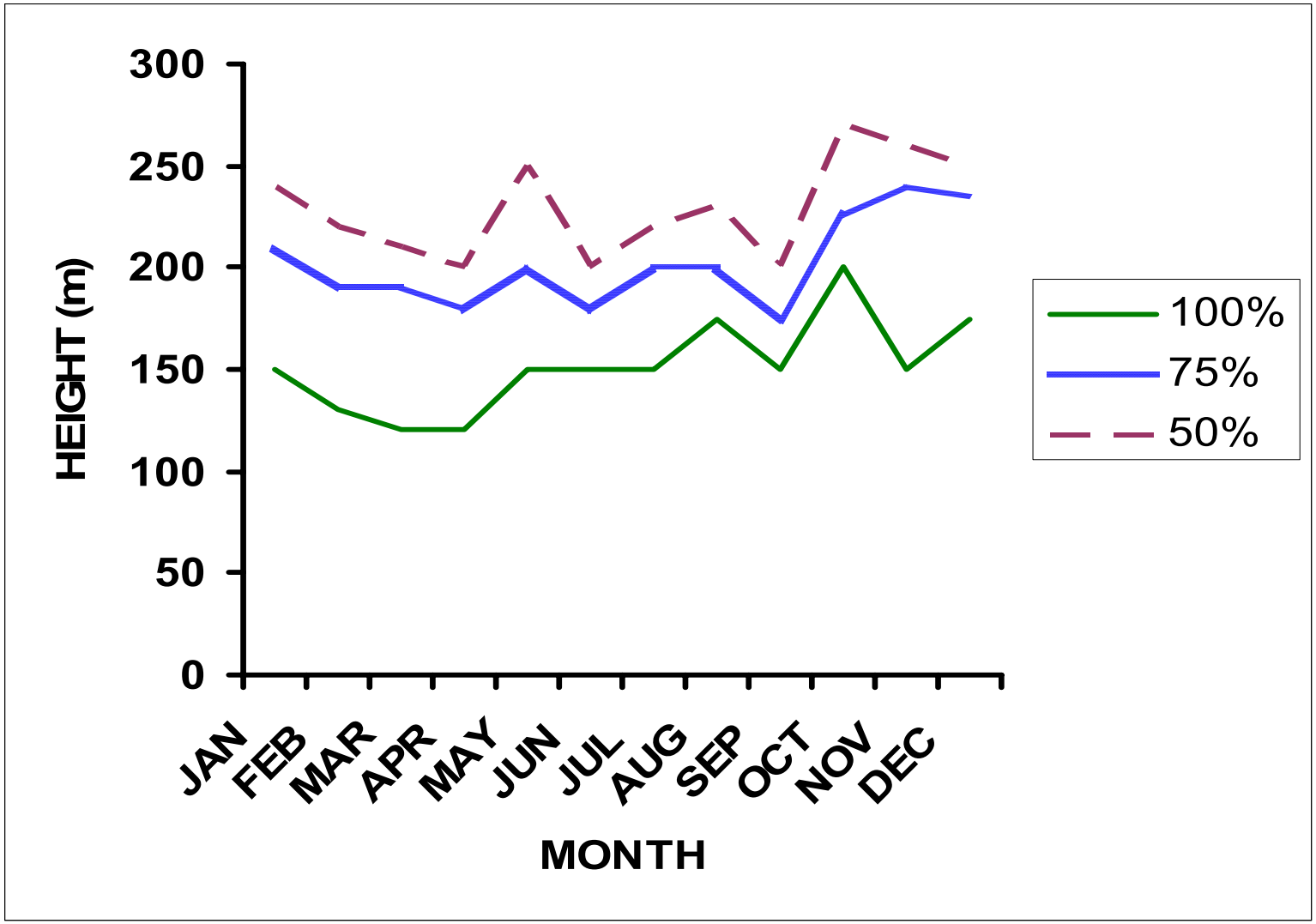

Fig.15 Monthly variation of NSBL height for different cumulative occurrence probabilities

prevails for rest of the night period. Further, that the stability F is seen mainly in and around the winter period October to January.

Considering unstable atmospheric classification, the stability class A is seen to occur for about 2 to 4 hr around noon. The occurrence is about 2 hr from pre monsoon to the monsoon period (February-September). The maximum period of occurrence for about 4-5 hr is seen for a couple of months during the post monsoon to pre– winter months (October-November).

The complete transition from stable to fully developed unstable atmosphere takes place (i.e., the change over of stability class E to B / A through C, indicated by rising layer or shallow plumes) takes place by 08-10 hr during the summer and post monsoon months. It is seen to be as late as 1200-1300 hr during winter. At times there may be no the transition from stable to unstable atmosphere throughout the day, particularly so under synoptic fog conditions.

It may be mentioned that the results shown in Figs 16b, c depict only the average trend of diurnal variation. However, under adverse weather conditions *viz*. occurrence of fog, rain, thunderstorm, frontal passage etc., there may be significant departures from the average trends shown in Fig.16a. Such deviations are generally seen during extreme winter period under dense fog conditions.

A typical example to demonstrate the deviation in the normally

observed trend of diurnal variation of stability class is shown in Fig.17. It is seen that unstable conditions, on a extremely cold day in January, are not observed at all. Through out the day, the atmosphere remained stable (stability E) while normally it is unstable around noon hours with stability A, B or C. Persistence of such conditions for days in succession are hazardous meteorological condition for air pollution and may stand responsible for pollution episode under accidental release of toxic gases etc. These considerations highlight the significance of using site specific real time data for air quality assessments.

Further, studies about the over all annual distribution of atmospheric stabilities (Fig.18) shows that the stable atmospheric conditions with stability class F has been observed for 11.8% of the time while the stability class E has been seen for 39.2%. Similar distribution for unstable atmospheric conditions shows the highly unstable conditions (stability A) occurring for 23.6%, moderately unstable (stability B) for 13.9% and weekly unstable condition or the stability C for 10.1% of the total observations.

7. THERMAL STRUCTURE ANOMALY – A NEW OBSERVATION

During the course of observations, an interesting observations calling for further R&D have been seen. During the winter period, it is normal to see, at any site, delayed or prolonged fumigation, slowly breaking or at times non breaking inversion conditions, elevated fog layer etc. However, a large scale sharply descending upper air mass, around sun rise hours in the morning (Fig.19), has been seen at

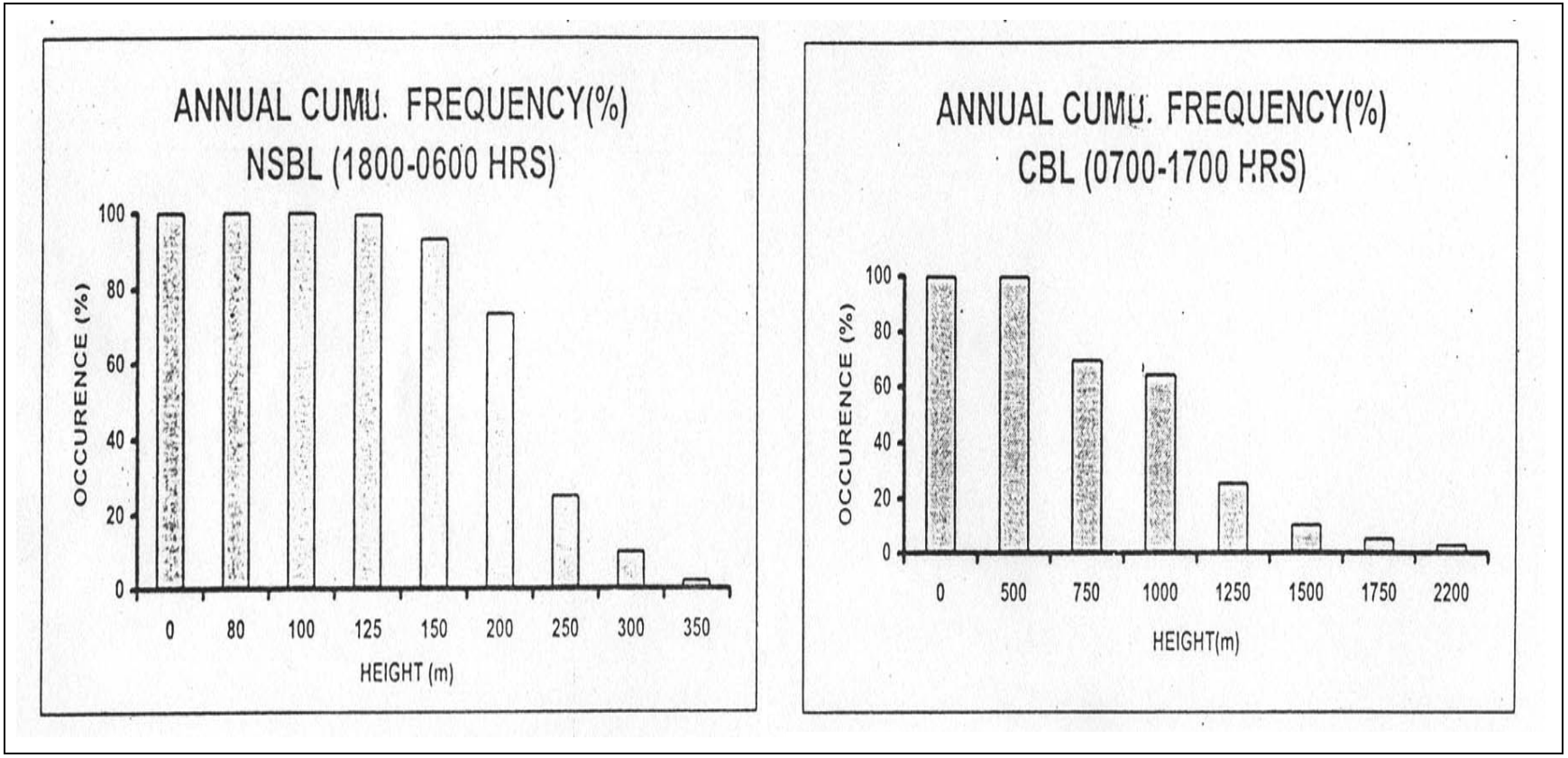

Fig.16a Annual cumulative occurrence percentage of the mixing height under stable and unstable boundary layer conditions at G.B. Pant Institute, Gangtok

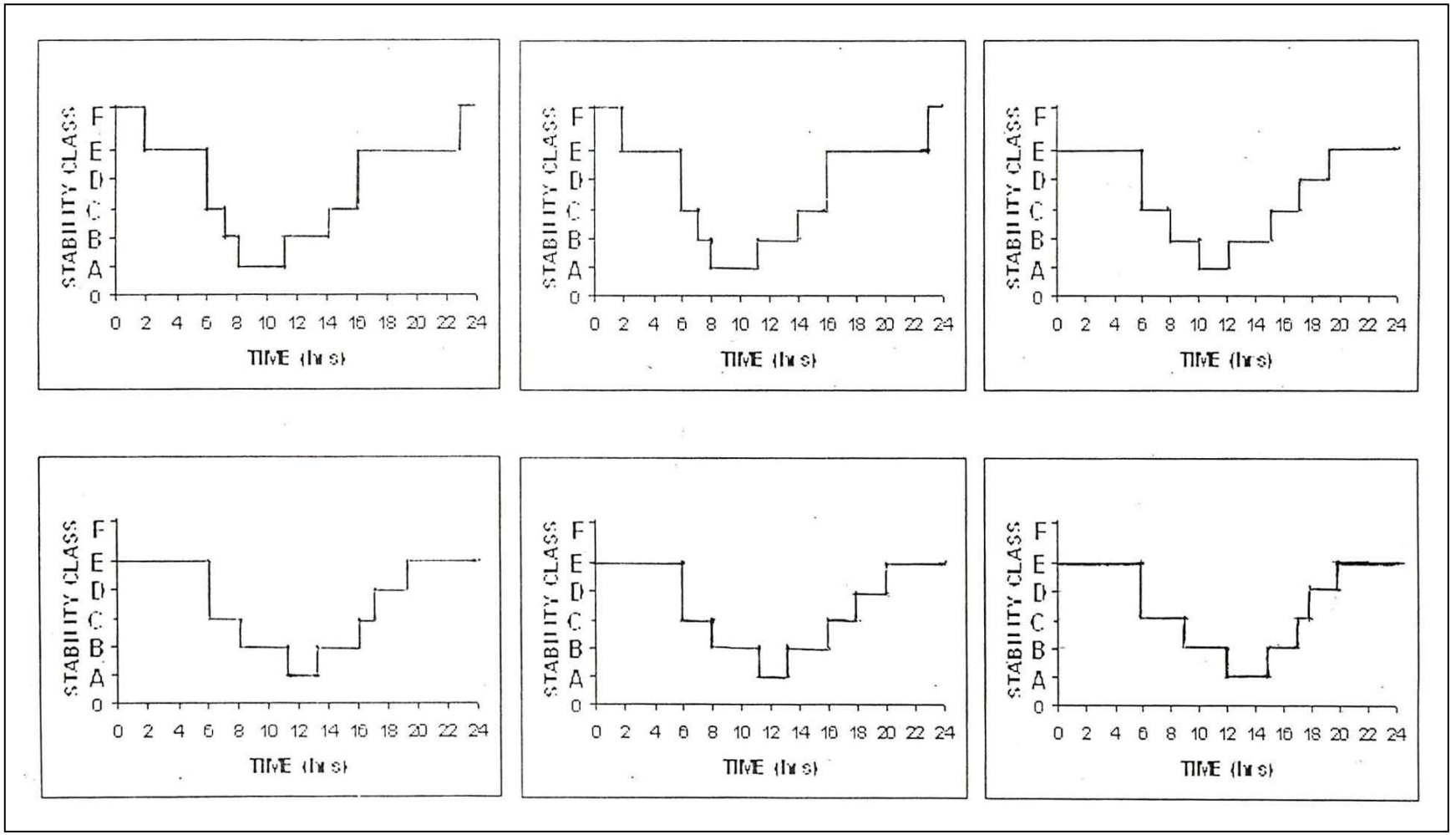

Fig.16b Monthly mean diurnal variation of stability class

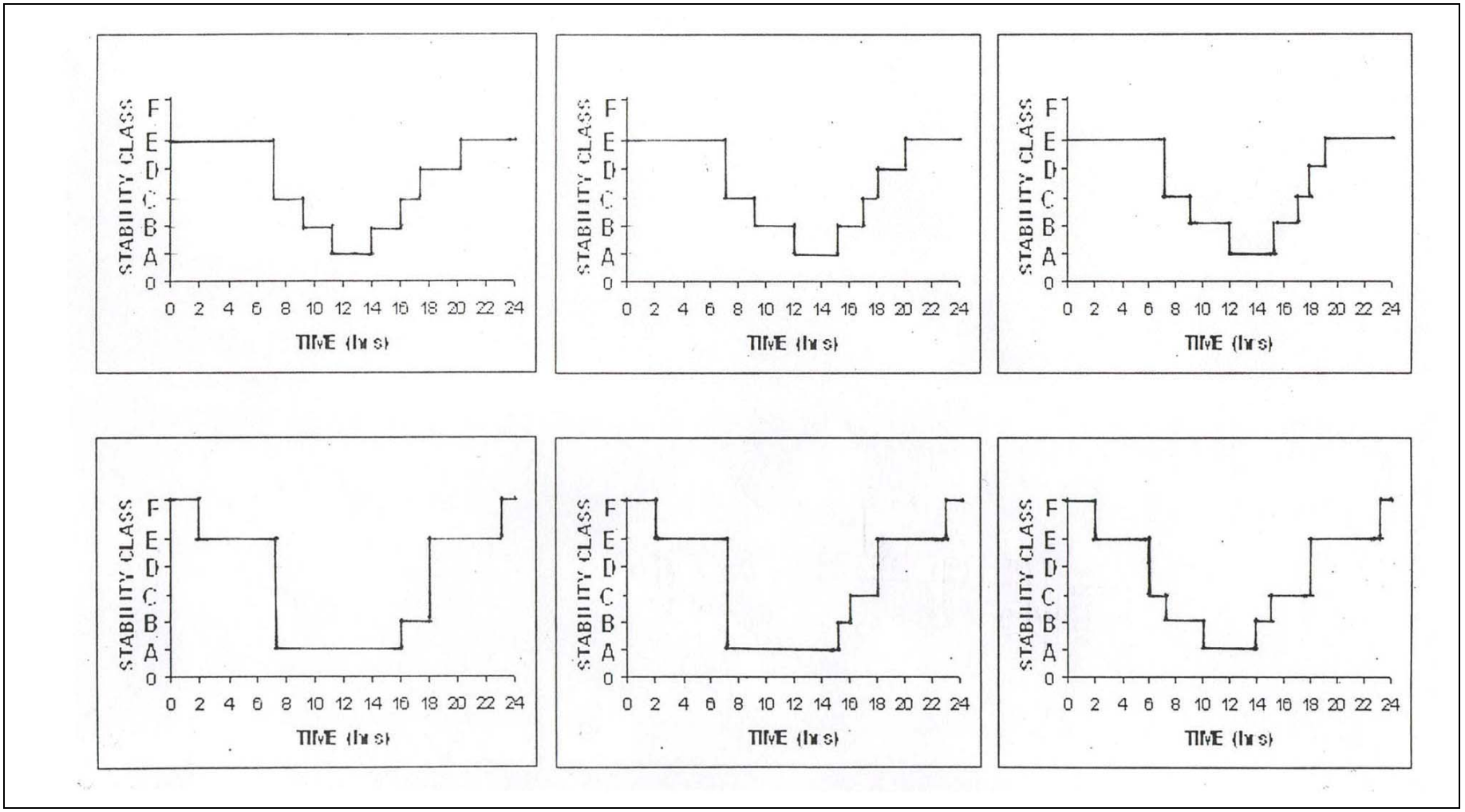

Fig.16c Monthly mean diurnal variation of stability class

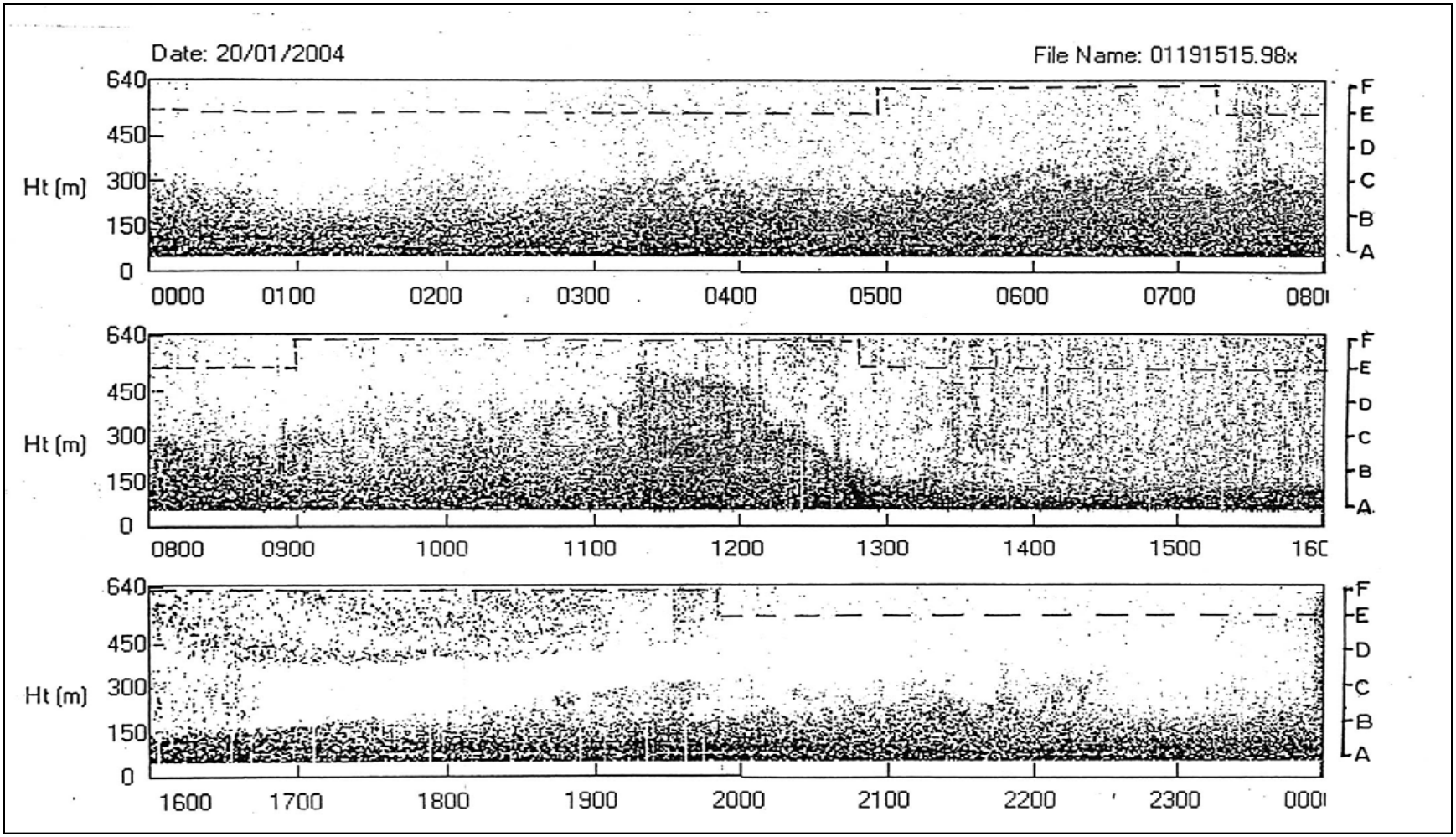

Fig.17 Deviation in the normally observed trend of diurnal variation of stability class

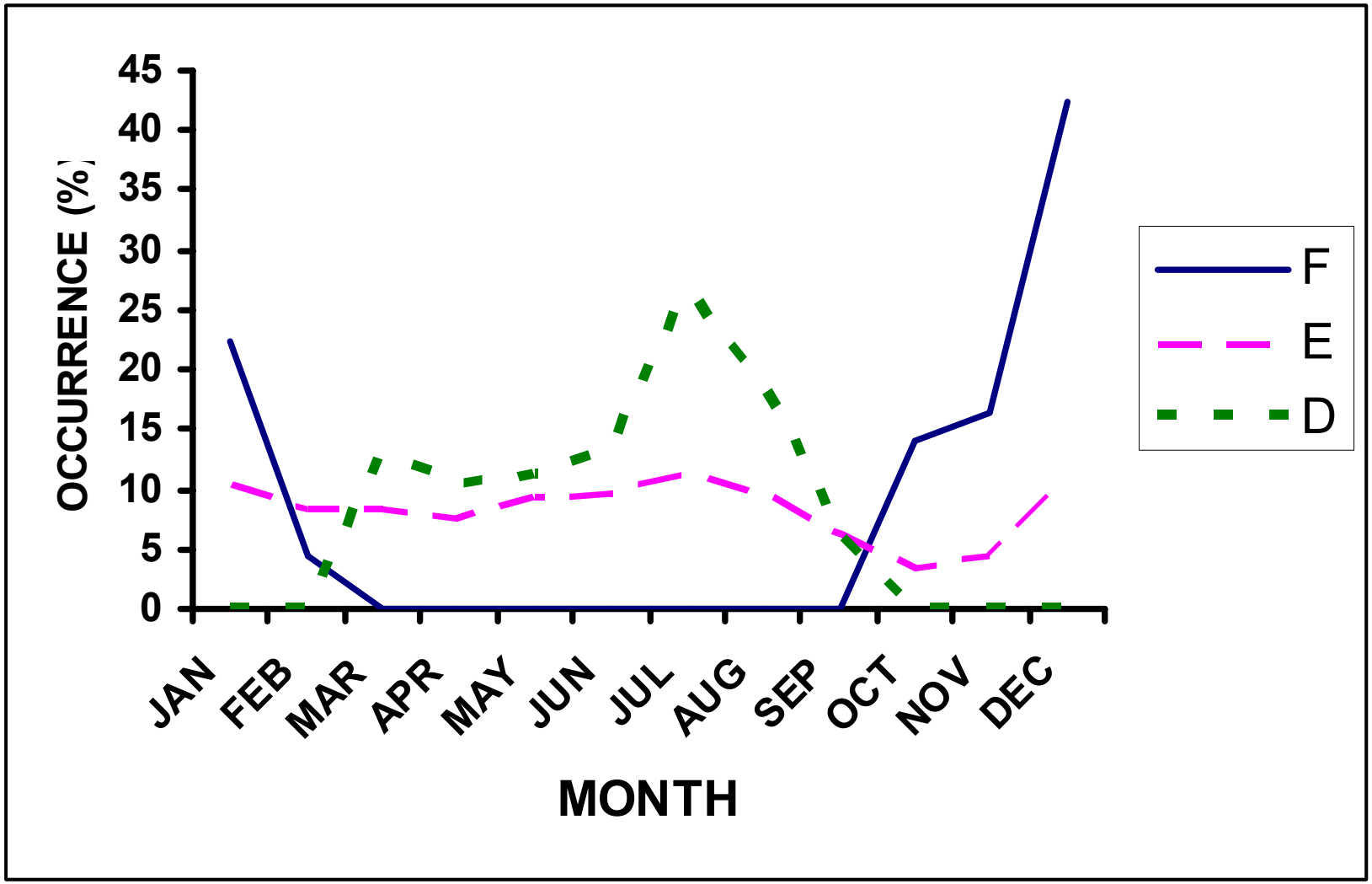

Fig.18 Monthly variation for relative occurrence percentage of ABL stability classes at Gangtok

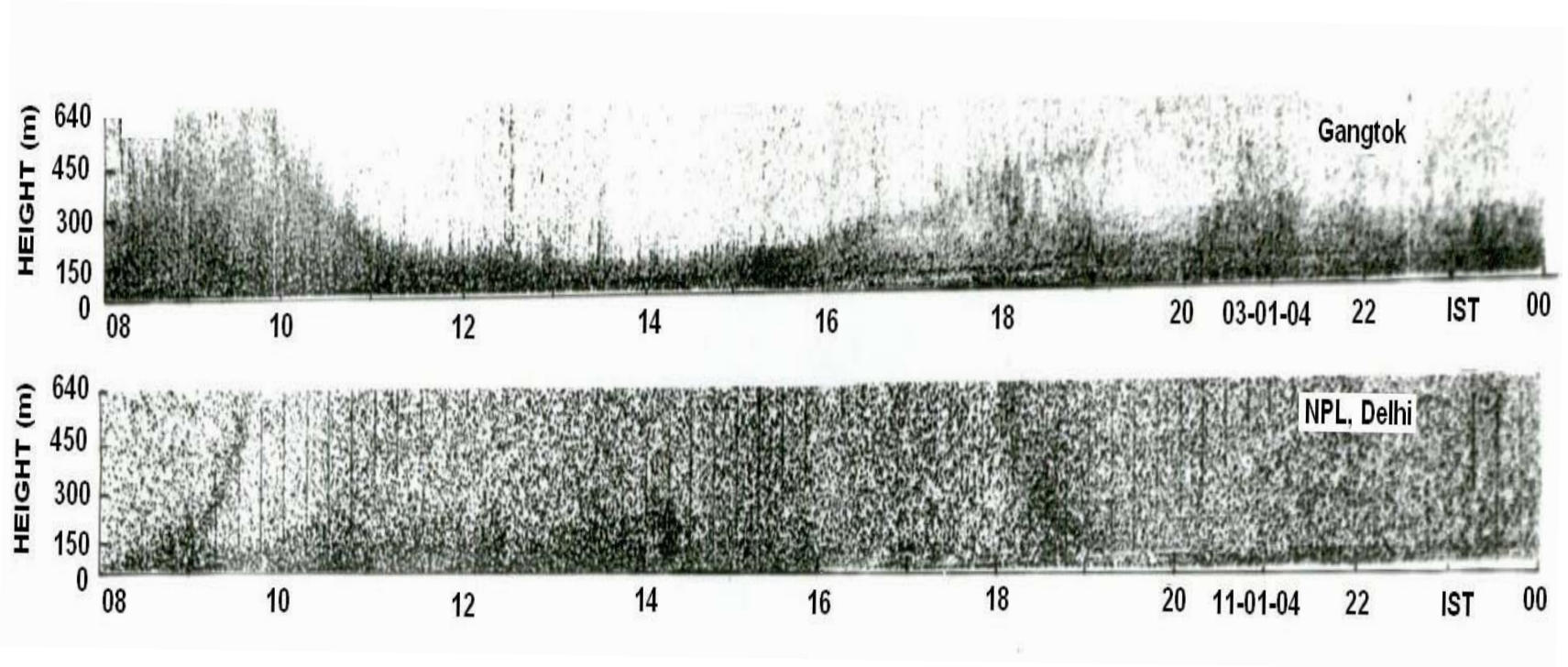

Fig.19 Comparative typical anomalous ABL thermal structure observed at high altitude (Gangtok) during winter

Gangtok. It is seen to remain settled near the ground throughout the day time. The layer gets lifted in the evening and it return, to the higher levels of ABL, with almost same sharpness that was observed while descending in the morning. Interestingly, a similar observation but with the opposite phases of ascending in the morning and descending in the evening has been at NPL (Delhi) during the same winter period. More over there is similarity in the observed slopes of ascending and descending at the two sites with different topography and altitudes. Further, care full examination of observation at NPL shows that the said ascending air mass is different than the normal rising layer or the eroding inversion. This eroding inversion is clearly seen separately in same record. The observation is yet to be understood, analyzed and interpreted with help of supporting meteorological data. However, the observation is first of its kind ever seen during the past two decades of Sodar observations at NPL. The observed features and that too at two entirely different characteristic sites make it a unique observation for further investigations.

8. DISCUSSION

The results are in general comparable with those reported for the urban and hilly areas. However, the observed maximum / minimum mixing height values for winter inversion are higher as compared with winter values of average inversion height for Delhi. Based on more than two decades (1983-2004) of Sodar observations (unpublished work) at NPL, New Delhi, and a minimum averaged inversion height of about 80

m and maximum of 150 m are seen over Delhi. The higher values at Gangtok are considered due to the contribution of topographically induced drainage flow in addition to nocturnal radiational cooling of the ground.

The mixing height for unstable ABL is also seen to slightly on higher side as compared with observations of plain area (Delhi). However, similar results for the hilly terrain (Guwahati) have been reported earlier by Singal and Kumar (1998).

Besides above an interesting observation, considered to be a ABL thermal structure anomaly at this stage, has been seen at Gangtok. A large scale sharply descending upper air mass in the morning hours, reaching near the ground and returning in the evening (see Fig.19) has been seen at Gangtok. A similar observation but in the opposite phase, at NPL (Delhi) makes it a unique observation for further investigations. Further, characteristic thin elevated layers have also been seen at Gangtok. Such layers have been seen in coastal regions of Antarctica. However, these are very preliminary observations and more extensive continuous data for at least couple of years and detailed studies in relation to supporting meteorological observations are required for more meaningful conclusions.

9. ACKNOWLEDGEMENT

We are thankful to the Director, National Physical Laboratory for providing necessary infra structural facilities, encouraging for Sodar R&D at NPL and permitting to carry out the present work. We are thankful to Director IIT, Delhi for giving an opportunity for carryout Sodar studies at Gangtok and funding the project work. Special Thanks are due to Professor Pramila Goyal, Project Coordinator and her teammates for their kind cooperation and loving attitude all through the period of studies.

10. SOME DEFINITIONS

Lapse Rate The rate of which the environmental temperature falls with height is known as Lapse rate. The dry adiabatic lapse rate is 9.8 °K/Km. The atmosphere is termed as stable, unstable and neutral according as the prevailing lapse rate is less than, more than or equal to the adiabatic lapse rate.

Inversion Atmospheric layer in which temperature increases with height is known as inversion. The inversion may be ground based or elevated depending on the meteorological conditions. The atmosphere under inversion conditions is stable and resists vertical motion – or – suppresses the prevailing turbulence.

Mixing height It is the height of the atmosphere above the earth's surface to which released air pollutants will extend primarily through the

action of atmospheric turbulence.

Boundary Layer It is a part of the lower atmosphere (troposphere) which is influenced by the presence of the earth and responds to cooling and heating of the earth. Boundary layer developed during night time stable atmospheric conditions is known as nocturnal stable boundary layer (NSBL).

Stability It is a qualitative indicator of atmospheric ability to disperse pollutants emitted into it from natural and man made sources. Six stability classes ranging from ‘A’ (extremely unstable) to ‘F’ (Highly stable) defined by Pasquill (1962) have been accepted in practice for use in air pollution modeling.

BIBLIOGRAPHY

BIBLIOGRAPHY

Balser, M. and Netterville, D. (1981). Measuring wind turbulence with doppler acoustic radar," *J. Appl. Meteorol*. **20**, 27.

Best, P.R., Kanowaski, M., Stumer, L. and Green, D. (1996). Convective dispersion modeling utilizing acoustic sounder information. *Atmos. Res*., **20**,173.

Beyrich, F. (1993). On the use of Sodar data to estimate mixing height. *Appl.Phys*. B57, 27-35

Brown, E.H. and Hall, F.F.Kr. (1978). Advances in atmospheric acoustics. ev. Geophys. Space Phys., 16, pp 47-110.

Clark, G.H., Chanash, E. and Bendum, E.O.K. (1977). Pattern recognition studies in acoustic sounding. *J. Appl. Meteorol*., 16, 1365.

Beyrich, F. (1993). On the use of sodar data to estimate mixing height. *Appl. Phys*. B57, 27-35.

Little, C.G. (1969). *Acoustic methods for the remote probing of the lower atmosphere*. Proc. IEEE, 57, 571-578.

Pasquill, F. (1962). *Atmospheric diffusion*, D. Van Nostrand Co. Ltd., London.

Coulter, R.L. (1979). A comparision of three methods for measuring mixing layer height. *Appl. Meteorol*. 18, 11,

Singal, S.P. (1988). *The use of an acoustic sounder in air quality studies.* 47 pp 520 –533.

Singal, S.P., Aggarwal, S.K. and Gera, B.S. (1980). Sodar (Acoustic Echo Sounder) in the use of air pollution meteorology, *J. Scient. Industri. Res*. 39, 73-86.

Singal, S.P. and Gera, B.S. (1982). Acoustic remote sensing of the boundary layer. *Proc. Ind. Acad. Sci*. (Engg. Sec.) 5(2) 131-157.

Singal, S.P. and Kumar, S. (1998). Sodar studies of air pollution associated meteorological parameters in the Hills of Assam, India. Proc. 9th International symp. on ISARS, 302-305.

Singal, S.P., Gera, B.S. and Aggarwal, S.K. (1984). Nowcasting by acoustic remote sensing Experiences with the systems established at the National Physical Laboratory, New Delhi. *J. Scient. Industr. Res*. 43, 469-488.

Singal, S.P., Aggarwal, S.K., Pahwa, D.R. and Gera, B.S. (1985). Stability studies with the help of acoustic sounding. *Atmos. Environ.* 19, 221-228.

Thomas, P. (1986). Stability classification by acoustic remote sensing. *Atmos. Res*. 20,165.

Twang Yu. Determining height of the nocturnal boundary layer. *Appl. Meteorol*. 17.

VOLUME-WISE CONTENTS

C O N T E N T S

VOLUME-I

INTRODUCTORY VOLUME

VOLUME-II

LAND ENVIRONMENT – GEOPHYSICAL ENVIRONMENT

VOLUME – III

LAND ENVIRONMENT - SOIL

VOLUME – IV

WATER ENVIRONMENT

VOLUME – V

AIR ENVIRONMENT

VOLUME – VI

BIOLOGICAL ENVIRONMENT

TERRESTRIAL AND AQUATIC RESOURCES

VOLUME – VII

BIOLOGICAL ENVIRONMENT

FAUNAL ELEMENTS

VOLUME – VIII

BIOLOGICAL ENVIRONMENT

FOOD RESOURCES

VOLUME – IX

SOCIO-ECONOMIC ENVIRONMENT

VOLUME – X

SOCIO-CULTURAL ENVIRONMENT